AIRFOIL PROGRAM SYSTEM "PROFIL05"

USER'S GUIDE

by Richard Eppler

© Prof. Dr. Richard Eppler, August 2006

Preface

The airfoil program system has been developed over a period of almost 50 years. A significant milestone was the description of the code in cooperation with NASA Langley Research Center in 1980 (ref. [1]). Shortly thereafter, a supplement to this description was published (ref. [2]), which included the options for boundary-layer displacement iteration and single roughness elements. Since then, many additional options have been incorporated, as described in additional supplements. Moreover, the book describing airfoil design using the code (ref. [3]) represents another milestone.

The version of the code listed in reference [1] is sold in the U.S. without my consent. (The same version was available from NASA through the Computer Software Management Information Center at the University of Georgia.) This version is obsolete.

Two major improvements were incorporated in 1996. First, a new transition criterion was developed that considers the instability history of the boundary layer (the previous criterion was local). Second, an empirical model for the drag due to laminar separation bubbles was included (the previous version provided only warnings of bubbles and no estimate of the drag).

Over the past decade, additional theoretical and experimental results concerning transition and laminar separation bubbles and much faster computers have become available. Thus, it was possible to develop a fast method for predicting transition by means of the e^N method and to improve the prediction of additional drag due to laminar separation bubbles.

The development of the code has been done in such a way that previous input data sets can still be used. The results may, however, differ from those produced by earlier versions of the code. Minor differences come from improvements to the panel method. Larger differences result from the new transition method and the bubble drag, which are now included in the normal (natural) transition mode. The previous transition criteria are no longer available.

The latest version of the code, along with the latest version of the user's guide, is available

for North America from:
Mr. Dan M. Somers
122 Rose Drive
Port Matilda, PA 16870-7535
USA

for all other countries from:
Prof. Dr. Richard Eppler
Leibnizstr. 84
D-70193 Stuttgart
Germany

I thank Mr. Dan Somers for many suggestions and Drs. Thorsten Lutz and Martin Hepperle for their assistance.

Stuttgart, October 2005.

Richard Eppler

Contents

1 Principles of Code **1**
1.1 Format of Input Lines . . . 1
1.2 Character Strings for Supplementing Plots . . . 2
1.3 Date and Time . . . 2

2 Overview of Input and General Options **2**
2.1 Overview of Input Lines . . . 2
2.2 General Options . . . 3
2.2.1 C Line . . . 3
2.2.2 REMO Line . . . 3
2.2.3 ENDE Line . . . 4

3 Airfoil Design **4**
3.1 TRA1 Line . . . 5
3.2 TRA2 Line . . . 6
3.3 RAMP Line . . . 11
3.4 ABSZ Line . . . 13

4 Potential-Flow Airfoil Analysis **14**
4.1 FXPR Line . . . 14
4.1.1 Coordinate Smoothing . . . 15
4.1.2 Insertion of Additional Points . . . 16
4.1.3 Input of Coordinates . . . 17
4.1.4 Coordinate Lines . . . 20
4.2 PAN Line . . . 20
4.2.1 Switching from Design to Analysis Mode . . . 20
4.2.2 Cascades . . . 21

5 Options for Both Design and Analysis Modes **22**
5.1 STRD Line . . . 23
5.2 STRK Line . . . 23
5.3 MACH Line . . . 26
5.4 FLAP Line . . . 27
5.4.1 Simple Flap . . . 27
5.4.2 Variable Geometry . . . 28
5.4.3 Modification of Individual Points . . . 30
5.4.4 Moment Reference Points . . . 31
5.5 ALFA Line . . . 33

5.6 DIAG Line . . . 35
5.6.1 Pressure-Envelope Diagram . . . 36
5.6.2 x-y-V Diagram . . . 36
5.7 PUXY Line . . . 40

6 Boundary-Layer Analysis 41
6.1 Fundamentals . . . 41
6.1.1 Criteria for Boundary-Layer Transition . . . 42
6.1.2 Profile Drag . . . 44
6.1.3 Bubble Drag . . . 44
6.2 EHNN Line . . . 45
6.3 RE Line . . . 45
6.3.1 Print and Plot Modes . . . 45
6.3.2 Reynolds Numbers and Transition and Bubble-Drag Modes . . . 46
6.3.3 Single Roughness Elements . . . 47
6.3.4 Labelling and Scaling . . . 48
6.3.5 Interpolation of Drag and Lift Coefficients . . . 49
6.4 FLZW Line . . . 49
6.5 PLW Line . . . 50
6.6 PLWA Line . . . 53
6.7 CDCL Line . . . 55
6.7.1 Extension of Frame . . . 56
6.7.2 Labelling . . . 57
6.7.3 Experimental Data . . . 58
6.7.4 Line Types . . . 60
6.7.5 Scaling . . . 60
6.7.6 Empty Grid . . . 61
6.7.7 Examples . . . 61
6.8 DPIT Line . . . 65

7 Rules for Input and Flow Chart 68
7.1 Input-Line Sequence . . . 68
7.2 Flow Chart . . . 70

References 71

1 Principles of Code

The sequence of execution within the code is controlled in a flexible manner by the input lines themselves. Each input line has a name in the first four columns. Thus, an ALFA line has "ALFA" in the first four columns and an RE line has "RE␣␣" (i.e., "RE" followed by two spaces). The spaces are part of the name and, therefore, those two columns must not be used for other purposes. The code reads the name and then branches to the corresponding section of the code. After performing the computations, printing, or plotting initiated by the input line, the code returns to the main routine and reads the next input line. In effect, the code is asking "What should I do next?"

Some of the lines initiate computations, printing, or plotting that requires results generated by other lines. Thus, the sequence of the lines is not completely arbitrary (see Chap. 7).

Normally, the data read from a line remain in effect until new data are read from a line having the same name. Exceptions to this rule are described in detail.

Every input case must be terminated by an ENDE line.

During the development of the code, many new options have been introduced. The modifications have always been guided by the principle that previous data sets should still be valid. For this reason, some input features are not as simple as they might be.

1.1 Format of Input Lines

For all input lines, except those containing airfoil coordinates or experimental data, the first 10 columns are read using the FORTRAN format `A4,3I1,I3`. Thus, each line contains:

in columns 1–4, an alphanumeric line name;

in columns 5–7, three integer numbers, *NUPA*, *NUPE*, and *NUPI*, having one digit each;

in columns 8–10, one integer number, *NUPU*, having three digits; and

in columns 12–80, up to 22 floating-point numbers, referred to as F-numbers F_1–F_n.

The input reading is performed in Subroutine DLFF. The following definitions apply.

- The symbol ␣ denotes a space. Thus, ␣␣␣␣␣ denotes four consecutive spaces.
- A DLFF word is a number, possibly with a minus sign and/or a decimal point. It may have as many digits as desired. It is always read as a floating-point number. The decimal point at the end of the word can be omitted. Leading zeroes ahead of the decimal point can also be omitted. A DLFF word is terminated by a comma or a space.

  For example,

  `12.0`␣ `12`␣ `-.003,` `12.3456789`␣
- A DLFF sentence consists of an arbitrary number of DLFF words separated only by a comma or a space. The sentence is terminated by two columns containing either a comma and a space or two spaces. For example,

  `12.0,12,12.01,400000,-.003,`␣
  `12.0`␣`12`␣`12.01`␣`400000`␣`-.003`␣␣

  (In this example, the first two words specify the same number.)

- If the character "F" occurs within a DLFF word, usually at the beginning of the word, Subroutine DLFF continues reading that word and that sentence in column 1 of the succeeding line. Thus, the 'continuation' line has neither an alphanumeric name nor the four integer numbers.
- A line may contain more than one DLFF sentence. A second call to Subroutine DLFF, without specifying the column in which reading should begin, initiates reading following the end of the preceding sentence. An example of a line containing two DLFF sentences is

  `12.0␣12,12.01␣40000␣␣5␣7,3.00368␣␣`

  The first sentence contains the four numbers 12, 12, 12.01, and 40000; the second, the three numbers 5, 7, and 3.00368.

All data are input as they will be used within the code (i.e., no multiplication factor is applied within the code). An exception is the RE line, in which the Reynolds numbers are specified in thousands. For example,

`RE␣␣␣␣␣␣␣␣␣3␣1000␣5␣500␣7␣10000`

which specifies Reynolds numbers of 1,000,000, 500,000, and 10,000,000 with transition modes 3, 5, and 7, respectively. (See Chap. 6.3.)

1.2 Character Strings for Supplementing Plots

Several options produce plots. These plots can be supplemented by labels in several ways, some of which are based on character strings contained in the input lines. The characters are formed by sequences of vectors. The vectors are not actually plotted but rather, like all graphic output, written to a file that must be postprocessed. A description (ref. [6]) is provided with the user's guide.

1.3 Date and Time

Most computer operating systems provide a calendar and a clock. To distinguish different results, the date and time are given in the output listing and in the plots. The delivered executable version of the code provides the date and time from the corresponding operating system.

2 Overview of Input and General Options

2.1 Overview of Input Lines

The input lines can be segregated into the four categories: design, potential-flow analysis, options for both design and analysis, and boundary-layer analysis. The function of each input line is summarized in the flow chart in Chapter 7.2.

The line names can be given in upper- or lower-case letters. Thus, "TRA1" and "tra1" are equivalent. Mixed case is not permitted, however. Thus, "Tra1" cannot be given.

- The input lines for the general options are described in Chapter 2.2.
- The input lines for airfoil design are:

TRA1 line, which specifies the arc limits and their corresponding α^*values;

TRA2 line, which specifies the pressure recovery and the closure contribution as well as the options for the trailing-edge iteration.

RAMP line, which specifies the transition ramps; and

ABSZ line, which specifies a factor by which the number of points on the circle is multiplied.

- The input lines for potential-flow analysis are:

  FXPR line, which reads a set of airfoil coordinates and

  PAN line, which switches from the design to the analysis mode and specifies cascades.

- The options for both design and analysis modes are specified in:

  STRD and STRK lines, which together plot airfoil shapes with various chords;

  MACH line, which computes compressibility effects on the velocity (or pressure) distributions.

  FLAP line, which alters the airfoil shape to that corresponding to the deflection of a simple flap or a variable-geometry device;

  ALFA line, which contains the angles of attack to be analyzed;

  DIAG line, which plots velocity (or pressure) distributions; and

  PUXY line, which writes the airfoil coordinates to a file.

- The input lines for boundary-layer analysis are:

  RE line, which specifies the transition modes and Reynolds numbers;

  FLZW line, which specifies the aircraft data required to compute the boundary-layer developments for which the Reynolds number varies with aircraft lift coefficient and local chord;

  PLW line, which specifies additional aircraft data required to compute a speed or power polar;

  PLWA line, which increments the aircraft data from the PLW line;

  CDCL line, which plots the section characteristics; and

  DPIT line, which performs the boundary-layer displacement iteration.

2.2 General Options

2.2.1 C Line

The C line specifies a comment, which follows the "C" and at least one space. The comment is written in the output listing.

2.2.2 REMO Line

The REMO line controls other general options.

NUPA, *NUPE*, and *NUPI* are ignored.

If the last digit of *NUPU* $\neq$ 0, all plots are rotated 90° counterclockwise.

The F-numbers specify the line widths for plotting.

Different line widths are used for the curves and the axes in the plots. The width specified by $PENLI$ is used for the curves and by $PENAX$, for the axes. Subroutine FORMEL, which draws the characters, sets the line width to one tenth the character height. This width is constrained by two parameters, $SMAX$ and FKK. After plotting a character, the line width is reset to the previous value. The F-numbers have the following meanings.

$F_1 = SMAX$, which is the maximum line width of the labels; the default value is 1 mm.

$F_2 = FKK$, which provides a smooth reduction of the line width between $SMAX$ and $FKK * SMAX$; the default value is 0.4.

$F_3 = PENLI$, which is the line width of the curves; the default value is 0.4 mm.

$F_4 = PENAX$, which is the line width of the axes; the default value is 0.25 mm.

A parameter is not changed if its input value is zero.

In the upper, left corner of each plot, "Eppler 05 V." and the date of the code version followed by "Run" and the current date and time are written. The default height of this text is 4 mm. In any column after column 14 or three columns after the last specification for other options, the following options can be specified.

*S followed by the two digits ab sets the label height to $a.b$ mm.

*P followed by a $character\ string$ replaces the default text with the character string. Thus, "*P" suppresses the default text in the upper, left corner.

*PN resets the text to the default text.

*D appends the date and time to the character string given after *P.

*Z followed by a $character\ string$ appends the character string to the previously specified text. Options *P and *D are, in this case, not valid (i.e., the *Z option cannot be specified in the same REMO line as the *P or *D options).

2.2.3 ENDE Line

This line terminates the run. The input lines are listed after the computed results.

3 Airfoil Design

The design of an airfoil is initiated by the TRA1 and TRA2 lines. It is suggested that these lines be saved, at least for those airfoils that are considered "final" in some sense. Airfoil designers soon collect many such sets and it is often helpful to insert comments in the TRA1 line and TRA2 lines. Any text input three columns after the last F-number is ignored unless it is preceded by "*C", in which case it will be written in the headline of the first output of the airfoil design. The *C option can be specified in each TRA1 line and all the comments (up to 48 characters) are then combined

and written in sequence.

As described in detail in references [1] and [3], the airfoil design is performed by a conformal mapping of the outside of a circle in the ζ-plane to the outside of the airfoil in the z-plane. Accordingly, the airfoil design is specified by several arcs on the circle with limits φ_i, having α^* values of α_i^*, and the parameters for the pressure-recovery functions and the closure contributions, including φ_w, $\bar{\varphi}_w$, φ_s, and $\bar{\varphi}_s$. The computation is based on N equiangular points on the circle. The value of N is specified and must be divisible by 4. The arc limits φ_i as well as φ_w, $\bar{\varphi}_w$, φ_s, and $\bar{\varphi}_s$ are not specified in degrees but, instead, relative to the point numbers. Thus,

$$\Delta\varphi = 2\pi/N = 360^\circ/N \tag{1}$$

and

$$\begin{aligned} \nu_i = \varphi_i/\Delta\varphi \qquad \lambda = \varphi_w/\Delta\varphi \qquad \bar{\lambda} = \bar{\varphi}_w/\Delta\varphi \\ \lambda^* = \varphi_s/\Delta\varphi \qquad \bar{\lambda}^* = \bar{\varphi}_s/\Delta\varphi \end{aligned} \tag{2}$$

A practical value for N is 60. Thus, $\Delta\varphi = 360^\circ/60 = 6^\circ$. In this case, $\nu_i = 15$ specifies an arc limit that corresponds to a point near midchord on the upper surface of the airfoil, whereas $\nu_i = 30$ is near the leading edge and $\nu_i = 45$ is near midchord on the lower surface. If ν_i is an integer number, the arc limit normally corresponds to a point on the airfoil. If ν_i is a decimal number, the arc limit falls between two points on the airfoil. The same is true for the λ values, which specify the beginning of the pressure-recovery and closure-contribution regions. Symmetric airfoils, of course, have $\lambda = \bar{\lambda}$ and $\lambda^* = \bar{\lambda}^*$.

The number of points on the airfoil NQ differs from N. Most points correspond to the equiangular points on the circle. The trailing edge, however, is defined by two points, one on the upper surface corresponding to $\varphi = 0^\circ$ and one on the lower surface corresponding to $\varphi = 360^\circ$. Moreover, additional points are automatically inserted near the leading edge, depending on its shape. Thus, NQ depends on the shape of the leading edge and is always greater than N.

The arc limit ν_{i_L} of the leading edge is not specified but rather computed by the code. This is indicated in the input by setting $\nu_{i_L} = 0$.

The input data for the design method is contained in four line types. The TRA1 line specifies the arc limits ν_i and their corresponding α_i^* values. The TRA2 line specifies the pressure-recovery and closure-contribution parameters, the iteration mode, and the amount of pressure recovery to be achieved by the closure contribution $K_H + \bar{K}_H$. The RAMP line specifies two arcs on each airfoil surface by which a transition ramp can be defined. The ABSZ line provides additional options. A detailed description of the use of the input parameters in airfoil design is given in reference [3].

3.1 TRA1 Line

NUPA and *NUPE* are ignored.

NUPI and *NUPU* together specify the airfoil identification number (i.e., up to four digits).

F_1 specifies ν_1.

F_2 specifies α_1^*, in degrees relative to the zero-lift line.

$(F_3,\ F_4) = (\nu_2,\ \alpha_2^*)$ and so on. A TRA1 line may contain up to 11 pairs ν_i, α_i^*. Reading is terminated by the end of the DLFF sentence (e.g., two spaces).

As many TRA1 lines as necessary can be given. Up to 120 arcs are allowed for each airfoil design.

The number of points on the circle comes from the last arc limit $\nu_i = N$. This number must be divisible by 4 and no greater than 120.

The leading-edge arc limit must be specified by $\nu_{i_L} = 0$. The value of ν_{i_L}, which is computed by the code, must fall between ν_{i_L-1} and ν_{i_L+1}. Thus, if ν_{i_L-1} is too large or ν_{i_L+1}, too small, no solution for ν_{i_L} can be found. In this situation, the code writes a message and then stops. The same is true if $\alpha^*_{i_L+1} > \alpha^*_{i_L}$.

It should be remembered that arc limits can be specified that do not correspond exactly to the points on the airfoil. Indeed, arc limits that fall between points (e.g., $\nu_i = 16.5$) yield velocity distributions that are slightly smoothed.

An example of a TRA1 line is

```
TRA1␣␣1098␣23.5␣8␣27.5␣10␣0␣12␣60␣2␣␣*C␣MIT␣SAILPLANE
```

This line results in $\Delta\varphi = 6^\circ$ and, therefore,

i	ν_i	φ_i	α^*_i
1	23.5	141°	8°
2	27.5	165°	10°
3	0	φ_{i_L}	12°
4	$60 = N$	360°	$2^\circ < \alpha^*_3$

If $\nu_i < \nu_{i-1}$, then ν_i is interpreted as $\Delta\nu$ and $\nu_i = \nu_{i-1} + \Delta\nu$ is set. This option is particularly convenient if, as discussed in reference [3], many arc limits are used having $\Delta\nu = 2$ and the arc limits fall between the airfoil points. Using this option, the above example can also be specified by

```
TRA1␣␣1098␣23.5␣8␣4␣10␣0␣12␣60␣2␣␣
```

The value of α^*_i for each arc S_i $(\nu_{i-1} < \nu < \nu_i)$ will be computed if $\Omega' = \frac{1}{V}\frac{dV}{dx}$ is specified for a given α_R. This is performed by the following option.

If, for the arc S_i, $\alpha^*_i > 90^\circ$ is input, Ω'_i is set to $\alpha^*_i - 90^\circ$ and α_R to α^*_1 for the upper surface or α^*_N for the lower surface and α^*_i is computed such that Ω'_i occurs in the middle of S_i for $\alpha = \alpha_R$.

This option was previously used to specify transition ramps. They are now much more easily specified using the RAMP line (Chap. 3.3).

3.2 TRA2 Line

The TRA2 line specifies the main pressure recovery on each surface, the length of the closure contribution necessary to achieve a closed airfoil shape, and, optionally, the addition of identifying letters to the airfoil name. The main pressure recovery is determined by a function $w(x)$ by which the velocity distribution along the upper surface as defined by the α^* values is multiplied. The function has a value of 1 forward of the beginning of the recovery, which is specified by λ for the upper surface and $\bar{\lambda}$ for the lower surface. The recovery itself is computed using two parameters K and μ, where K determines the amount of recovery ω and μ determines the shape of the recovery. The combined effect of K and μ is complicated. Therefore, the recovery can be specified by other, more explicit parameters (e.g., μ and ω, see figure reframpm) as well.

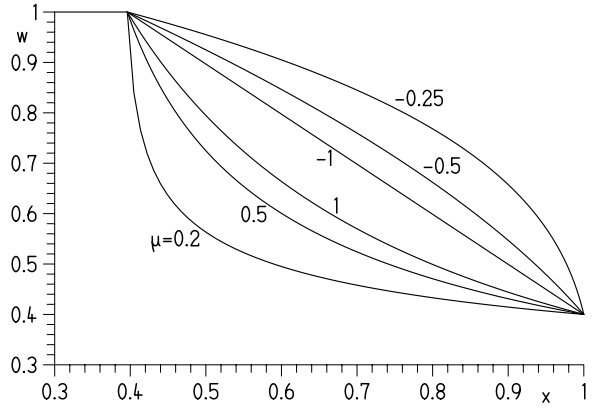

Figure 1: Effect of μ on recovery shape.

If *NUPA* > 0, the airfoil number will be prefixed by one or two letters with or without a space between these letters and the airfoil number, as shown in the table to the right.

NUPA	Letter(s)	Space
1	E	Yes
2	S	No
3	HQ	No
4	HX	No
5	TL	No
6	MH	No
7	DO	No
8	YY	Yes
9	ZZ	No

If "*8" followed by two letters are given in a TRA2 or REMO line at least two spaces after the last number, these two letters replace "YY" in the table; "*9" followed by two letters accomplishes the same for "ZZ".

The replacement letters precede the airfoil number if *NUPA* $= 8$ or 9, with a space if *NUPA* $= 8$ and without a space if *NUPA* $= 9$.

NUPE, *NUPI*, and *NUPU* are ignored and, therefore, columns 7–10 can be used for the airfoil identification number, if desired.

F_1 specifies λ^*, which is the beginning of the closure contribution on the upper surface.

F_2 specifies λ, which is the beginning of the main pressure-recovery region on the upper surface.

F_3 specifies $RSM(us)$, which is the recovery specification mode for the upper surface. It determines the interpretation of F_4 and F_5 as shown in the table to the right.

$RSM(us)$	F_4	F_5
0	K	μ
1	ω'	ω
2	μ	ω
3	μ	ω'

F_6 specifies $\bar{\lambda}^*$; $N - \bar{\lambda}^*$ is the beginning of the closure contribution on the lower surface.

F_7 specifies $\bar{\lambda}$; $N - \bar{\lambda}$ is the beginning of the main pressure-recovery region on the lower surface.

F_8 specifies $RSM(ls)$, which is the recovery specification mode for the lower surface. It determines the interpretation of F_9 and F_{10} as shown in the tableto the right.

$RSM(ls)$	F_9	F_{10}
0	$\bar{K}$	$\bar{\mu}$
1	$\bar{\omega}'$	$\bar{\omega}$
2	$\bar{\mu}$	$\bar{\omega}$
3	$\bar{\mu}$	$\bar{\omega}'$

The values of K, μ, $\bar{K}$, and $\bar{\mu}$ are normally rounded to three digits after the decimal point; the values of α^*, to two digits. F-numbers F_3 and F_8 allow the rounding to be changed. If the first digit after the decimal point is a, then the rounding is done to $3 + a$ digits for K, μ, $\bar{K}$, and $\bar{\mu}$,

and to $2 + a$ digits for α^*. The latter is significant only if some of the α^* values are iterated (see below). Both F_3 and F_8 should specify the same value for a.

F_{11} specifies $ITMOD$, which is the iteration mode used to achieve the desired value K_R of K_S.

F_{12} specifies K_R, which is the desired value of $K_S = K_H + \bar{K}_H$.

F_{13} specifies K_{tol}, which is the tolerance on the achievement of K_R; $K_{tol} = 0$, normally.

The following iteration modes, specified by F_{11}, can be used to achieve the desired trailing-edge angle as indicated by K_S.

If $ITMOD = 0$, no iteration is performed; F_{12} and F_{13} are ignored and K_H and $\bar{K}_H$ are determined by the other design parameters.

If $ITMOD = 1$, all α_i^* for the upper surface ($i \le i_L$) are replaced by $\alpha_i^* + \Delta\alpha^*$.

If $ITMOD = 2$, all α_i^* for the lower surface ($i > i_L$) are replaced by $\alpha_i^* + \Delta\alpha^*$.

If $ITMOD = 3$, all upper-surface α_i^* ($i \le i_L$) are replaced by $\alpha_i^* + \Delta\alpha^*$ and all lower-surface α_i^* ($i > i_L$) are replaced by $\alpha_i^* - \Delta\alpha^*$.

For iteration modes 1–3, certain arcs can be excluded from the iteration by specifying a number b after the decimal point. Thereby, b arcs from the trailing edge forward on the corresponding surface are excluded from the iteration. For example, $ITMOD = 2.7$ excludes the seven arcs on the lower surface forward of the trailing edge from the iteration.

If $ITMOD = 4$, K is replaced by $K + \Delta K$.

If $ITMOD = 5$, $\bar{K}$ is replaced by $K + \Delta K$.

If $ITMOD = 6$, K is replaced by $K + \Delta K$ and $\bar{K}$ is replaced by $\bar{K} + \Delta K$.

This option should not be used if K and $\bar{K}$ have opposite signs, for example, if both values are determined by $RSM = 2$ and μ and $\bar{\mu}$ have opposite signs. In this case, the effects of ΔK on K_s are opposite for the upper and lower surfaces and the iteration may diverge or, at least, produce unintended results.

If $ITMOD = 7$, $\alpha_{i_L}^*$ is replaced by $\alpha_{i_L}^* + \Delta\alpha^*$.

If $ITMOD = 8$, $\alpha_{i_L+1}^*$ is replaced by $\alpha_{i_L+1}^* + \Delta\alpha^*$.

If $ITMOD = 9$, $\alpha_{i_L}^*$ is replaced by $\alpha_{i_L}^* + \Delta\alpha^*$ and $\alpha_{i_L+1}^*$ is replaced by $\alpha_{i_L+1}^* - \Delta\alpha^*$.

In all iteration modes, $\Delta\alpha^*$ or ΔK is determined such that $K_H + \bar{K}_H = K_S = K_R$, as specified by F_{12}. During the iteration, $\Delta\alpha^*$ is rounded to $2 + a$ digits and K to $3 + a$ digits to the right of the decimal point. Therefore, K_S may not be exactly equal to K_R.

The TRA2 line initiates the design of the specified airfoil. The x/c and y/c airfoil coordinates, the inner normal angles, and the velocity function $v/\cos(\varphi/2 - \alpha_i^*)$ are stored in blank COMMON arrays X, Y, ARG, and VF, respectively.

Normally, the code produces two tables containing all the ν_i values, including ν_{i_L}, and their corresponding α_i^* values, as well as the pressure-recovery and closure-contribution parameters, in the first line for the upper surface and in the last line for the lower surface. The first table contains the input values; the second, the values from the final iteration. Between these two tables, one line per iteration is written containing the values of K_S and $\Delta\alpha^*$ or ΔK for that iteration. Other print modes are specified by mpr in the ABSZ line (Chap. 3.4).

For example, the TRA2 line for airfoil 1098 is

```
TRA2␣␣1098␣4␣14.5␣2␣1␣0.65␣4␣14.5␣2␣1␣0.65␣6␣.4␣0␣0
```

The listing produced by this TRA2 line and the previous TRA1 line (see Chap. 3.1), assuming the default print mode (i.e., $mpr = 1$, see "ABSZ Line", Chap. 3.4), is given below. The values of K and $\bar{K}$ are changed by the iteration. The final values, listed in the second table, are underlined twice. The other values influenced by the changes in K and $\bar{K}$ are underlined once. (The underlining has been added for clarity and is not produced by the code.)

```
 EPPLER-CODE PROFIL98 V. 16.6.98  RUN  17.6.98  10:28

 TRANSCENDENTAL EQUATION RESULTS AIRFOIL 1098     ITERATION  0  MODE 6
    NU    ALPHA*  OMEGAP  OMEGA    K      MU     K H   LAMBDA LAMBDA*
  23.8000  8.00   1.137  0.650  0.598  1.000  0.583060  14.50   4.00
  27.8000 10.00
  32.0050 12.00
  60.0000  2.00   1.137  0.650  0.598  1.000  0.066661  14.50   4.00

 ITERATION 1  KS= -0.360403   DELTA= -0.07527818  ROUNDED -0.075000
 ITERATION 2  KS=  0.392433   DELTA= -0.00075381  ROUNDED -0.001000
 ITERATION 3  KS=  0.402662   DELTA=  0.00026028  ROUNDED  0.000000

 TRANSCENDENTAL EQUATION RESULTS AIRFOIL 1098     ITERATION  3  MODE 6
    NU    ALPHA*  OMEGAP  OMEGA    K      MU     K H   LAMBDA LAMBDA*
  23.8000  8.00   1.182  0.641  0.622  1.000  0.459530  14.50   4.00
  27.8000 10.00   -----  -----  =====
  32.0050 12.00
  60.0000  2.00   1.182  0.641  0.622  1.000 -0.056868  14.50   4.00
                  -----  -----  =====
 THICKNESS 18.84%, CM0=-0.1232, ALFA0= 4.8721 DEG., ETA= 1.1364
```

Airfoils having sharp or thin leading edges are usually not defined precisely enough in that region by the number of points specified in the TRA1 line, even if the maximum number is specified.

Moreover, another problem arises, even if the airfoil shape is well defined. The point on the airfoil that corresponds to the aerodynamic leading edge, ν_{i_L}, usually does not coincide with one of the computed airfoil points. Thus, for high or low lift coefficients, the leading-edge suction peak occurs at a location that is not an airfoil coordinate. Because the velocities for all the plots and the boundary-layer computations are computed only at the airfoil coordinates, the resulting suction peak is, therefore, usually lower than it should be and the boundary-layer development is computed with a shallower adverse pressure gradient near the leading edge. The low-drag range is then predicted to be slightly too wide. This small error is unconservative and compounds an error in the same direction arising from the integral method used for the boundary-layer computation.

Accordingly, additional points are automatically inserted near the leading edge; the code determines how many additional points are required; the sharper the leading edge, the more points added. The points are added in the circle plane at

$$\nu_{i_L} + \Delta\nu_j$$

where

$$\Delta\nu_j = -0.5, -0.25, 0, 0.25.0.5$$

Finally, the values

$$\Delta\nu_j = \pm 0.125, \quad \pm 0.0625, ...$$

are used according to the amount of camber near the leading edge. No more than 13 points are inserted, which is adequate even for very sharp leading edges.

It should be remembered that the airfoil points are normally computed for integer values of ν,

whereas ν_{i_L} is computed during the design procedure and not known in advance. The additional points are thus located relative to the unknown leading edge. If an additional point falls too close to an integer one, the integer one is omitted. The value $\Delta\nu_j = 0$ corresponds to the airfoil point to be computed for ν_{i_L}. This is the leading edge in an aerodynamic sense. At that point, the airfoil has its maximum camber and its maximum suction peak. This point does not necessarily, however, coincide with the geometric leading edge (i.e., $x/c = 0$).

As a consequence of the additional points, all airfoils are defined by more points than specified in the TRA1 line. This is of no concern unless the airfoil is analyzed using the panel method. For example, FLAP lines may cause the number of points to increase before the panel method is called. Because the total number of points is restricted to 129, no more than 108 points should be specified in the design mode. Due to the precise definition of the leading-edge region, 60 points normally yield very precise shapes.

The code works internally with many more points in the most critical step of the conformal mapping. This is transparent to the user. The results may, however, differ slightly from those of older code versions, mainly for airfoils with very sharp leading edges.

Those lines in previous data sets that specify additional points near the leading edge (e.g., TRA1 lines with $F_1 > 998$) need not to be deleted; they are now simply ignored.

Figure 2 shows the leading edge of a very thin airfoil with $N = 60$ in the TRA1 line with and without additional points near the leading edge. (Note that the shape without additional points cannot be generated using the current version of the code.) The computed airfoil points are identified on both airfoils by tic marks perpendicular to the airfoil surface (see "STRK Line", Chap. 5.2).

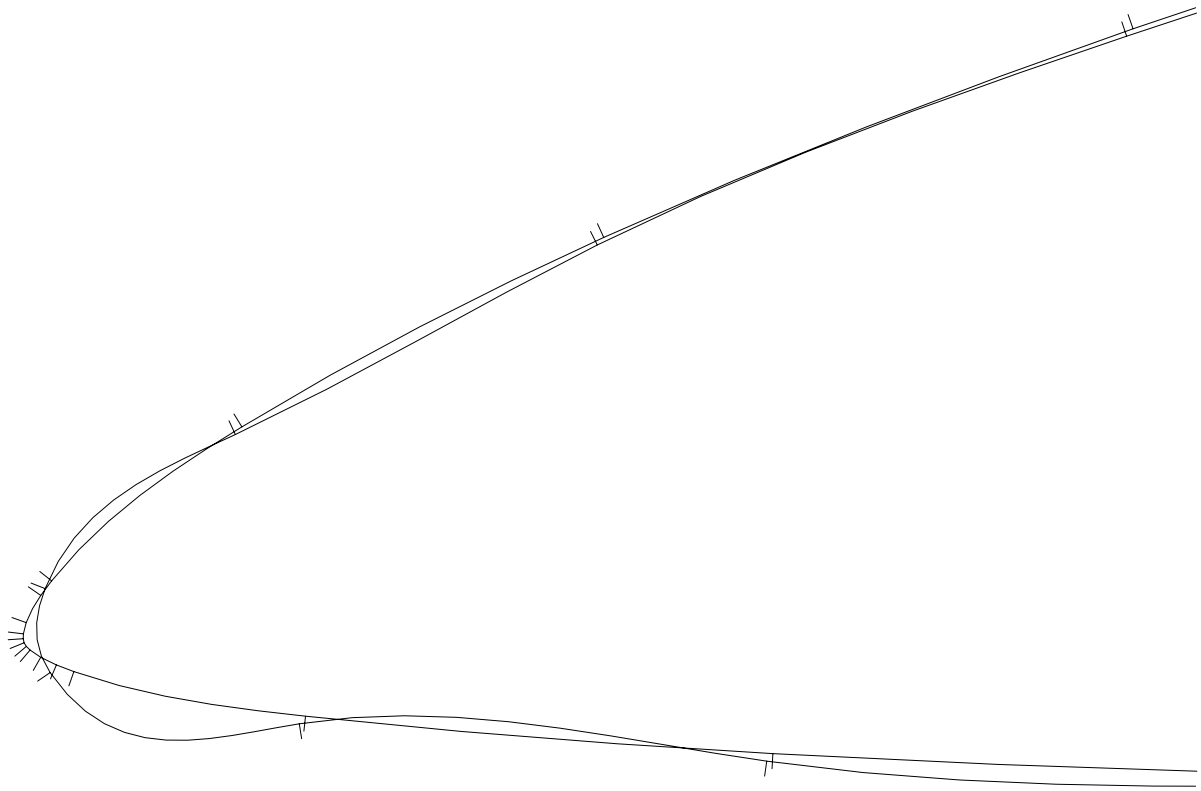

Figure 2: Thin airfoil with and without additional points near leading edge.

3.3 RAMP Line

The RAMP line allows transition ramps to be designed without specifying several arcs with different α_i^* forward of the pressure recovery. Instead, the length of the pressure-recovery function as specified by λ in the TRA2 line is extended forward by $\Delta\nu_f$. The recovery function between the trailing edge and $\lambda - \Delta\nu_r$, which is the aft end of the ramp, is not altered. The shape of the ramp is determined by $\Delta\nu_r$ and $\Delta\nu_f$. Over the length of the ramp, which extends from $\lambda + \Delta\nu_f$ to $\lambda - \Delta\nu_r$, the recovery function is replaced by a parabola with an inclined axis of symmetry. The parabola smooths the corner that would otherwise occur at the beginning of the recovery function.

Several examples of transition ramps are given in figure 3, where the broken line is the recovery function from the TRA2 line without a ramp and the solid line, with a ramp. The ramp is specified by $\Delta\nu_f$ and $\Delta\nu_r$ only. These parameters are angles on the circle in the conformal mapping. It should be remembered that the length in x/c between equiangular points is smaller near the leading and trailing edges and larger near midchord.

Figure 3 illustrates the ease with which the shape of the ramp can be controlled. For example, on the upper surface of aircraft wings, the maximum curvature should usually occur toward the aft end of the ramp because boundary-layer transition occurs there at lower lift coefficients and higher Reynolds numbers. The opposite is true for the lower surface. Controlling the curvature is accomplished by changing $\Delta\nu_r$ and/or $\Delta\nu_f$. Decreasing $\Delta\nu_r$ increases the curvature of the ramp at its aft end and vice versa; increasing $\Delta\nu_f$ has the same effect. The first four plots illustrate this effect for a recovery function with $\mu = 1$, which is only slightly concave. The last four plots show the same effect for a recovery function with $\mu = 0.25$, which is very concave and initially very steep. Clearly, the shape of the recovery function must be considered when designing the ramp. For concave recovery functions, if $\Delta\nu_f$ is too small, the intersection of the tangent to the recovery function and the horizontal line $w = 1$ lies forward of the beginning of the ramp. In this case, the code writes a message and ignores the ramp design. In such cases, either $\Delta\nu_f$ must be increased or $\Delta\nu_r$ must be decreased. The length of the ramp is constrained only by the length of the given airfoil surface.

It is permitted to change α^* within the ramp, as can also be done within the recovery function. It is recommended, however, that only one α^* be specified for both the recovery function and the ramp.

NUPA, *NUPE*, *NUPI*, and *NUPU* are ignored;

$F_1 = \Delta\nu_f$ for the upper surface;

$F_2 = \Delta\nu_r$ for the upper surface;

$F_3 = \Delta\nu_f$ for the lower surface; and

$F_4 = \Delta\nu_r$ for the lower surface.

The RAMP line is valid for the current airfoil design only and must be inserted ahead of the TRA2 line. At the end of Subroutine TRAPRO, which computes the airfoil coordinates, the values of $\Delta\nu_r$ and $\Delta\nu_f$ are reset to the default values (i.e., zero), which specify no ramp. The option of specifying Ω' instead of α^* in the TRA1 line (Chap. 3.1) is independent of the RAMP line.

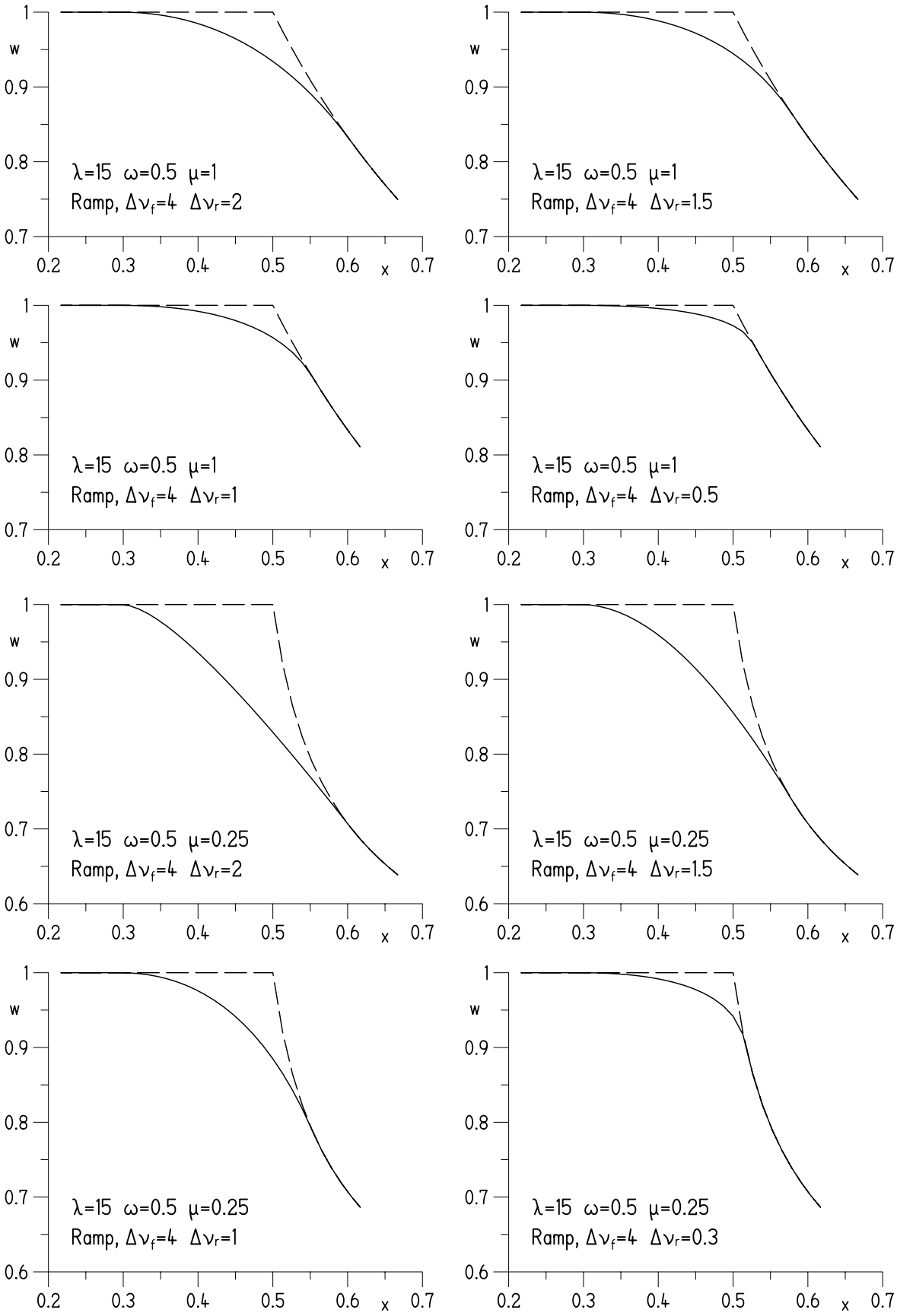

Figure 3: Effect of input variation on ramps.

The following input yields the airfoil shown in figure 4.

```
TRA1     77 0 10 60 5
RAMP        4 2 3 3
TRA2     77 4 14.5 2 -1 .7 4 12.5 2 1 .7 6 .3 0
ALFA      2 5 10
DIAG                  -1 .08 1 2 .1 1 2 -.2 1
```

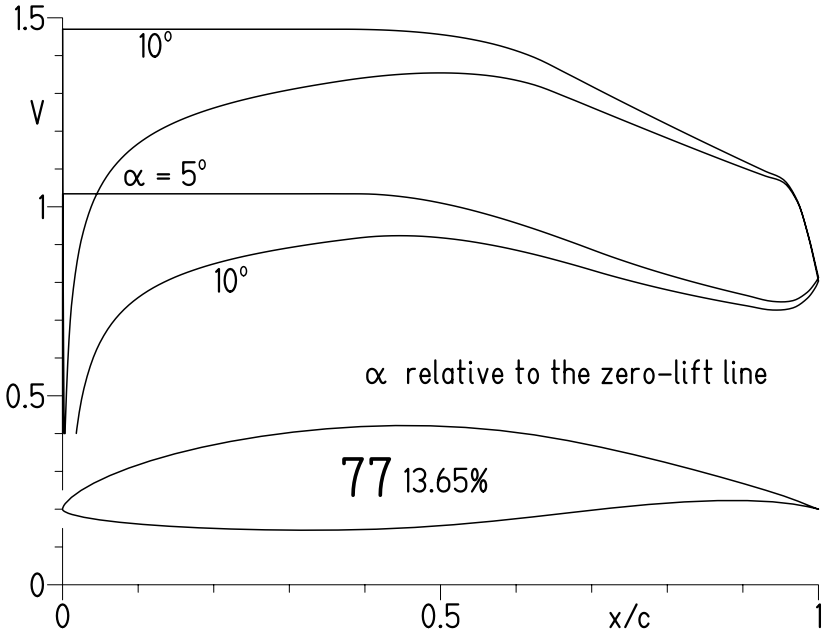

Figure 4: Airfoil with ramps on upper and lower surfaces.

3.4 ABSZ Line

Four values can be changed by the ABSZ line: the print mode mpr for the design iteration, the number of lines per page in the listing, the number of points NQ in the design method, and a precision ϵ in the panel method.

If *NUPA* $\neq 0$, $mpr =$ *NUPE*, where

$mpr = 0$ suppresses the listing from the solution of the transcendental equation,

$mpr = 1$ produces the (default) listing as described in the preceding section, and

$mpr > 2$ produces a listing for every iteration.

NUPI and *NUPU* are ignored.

If $F_1 \neq 0$, the number of lines per page $NPG = F_1$; the default value is 68.

If $F_2 \neq 0$, $ABFA = F_2$; the default value is 1.

If $F_3 \neq 0$, $EPSPA = 0.001F_3$; the default value is 0.0001.

The variable $ABFA$ is a factor by which all ν_i values in the TRA1 lines as well as λ, $\bar{\lambda}$, λ^*, and $\bar{\lambda}^*$ in the TRA2 line and $\Delta\nu_f$ and $\Delta\nu_r$ in the RAMP line are multiplied. This factor allows the number of points N to be changed for a given airfoil design for which TRA1, TRA2, and RAMP lines already exist. If the final arc limit in the TRA1 line is N, then $N \times ABFA$ must still be divisible by 4.

Thus, the usual number of points $N = 60$, specified in the TRA1 line, can be changed to $N = 108$, for example, by setting $ABFA$ to 1.8. Note that, if the arc limits in the TRA1 lines were selected such that they fall midway between the points on the airfoil, this will no longer be true if $ABFA \neq 1$. The value of $ABFA$ must not be so large that the total number of points exceeds 120.

$EPSPA$ specifies ϵ in the panel method, where the subpanelling is a function of ϵ. As ϵ decreases, more subpanels are used when the induced velocity is computed at a point located very close to the panel.

All four values, mpr, NPG, $ABFA$, and ϵ, remain in effect until the next ABSZ line is read. Thus, a new ABSZ line with $F_2 = 1$ resets $ABFA$ to its default value.

4 Potential-Flow Airfoil Analysis

The potential-flow analysis method requires only a set of airfoil coordinates, which can come from the design method or from the input. Because airfoil coordinates do not conveniently fit into the format used for all the other input lines, they are read by a separate subroutine FIXLES, which is called when an FXPR line is read. This subroutine reads or generates the coordinates and writes them into blank COMMON arrays X(121) and Y(121) in the appropriate sequence (i.e., from the trailing edge forward along the upper surface, around the leading edge, and back along the lower surface to the trailing edge). The number of points $NQ \leq 121$ is stored in the blank COMMON variable NQ.

Once the coordinates are available, the slope of the upper surface δ_{us} near the trailing edge is written into variable DLT in COMMON/PRAL/; the lower-surface slope δ_{ls}, into DLTU. These slopes are defined such that, for symmetric airfoils, $\delta_{ls} = \delta_{us}$. Because many airfoils are not very smooth in the region surrounding the trailing edge, a point (x_i, y_i) on the upper surface and a point (x_j, y_j) on the lower surface are selected such that $x_i/c \approx 0.9$ and $x_j/c \approx 0.9$. Then

$$\delta_{us} = y_i/(c - x_i) \qquad \text{and} \qquad \delta_{ls} = -y_j/(c - x_j)$$

are set. These values are used when the lift and pitching-moment coefficients are corrected for boundary-layer separation effects.

Once all these values have been provided by Subroutine FIXLES, the panel method is invoked. Arrays X(121) and Y(121) are not changed. The resulting vorticities, which, in the present notation are identical to the velocities, for $\alpha = 0°$ and $\alpha = 90°$ are stored in arrays VF(121) and ARG(121), respectively. Thus, all the data are available to function VPR, which computes the velocity at every airfoil point for every angle of attack.

4.1 FXPR Line

The FXPR line specifies the print mode mpa for the results of Subroutine PANEL, how the airfoil coordinates are provided from the subsequent lines, and an option for inserting additional points along a spline fit of the original airfoil points.

If *NUPA* = 0, the print mode mpa remains unchanged; the default value is 1.

If *NUPA* $\neq$ 0, $mpa =$ *NUPE*, where

$mpa = 0$ suppresses the listing,

$mpa = 1$ or 2 lists only the headline containing the lift coefficients for $0°$ and $90°$ angle of attack and the zero-lift angle, and

$mpa \geq 3$ lists the headline plus the coordinates, the vorticities for $0°$ and $90°$ angle of attack, and the surface slopes.

NUPI controls a coordinate transformation after which the leading edge is at $x = 0$, $y = 0$ and the tangent at this point is vertical. The trailing edge (i.e., the midpoint between the two trailing-edge points) is transformed into $x/c = 1$, $y = 0$. The transformation generates a new leading-edge point for all nonsymmetrical NACA and Wortmann airfoils, which increases the number of points NQ by 1.

If *NUPI* $= 0$, no transformation is performed.

If *NUPI* $\neq 0$, the transformation is performed after the coordinates are read and possibly smoothed.

NUPU $= N + 10S$, $(N, S \leq 9)$ IF $S > 0$, the coordinates are smoothed.

The value N controls the derivation of the airfoil coordinates from the subsequent line or lines. A summary of the options follows; the details are given in Chapter 4.1.3.

If $N = 0$ or 1, the ordinates (i.e., y/c) of a Wortmann airfoil are read; the abscissas (i.e., x/c) are computed.

If $N = 2$, arbitrary coordinates x_i/c and y_i/c are read.

If $N = 3$, the upper-surface coordinates of a symmetric NACA 6-series airfoil (i.e., thickness distribution) are read; the mean line and the coordinates of a cambered NACA 6-series airfoil are then computed.

If $N = 4$, the coordinates of an NACA 4-digit-series airfoil are computed.

If $N = 5$, the coordinates of an NACA 5-digit-series airfoil are computed.

If $N = 7$, a curve of the form

$$y_m = ax(c - x)^2 + bx^2(c - x)$$

is computed and the x-axis of a previously given airfoil is transformed into this curve, which yields additional camber.

If $N = 8$, the x-axis of a previously given airfoil is transformed into a circular arc.

If $N = 9$, the coordinates of a symmetric EXTRA airfoil, consisting of an ellipse and two straight lines, are computed.

The F-numbers F_i specify additional points to be splined in (see Chap. 4.1.2).

4.1.1 Coordinate Smoothing

The second digit S of *NUPU* in an FXPR line allows the coordinates, read from the subsequent lines, to be modified to eliminate irregularities. Wortmann and some other older airfoils require such smoothing. Two options are available. If $S \geq 1$ and $N = 1$, a mild smoothing is performed S times; $S = 3$ is sufficient for most airfoils. This option applies only to Wortmann airfoils. If $S \neq 0$ and $N \neq 1$, a different smoothing, based on a compensation spline, is performed once. (Wortmann airfoils can be smoothed using this routine if $N = 0$.) Both smoothing routines modify the airfoils as little as possible. The second routine initiates a coordinate transformation exactly as *NUPI* $\neq 0$

does. The first routine may result in a point $x = 0$, $y \neq 0$, even though all Wortmann airfoils already have a point at $x = 0$, $y = 0$. An example is given at the end of Chapter 5.6.

4.1.2 Insertion of Additional Points

The F-numbers in the FXPR line (and in the PAN and FLAP lines) specify additional points to be splined in between the original coordinates as read or generated following the FXPR line.

The F-numbers F_i are interpreted as $sab.c$, where s is an optional minus sign and a, b, and c may contain more than 1 digit each. (See example below.)

> If $ab = 0$, one point is inserted at $x/c = 0.c$ on the upper surface or on the lower surface, if s is a minus sign.
>
> If $ab \neq 0$, c contains only one digit. The number b contains two digits if $c = 4$ or 5 and only one digit otherwise. Then b new points are inserted between points a and $a + 1$. If s is a minus sign, b new points are inserted between points $NQ - a$ and $NQ - a + 1$, which specify the locations of the new points relative to the trailing edge. This is helpful if NQ has been changed since the design or coordinate input, for example, by the addition of points near the leading edge or a transformation of the coordinates. The new points are spaced equidistantly along the straight line between the two original points if $c \geq 5$. Otherwise, the points are spaced such that, in
>
> $$x/c = (1 + \cos\varphi)/2$$
>
> the differences between the angles φ corresponding to the new points are equal (i.e., equiangular spacing).

In previous data sets, no more than nine points could be splined in between two original points and usually $c = 00$ was used for equiangular spacing and $c = 99$, for equidistant spacing. Such data sets are still processed correctly.

The insertion of additional points frequently improves the accuracy of the results if portions of the airfoil have sparsely distributed points. Near the trailing edge, where the velocity changes rapidly, the new points should be spaced equiangularly.

This option must be exercised carefully, however. The indices of all the points in arrays X and Y falling after the inserted points are increased by the number of inserted points. The simplest way to avoid confusion is to specify the F-numbers with decreasing values of a. Thus, a in F_1 should be greater than a in F_2, which should be greater than a in F_3, and so on. The same is true if negative F_i are used for the lower surface.

For example, the NACA 6-series airfoils are defined by 26 points on each surface, which results in a total of 51 points, with the leading edge at point 26. (One of the two identical leading-edge points is omitted.) The points near the trailing edge (i.e., $x_1/c = 1.00$, $x_2/c \approx 0.95$, and $x_3/c \approx 0.90$) as well as those near the leading edge are too widely spaced to obtain accurate results from the panel method.

```
FXPR␣␣␣␣␣3␣502␣491␣261.9␣251.9␣21␣12
FXPR␣␣␣␣␣3␣-251.9␣-21␣-12␣251.9␣21␣12
FXPR␣␣␣␣␣3␣-2501.5␣-201.4␣-102.4␣2501.5␣201.4␣102.4
```

All three lines have the same effect. The second and third lines use the option of negative F_i. The third line uses two columns for b (i.e., two digits), which is not necessary in this example. The last

two lines also function correctly if a new point was inserted at the leading edge using *NUPI* $\neq 0$; the first line would have to be changed in this case.

In this example, two points are inserted on each surface between $x/c = 0.95$ and 1.00 in the equiangular spacing mode; one point, on each surface between $x/c = 0.90$ and 0.95 in the equiangular spacing mode; and one point, between the leading edge and the first point on each surface in the equidistant spacing mode. Thus, a total of eight points is inserted.

Another example is given in the next section under the specification of Wortmann airfoils.

4.1.3 Input of Coordinates

Subroutine FIXLES delivers the coordinates of an airfoil to be analyzed. In the FXPR line, *NUPU* specifies the option. The line after the FXPR line is always required. It contains the airfoil name (up to 12 characters) followed by two spaces and then one DLFF sentence containing NQ, A, R, and T. The airfoil name is always read and written in the listing; the numbers NQ, A, R, and T are not always used. If one of the DLFF words is specified, all preceding words must be given, even if they are not used. The words following the last, specified word may be omitted.

If *NUPU* ≥ 4, the FXPR line and the succeeding line contain everything necessary to compute the corresponding coordinates. If *NUPU* ≤ 3, additional information, specified in subsequent lines, is required.

Wortmann Airfoils

If *NUPU* $= 0$ or 1 (optionally, $+ 10S$, where $S < 10$), Wortmann (FX) airfoils are specified. NQ, R, and T are ignored; A specifies a modification factor THF.

Only the ordinates (i.e., y/c) must be given in the succeeding lines, beginning at the trailing edge as presented in reference [7]. The abscissas (i.e., x/c) are computed in Subroutine FIXLES. The various formats of the succeeding lines containing the ordinates are described in the Chapter 4.1.4.

In reference [7], two sizes of coordinate sets are presented: one with 49 points on each surface, the other with 44. In the latter case, several points near the trailing edge have been omitted. Accordingly, the code counts the number of input points and then computes the corresponding x/c values. In the former case, the airfoil is defined by 97 points; in the latter, by 87. (The leading-edge point is included on both surfaces in reference [7], whereas only one point is required in the code.)

In the latter case, which has only 44 input points, the spacing of the points is not very suitable for the panel method. It is recommended that the points omitted in reference [7] be splined back in. This is accomplished by the following FXPR line. (See Chap. 4.1.2.)

```
FXPR␣␣␣␣␣1␣851␣841␣831␣821␣811␣61␣51␣41␣31␣21
FXPR␣␣␣␣␣1␣-61␣-51␣-41␣-31␣-21␣61␣51␣41␣31␣21
```

Both lines insert the same points.

There is one more option available for Wortmann airfoils. Although not recommended, the thickness and the camber of Wortmann airfoils can be modified. To accomplish this, A is used as a factor THF.

If $THF > 0$, the thickness distribution is multiplied by THF without changing the mean line.

If $THF < 0$, all y/c values are multiplied by $-THF$. Thus, the y/c values of the mean line are also modified.

For example,

```
FXPR␣␣␣␣31
FX␣63-126␣␣0␣-.9235
```

These two lines invoke the first smoothing routine (see Chap. 4.1.1) and multiply all the y/c values by 0.9235.

Input of x/c and y/c for All Points

If *NUPU* = 2, the x/c and y/c values for all points must be specified.

NQ is ignored. (The number of points is determined from the input coordinates.)

If $A \neq 0$, all the x/c and y/c values are divided by the larger of X(1) and X(NQ) (i.e., the more aft trailing-edge point). This normalization of the coordinates is not necessary if the x and y values are already in the form x/c and y/c, where c is the chord.

R and T are ignored.

This is the most general coordinate-reading option. A total of NQ points are defined, each one by x_i and y_i. The points can be specified in two different sequences. Both trailing-edge points, even if identical, must be given. If they are not identical, the panel method will invoke a wake model. The details of the sequences and the format of the coordinate lines are described in Chapter 4.1.4.

NACA 6-Series Airfoils

If *NUPU* = 3, an NACA 6-series airfoil (ref. [8]) is specified.

Only the thickness distribution is given; the mean line and its slope are computed.

NQ is ignored. (The number of points is determined from the input coordinates.)

A, R, and T specify the NACA 6-series mean line and a thickness ratio, where

$A = a$, which is the extent of the constant vorticity along the mean line (i.e., the point where the vorticity begins to linearly decrease).

$R = c_{\ell_i}$, which is the design lift coefficient, which determines the amount of camber.

T = thickness factor; normally, $T = 1$.

The succeeding lines contain the coordinates of the upper surface of a symmetrical NACA 6-series airfoil, from the leading edge to the trailing edge, as presented in reference [8]. The number of airfoil points NQ depends on the number of points for the symmetrical airfoil, which is determined from the input. The format of the succeeding coordinate lines is described in Chapter 4.1.4.

It should be noted that the spacing of the points, as given in reference [8], is not very suitable for the panel method. The option for splining in additional points should be exercised, not only near the trailing edge but also near the leading edge. An appropriate example is given in Chapter 4.1.2.

NACA 4-Digit-Series Airfoils

If *NUPU* = 4, an NACA 4-digit-series airfoil (ref. [9]) is specified.

The airfoil name (e.g., NACA 4415) is given in columns 1–9, followed by two spaces, and then the total number of points NQ to be computed.

A, R, and T are ignored.

No other lines are required. The necessary airfoil parameters (see ref. [9]) are derived from the airfoil number given in columns 6–9.

NACA 5-Digit-Series Airfoils

If *NUPU* = 5, an NACA 5-digit-series airfoil (ref. [10]) is specified.

The airfoil name (e.g., NACA 23012) is given in columns 1–10, followed by two spaces, and then the total number of points NQ to be computed.

A, R, and T are ignored.

No other lines are required. The necessary airfoil parameters (see ref. [10]) are derived from the airfoil number given in columns 6–10.

The NACA 5-digit-series airfoils having reflexed mean lines (i.e., the third digit is 1) cannot be generated. For these airfoils, the general coordinate-reading option (i.e., *NUPU* = 2) must be used.

It should be noted that the coordinates presented in references [8] and [10] for the NACA 5-digit-series airfoils contain minor inaccuracies and, therefore, small discrepancies between the previously published coordinates and those generated by the code are possible.

Transformation Using Third-Degree Polynomial Line

If *NUPU* = 7, the x-axis of a given airfoil is transformed into a third-degree polynomial curve of the form

$$y_m = ax(c-x)^2 + bx^2(c-x)$$

The boundary conditions are

$$y_m(0) = y_m(c) = 0 \qquad y'_m(0) = A \qquad y'_m(c) = -R,$$

where c = chord, and T is ignored.

The original airfoil must have been specified before the FXPR line with *NUPU* = 7 is read. Non-symmetrical airfoils can also be modified using this option. Each point x_n, y_n of the original airfoil is modified as follows. First, the point $y_m(x_n)$ on the mean line $y_m(x)$ is computed. Then, the new point is located perpendicular to the tangent of the curve $y_m(x)$ at x_n. The distance to $y_m(x)$ is y_n.

Transformation Using Circular Arc

If *NUPU* = 8, the x-axis of a given airfoil is transformed into a circular arc. The only diffenence between this option and the preceding one is that the new curve $y_m(x)$ is now a circular arc through $x = 0$ and $x = c$, with a slope at $x = 0$ of A degrees. This option is normally only used for cascades.

EXTRA Airfoils

If *NUPU* = 9, a symmetrical EXTRA airfoil is specified.

These symmetric airfoils for aerobatic aircraft are defined by an ellipse and two straight lines.

NQ is the total number of points to be computed.

$A = a/c$, which is the length of the half axis of the ellipse, in percent chord. (This is also the x value of the maximum thickness.)

$R = h/c$, which is the thickness of the trailing edge, in percent chord.

$T = t/c$, which is the airfoil thickness, in percent chord.

A typical EXTRA airfoil with its input are given in Fig. 5

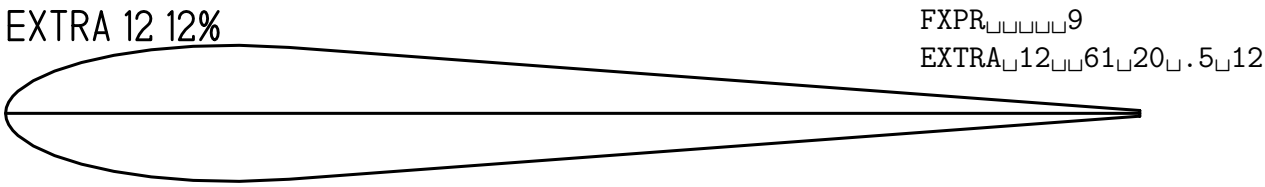

Figure 5: EXTRA airfoil having 12-percent-chord thickness at $x/c = 0.2$.

4.1.4 Coordinate Lines

Only the options specified by *NUPU* = 0–3 require succeeding lines containing coordinates. Wortmann airfoils (i.e., *NUPU* = 0 or 1) are specified by pairs of ordinates $(y/c)_{us}$ and $(y/c)_{ls}$ for which x/c values are computed by the code. The airfoils defined by arbitrary coordinates (i.e., *NUPU* = 2) are specified by one pair of coordinates x_n and y_n for each point. The thickness distributions of NACA 6-series airfoils (i.e., *NUPU* = 3) are specified in the same way. Thus, pairs of numbers are specified in the input lines, which are read in the same way for all four options.

The coordinate lines contain one pair of numbers per line. The numbers must be separated by at least one space. The format of the first coordinate line is used to read all the succeeding coordinate lines.

The various options require different pairs as follows. If *NUPU* = 0 or 1 (i.e., Wortmann airfoils), each pair contains the ordinate y/c of the upper surface and the ordinate of the lower surface for one abscissa x/c. The pairs start at the trailing edge, as presented in reference [7]. The total number of points NQ is determined from the input. If *NUPU* = 2, the pairs can be input in two different sequences: the normal sequence used in the code (i.e., from the trailing edge forward along the upper surface, around the leading edge, and then back along the lower surface to the trailing edge) or from the leading edge to the trailing edge on the upper surface and then from the leading edge to the trailing edge on the lower surface. The code reorders the latter into the normal sequence.

If *NUPU* = 3, the pairs start at the leading edge, as presented in reference [8].

4.2 PAN Line

The PAN line switches from the design to the analysis mode and, therefore, is required if the panel method is to be employed following a design (i.e., TRA1 and TRA2 lines). The PAN line contains the same options for the print mode and the insertion of points as does the FXPR line. A cascade can also be defined in a PAN line.

4.2.1 Switching from Design to Analysis Mode

If 0 *NUPA* = 0–8, *NUPE* and *NUPA* together control the print modes (see "FXPR Line", Chap.4.1).

NUPI controls the coordinate transformation (see"FXPR Line", Chap. 4.1).

NUPU is ignored.

The F_i specify the additional points to be splined in (see"FXPR Line", Chap. 4.1).

4.2.2 Cascades

If *NUPA* = 9, the parameters of a cascade (fig. 6) are specified by F_1–F_4, where

$F_1 = \Delta x/c$;

$F_2 = \Delta y/c$;

$F_3 = n_c$, which is the number of cascade members; and

$F_4 = c$, which is the chord in mm.

If $F_4 \neq 0$, a diagram (e.g., fig. 6) is produced in which the current airfoil is plotted twice with the chord specified by F_4. The horizontal and vertical distances between the two airfoils are $\Delta x/c$ and $\Delta y/c$, respectively.

The distance between the cascade members is defined by $\Delta x/c$ and $\Delta y/c$, as shown in figure 6. A

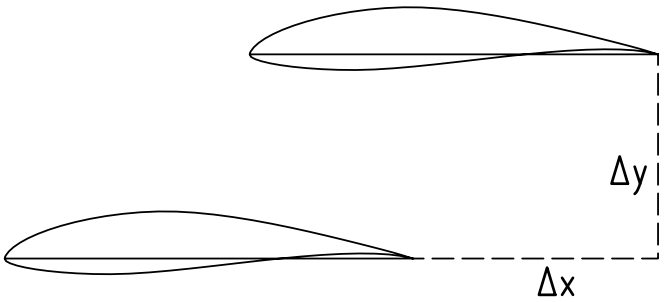

Figure 6: Cascade parameters.

finite number of cascade members must be specified by F_3. A PAN line with *NUPA* = 9 merely stores the cascade parameters and does not invoke the panel method, which must be done by another PAN line with *NUPA* < 9.

The computation of cascades is a generalization of the panel method. When an individual airfoil is analyzed, vorticity distributions are placed along the surface of the airfoil. The distributions are determined such that the flow conditions on the airfoil surface are satisfied. When a cascade of airfoils is analyzed, the vorticity distributions must be placed on all members of the cascade and the amount of vorticity is again determined from the flow conditions on the surface of each member. A cascade is usually assumed to have an infinite number of members, in which case, the flow conditions are satisfied on all members if they are satisfied on one member.

For infinite cascades, a higher-order panel method cannot be developed with closed formulas. This is only possible with simple low-order panel methods. To maintain higher-order precision, the cascade members are treated exactly by the higher-order method used for the single airfoil. If the cascade has narrow gaps between the members, the higher-order method is necessary to provide adequate precision. Because it is not possible to have an infinite number of members and a higher-order panel method, the number of members must be specified. If the number of cascade members n_c is 15, a good approximation to an infinite cascade results. An odd number of cascade members is recommended because the airfoil under consideration is then in the middle of the cascade.

The convergence of the method can be checked by comparing two solutions for the cascade having the same airfoil but different numbers of members. The most sensitive result is the second value of c_ℓ in the listing from Subroutine PANEL. This c_ℓ value, for $\alpha = 90^\circ$, is equal to the lift-curve slope of the airfoil according to potential-flow theory.

The cascade parameters remain unchanged until a new PAN line with *NUPA* $= 9$ is read.

The following input generates figure 6 as well as the velocity distributions for the SH8 airfoil at an angle of attack of 9° relative to the zero-lift line shown in figure 7. The number of cascade members n_c is 15 and the distance between the members is $\Delta x/c = 0.5$ and $\Delta y/c = 1.0$.

```
REMO1              *P@RTEST @1CASCADE @1OPTION   FIGS. 6+5
TRA1     8 27.5 10 29.5 11 0 12 60 4
TRA26    8 4 17.5 2 -1 .7 4 17.5 2 -1 .7 6 0 0
ALFA     2 4 9
DIAG     1          1 .5 4 1 -.2 1 -2 .3 3 2 -.4 4
PAN 9      .5 .7 15
PAN
ALFA
DIAG     2          1 .05 1 1 -.6 2 2 .05 1 2 -.2 2  *1C  *2C  *3C  *4C
REMO1                    *P
PAN 9      .6 .5 3 90
ENDE
```

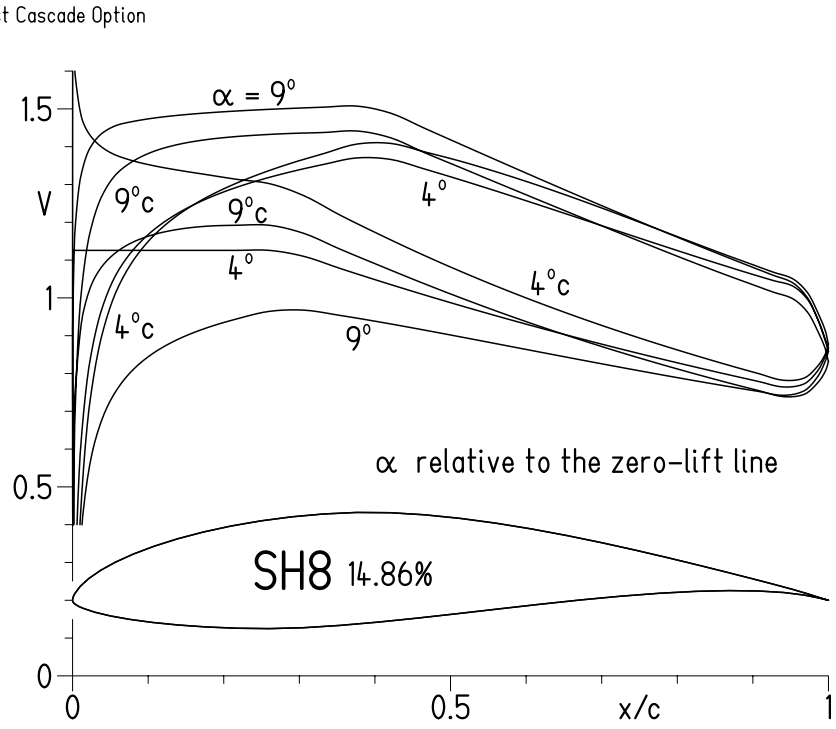

Figure 7: Velocity distributions for SH8 airfoil alone and in a cascade having 15 members (denoted by "c").

5 Options for Both Design and Analysis Modes

After defining an airfoil, in either the design or analysis mode, several options are available for additional printed and plotted output. All the options are independent of the mode (design or analysis) in which the airfoil was defined.

5.1 STRD Line

The STRD line prepares the data for plotting airfoils having various chords.

NUPA is ignored.

NUPE and *NUPI* together form the number $nn = 10$*NUPE* + *NUPI*, which is the number of the output file containing an augmented set of coordinates (see "STRK Line", Chap. 5.2). The default value of nn is 0.

NUPU is the plot mode mxz for subsequent plotting initiated by STRK lines.

If *NUPU* $\neq 0$, $mxz =$ *NUPU*.

If $mxz > 0$, the x-axis is plotted.

If $mxz < 0$, the x-axis is not plotted.

If *NUPU* $= 0$, mxz remains as previously set. The default value is 0.

$100F_1 = YBL$, where $|YBL|$ is the height of the diagram in mm. The sign of YBL determines the interpretation of F_2.

$100F_2 = RUA$, where,

if $YBL < 0$, RUA is the vertical distance in mm between the chord line of one airfoil and that of the next; and,

if $YBL > 0$, RUA is the vertical distance in mm between the upper surface of one airfoil and the lower surface of the next.

$F_3 = SILAFA$, which is a scale factor for the label inserted above the leading edge of each airfoil. The label contains the name of the airfoil and the thickness. The label height is $SILAFA$ times the airfoil chord. The airfoil name can be specified as in other diagrams. The default value of $SILAFA$ is 0.008, which is suitable for chords greater than 400 mm. The value of $SILAFA$ remains in effect until a new value is specified. If $SILAFA < 0$, no label is plotted.

F_4 specifies the line width. The default value is the value $PENLI$, which can be specified in the REMO line (Chap. 2.2.2). The default value of $PENLI$ is 0.4 mm.

5.2 STRK Line

The STRK line initiates a diagram and a listing of the airfoil coordinates generated by the preceding TRA1 and TRA2 lines or FXPR line for various chords. An STRK line must be preceded by an STRD line.

If *NUPA* $\neq 0$, an augmented set of coordinates for each chord is listed. Each airfoil diagram increases nn by 1 and then opens a new file LASnn.NCC. Such files can be used for numerically-controlled milling machines, for example. The coordinates are spaced such that the straight line from one point to the next deviates from the spline fit through the points by less than a constant times 2^{-NUPA}. Thus, the number of coordinates listed increases with *NUPA*. The value of *NUPA* is not stored; it must always be specified in the STRK line that initiates the diagram.

If *NUPE* $\neq 0$, the points resulting from the design or analysis mode are identified by symbols. The value of *NUPE* specifies the symbol and is valid for only one plot. Only symbols 1–9 (see fig. 12) can

be specified because *NUPE* has only one digit. In this case, *NUPE* = 9 specifies symbol 10 instead of symbol 9. Figure 2, which shows the additional points near the leading edge, was produced using this option with *NUPE* = 9.

If *NUPI* $\neq$ 0, the listing is produced but the diagram is suppressed.

If *NUPI* = 0, both the listing and the diagram are produced.

If *NUPU* = 1–999, the $|F_i|$ specify up to 22 chords c_i in mm, which are used for both the listing and the diagram (if *NUPI* = 0). If $F_i < 0$, any open diagram is terminated before the diagram containing the airfoil having chord c_i is opened. If $F_i > 0$, the airfoil with chord c_i is plotted in the diagram that is open to further plotting. If no diagram is open or if the open diagram does not contain sufficient vertical space, a new diagram is opened before the airfoil with chord c_i is plotted. Any airfoil having a chord $c_i < 1$ mm is not plotted. Thus, the diagram is terminated by -1 mm $< c_i < 0$.

If *NUPU* = 0, the chords from the preceding STRK line are used.

If *NUPU* = 999, the F_i are the x/c locations x_{le} of the leading edges of the airfoils in the next STRK line with *NUPU* $\neq$ 999. Negative x_{le} are permitted. The default value of x_{le} is 0.

The trailing edge $c + x_{le}$ of the first airfoil to be plotted in a diagram determines the width of the diagram. The width can also be set by a positive x_{le} and $c < 1$ mm, in which case, the airfoil that determines the width is not plotted. The plots that exceed the width of the diagram are merely truncated (i.e., clipped). This applies to the leading edge, if $x_{le} < 0$ is specified, and to the trailing edge, if the chord exceeds the width of the diagram.

If the leading-edge locations are not alterred by a preceding line with *NUPU* = 999, the largest chord should be given first, if all the other airfoils are to be plotted in their entirety.

If only the leading-edge region is to be plotted to a large scale, a normal width is specified for the first airfoil. The second airfoil is specified with a very large chord. Everything aft of the leading-edge region is thus truncated. Figure 2 was produced using this option as well.

If only the trailing-edge region is to be plotted to a large scale, the first airfoil is specified with $x_{le} \ll 0$ and a chord c that corresponds to the available paper size s (i.e., $c = s - x_{le}$).

Other regions (e.g., the flap hinge) can also be plotted to a large scale. First, the width of the plot is specified and then the airfoil with large c and $x_{le} < 0$, such that the desired region falls within the diagram.

The following example plots two different airfoils in one diagram.

```
TRA1 and TRA2 lines (first airfoil)
STRD     1 500 5
STRK     1 500
TRA1 and TRA2 lines (second airfoil)
STRK     1 500 -0.5
```

Both airfoils have a chord of 500 mm and are separated vertically by 5 mm. The chord lines of both airfoils are plotted and the diagram is terminated by the second STRK line. If the second STRK line had specified *NUPU* = 0, the chord from the preceding STRK line would have been used and the diagram would have remained open to further plotting.

The following example produces the diagrams shown in figure 8.

```
REMO1              *P@1@RE@2XAMPLE OF AIRFOIL PLOT
TRA1     1 28.5 3 0 10 60 2
TRA24    1 4 18.5 2 -1 .7 4 18.5 2 -1 .7 6 .3 0
STRD    -1 32 5 -1 .15
STRK     2 150 100 -.1
STRD     1 -62 14 .016 .15
STRK     2 150 140      *NSUPER X
TRA1     2 27.5 5 0 10 60 5
TRA24    2 4 18.5 2 -1 .7 4 18.5 2 -1 .7 6 .3 0
STRK     1 150 140 -.1     *NSUPER Y
```

The first diagram (fig. 8) contains only the first airfoil with two chords, 150 and 100 mm, and is closed by the chord of -0.1 mm, which is not plotted. The vertical distance between the airfoils is 1 mm and the x-axis and the labelling of the airfoils are suppressed by *NUPU* $= -1$ and $F_3 = -1$ in the STRD line. The line width is set to 0.15 mm by F_4 in the STRD line. Only the labelling specified in the REMO line is plotted.

The second STRD line, with *NUPU* $= 1$ and $F_3 = 0.016$, initiates the second diagram (fig. **??**),

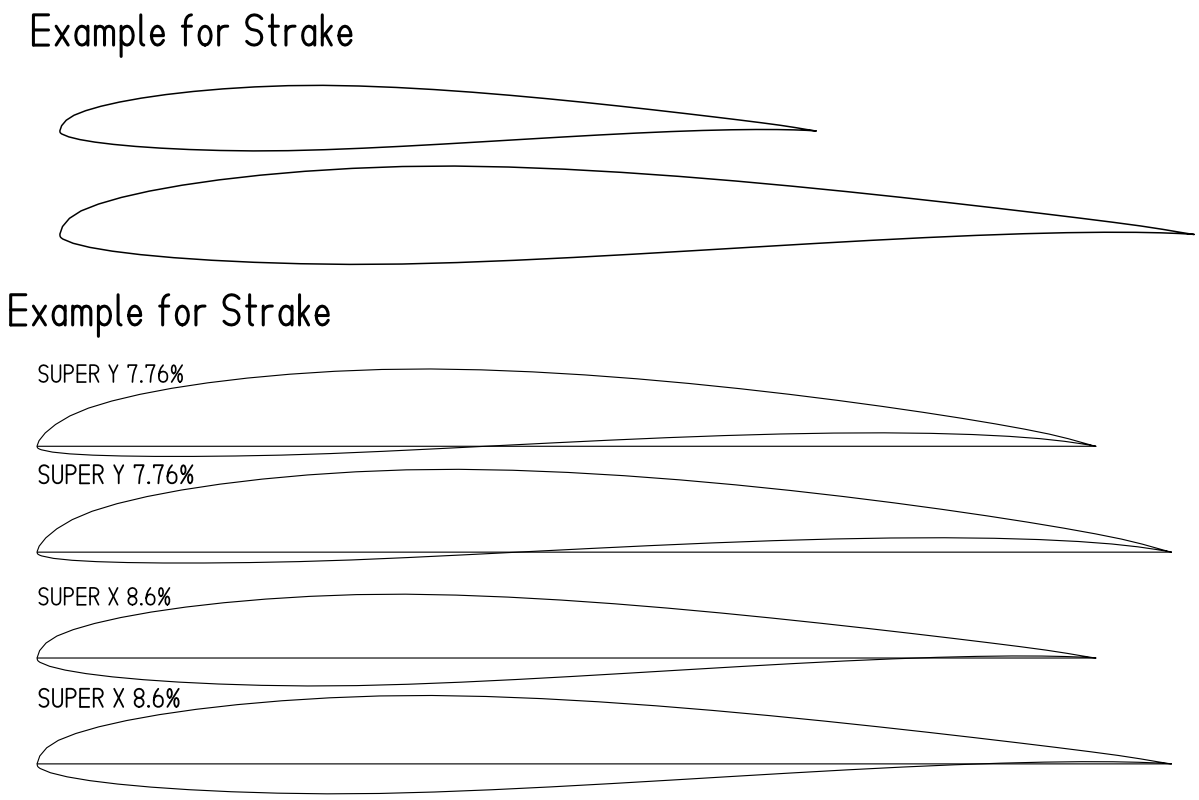

Figure 8: Two diagrams from example for STRD and STRK lines.

which contains the x-axis and the labels. The distance between the chord lines is 14 mm. The succeeding STRK line plots the airfoil with chords of 150 and 140 mm and leaves the diagram open to further plotting. The name of the first airfoil is set to "SUPER X". Then, a second airfoil is computed and plotted with chords of 150 and 140 mm, its name is set to "SUPER Y", and the diagram is closed. Note that the second STRD line is valid for more than one STRK line.

5.3 MACH Line

The MACH line initiates two runs of the panel method; the first one, with the original coordinates of the airfoil, and the second one, with a new set of coordinates in which the ordinates y/c are multiplied by the factor $\beta = \sqrt{1 - M^2}$.

Following a MACH line, all velocity and pressure computations consider the compressibility effects according to the method of reference [11], including the listing of the velocity or pressure distributions after an ALFA line, the plot of the velocity or pressure distributions after a DIAG line, and all boundary-layer computations.

NUPA, *NUPE*, *NUPI*, and *NUPU* are ignored.

$F_1 = M$, which is the Mach number. The default value is 0.

Contrary to several other lines (e.g., ALFA, RE , FLZW, and PLW), the input from which remains in effect until replaced by that from a new line of the same type, the MACH line remains in effect only until a new airfoil is defined by TRA1 and TRA2 lines or by an FXPR line and the corresponding coordinate lines. After either of these line sequences, the Mach number is reset to 0 and another MACH line is required if the new airfoil is to be computed with $M \neq 0$.

It is not necessary to insert the MACH line immediately after the definition of an airfoil. Thus, it is possible to evaluate the differences between the incompressible and compressible flows.

The following example (fig. 9) plots a diagram containing two velocity distributions for one airfoil: the first is incompressible; the second, compressible, with $M = 0.55$. (Note that some of the labels are not specified by the example input.) The diagram includes the sonic limit if it is near the maximum velocity on the airfoil. The Mach number M and the value $Mc_\ell{}^2$ for the last α are also plotted. The compressibility correction is invalid if the sonic limit is exceeded.

```
TRA1, TRA2 lines
ALFA     2 3 8
DIAG     1
MACH       .55
ALFA
DIAG     2
```

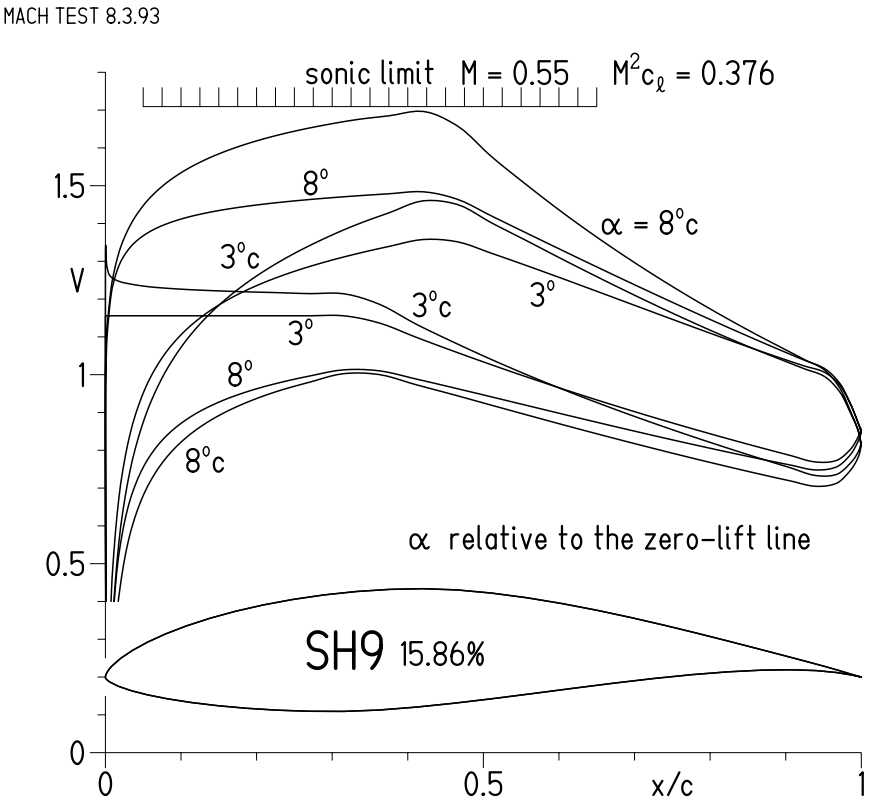

Figure 9: Velocity distributions for SH9 airfoil at $M = 0$ and $M = 0.55$ (identified by "c").

5.4 FLAP Line

The FLAP line exercises four options. First, the shape of an airfoil can be altered to correspond to that due to the deflection of a simple flap. Because the panel method does not allow sharp corners in the airfoil surface, a transition arc between the flap and the forward portion of the airfoil must be introduced. Such a transition arc occurs 'naturally' on the convex side of a real wing, but not on the concave side, where a corner is formed. This concave corner, however, is 'smoothed' by a locally separated region and, therefore, it is reasonable to introduce a transition arc there as well. This option is initiated by *NUPU* = 0.

The second option allows the analysis of chord-increasing flaps. It should be noted that, while the airfoil shape that results from this variable-geometry option may have an increased chord, it does not contain a slot and, thus, is still a single-element as opposed to a multielement airfoil. This option is initiated by *NUPU* = 1–5.

The third option, specified by *NUPA* $\neq$ 0, allows the modification of single points on the airfoil.

The fourth option, specified by *NUPI* $\neq$ 0, concerns only the reference point for the hinge moment.

For all options that modify the shape of an airfoil,

if *NUPE* $\geq$ 8, the modified airfoil replaces the original one. In this case, the original airfoil is completely lost and the new (modified) one can be further modified by additional FLAP lines. In this way, it is possible, for example, to introduce a secondary flap, such as a Flettner flap, or to introduce a flap on an airfoil after having modified its shape using the variable-geometry option. If another FLAP line is inserted after a FLAP line with *NUPE* $<$ 8, a new modification of the old (original) airfoil will be initiated, whereas inserting another FLAP line after a FLAP line with *NUPE* $\geq$ 8 will cause the shape as resulting from the first FLAP line to be modified.

If *NUPE* = 9, the thickness of the modified airfoil relative to its chord is evaluated. The new thickness replaces the thickness of the original airfoil. For example, the deflection of a simple flap changes the relative thickness because the airfoil chord changes.

If *NUPE* = 8, the evaluation of the new thickness is not performed and the thickness remains unchanged. This is common practice in the case of simple flaps.

The panel method is invoked automatically after a FLAP line with *NUPU* = 0, 4, or 5 or *NUPA* $\neq$ 0.

Note that the number of points may be increased by FLAP lines. The maximum number of points on the original airfoil must be no more than 121. The panel method can accommodate up to 129 points. The modification of an airfoil with 121 points by a FLAP line with *NUPU* = 0 (i.e., a simple flap) is, therefore, possible. The variable-geometry option is also allowed to increase the number of points up to 129. A modification that yields more than 129 points, however, causes the code to stop.

5.4.1 Simple Flap

If *NUPU* = 0, the airfoil shape is modified to simulate the deflection of a simple flap.

NUPA must be zero.

F_1 specifies the length of the flap in percent chord.

F_2 specifies the vertical location of the flap hinge in percent chord.

Thus, the flap hinge point is located at $x_h/c = 1 - 0.01F_1$ and $y_h/c = 0.01F_2$.

F_3 specifies one half the transition arc length s_T/c in percent chord for the upper surface. Typically, $s_T/c =$ 0.04–0.06, depending on the amount of flap deflection.

F_4 specifies the flap deflection δ_f in degrees, positive downward.

F_5 specifies one half the transition arc length s_T/c in percent chord for the lower surface. If $F_5 = 0$ or blank, the transition arc length for the upper surface is also used for the lower surface.

For example,

FLAP␣␣␣␣␣␣␣25␣2␣3␣10

which specifies a simple, 25-percent-chord flap with a downward deflection of 10°. The flap hinge is located vertically at $y/c = 0.02$ and the transition arc length is $s_T/c = 0.06$ for the upper surface as well as for the lower surface.

5.4.2 Variable Geometry

If *NUPU* = 1–5, the variable-geometry option is specified.

The points are renumbered during the execution of each of the following FLAP lines.

If *NUPU* = 1, points are deleted. The digits of the F-numbers are denoted

$$F_i = (-)aaa.bb$$

Points aaa to $aaa + bb$ are deleted. If $bb = 00$, only point aaa is deleted.

The points after point aaa are renumbered. If it is intended that aaa i always be the point number on the original airfoil, aaa of succeeding F_i must decrease. If the minus sign is given, aaa is replaced by $NQ - aaa$ and the points are deleted relative to point NQ, which is the last point. This is useful on the lower surface. All negative F_i must occur before positive ones. Only the first positive F_i may have a greater aaa than the last negative F_i.

For example,

FLAP␣␣␣␣␣1␣-8.08␣5␣2.01

which deletes points $NQ - 8$ through NQ, 5, and 2 and 3.

If *NUPU* = 2, points are inserted on the upper surface.

$F_1 = 100x_1/c$

$F_2 = 100y_1/c$

$(F_3,\ F_4) = (100x_2/c, 100y_2/c)$ and so on.

The new points are inserted in the correct sequence between or aft of the points remaining after the deletions resulting from the FLAP line with *NUPU* = 1. The sequence of the points to be inserted is arbitrary.

For example,

FLAP␣␣␣␣␣2␣120␣-5␣110␣-2

which inserts two points that extend the upper surface ($x/c = 1.10,\ y/c = -0.02$ and $x/c = 1.20,\ y/c = -0.05$).

If *NUPU* = 3, points are inserted on the lower surface.

For example,

FLAP␣␣␣␣␣3␣100␣-2.5␣120␣-5

which inserts two points that extend the lower surface ($x/c = 1.00,\ y/c = -0.0250$ and $x/c = 1.2000,\ y/c = -0.0500$).

Normally, some points must be deleted by a FLAP line with *NUPU* = 1 before new points are inserted.

If *NUPU* = 4 or 5, additional points are splined in. The F-numbers are interpreted just as they are for the FXPR line, including the option of negative F_i.

$$F_i = (-)aab.dd$$

If *NUPU* = 5, in addition to the splining in of points, a transformation is performed that rotates the modified airfoil around $x = 0$, $y = 0$ and stretches it so that the first point becomes $x/c = 1,\ y/c = 0$. The option *NUPE* = 9 can also be used.

Care must be exercised because deleting points (i.e., *NUPU* = 1) as well as inserting new points (i.e., *NUPU* = 2 or 3) changes the sequence numbers of the points and the total number of points NQ. For splining in additional points, the alterred point numbers must be taken into account. An example is given in figure 10.

For example,

FLAP␣␣␣␣␣4␣-24␣-16␣22␣13

which inserts a total of 15 points, all with equiangular spacing: four points between points $NQ - 2$ and $NQ - 1$, six points between points $NQ - 1$ and NQ, two points between points 2 and 3, and three points between points 1 and 2.

The application of the four FLAP lines given in this section to an NACA 23015 airfoil, defined originally by 61 points, is shown in figure 11. The following steps occur.

The original upper surface is maintained up to the original trailing edge, although some points near the original trailing edge are deleted because the close spacing there is no longer necessary although it is near the new trailing edge ($x/c = 1.20,\ y/c = -0.05$), as described below.

On the lower surface, points $NQ - 8$ through NQ are deleted, which includes the lower-surface, trailing-edge point.

On the upper surface, two points are inserted at $x/c = 1.10$ and $x/c = 1.20$. Two points are splined in between the original trailing edge and the new point at $x/c = 1.10$; three points, between $x/c = 1.10$ and $x/c = 1.20$.

On the lower surface, the last point of the original airfoil that was not deleted is near $x/c = 0.84$. Its number is 51, after the deletion of three points and insertion of two on the upper surface. Aft of that point, only two points are inserted: one at $x/c = 1.00$ (number 52 or $NQ - 1$) and the other at $x/c = 1.20$ (number 53 or NQ). The distances between these points as well as between the last point on the original airfoil and the first inserted point are larger than those on the upper surface. Therefore, four and six points, respectively, are splined in using negative F_i. This procedure does not require knowledge of the absolute point numbers and still functions properly if, for example, the transformation (i.e., *NUPI* = 1) that produces the vertical tangent at $x = 0$, $y = 0$ is performed by the FXPR line (see Chap. 4.1). This is actually performed in this example.

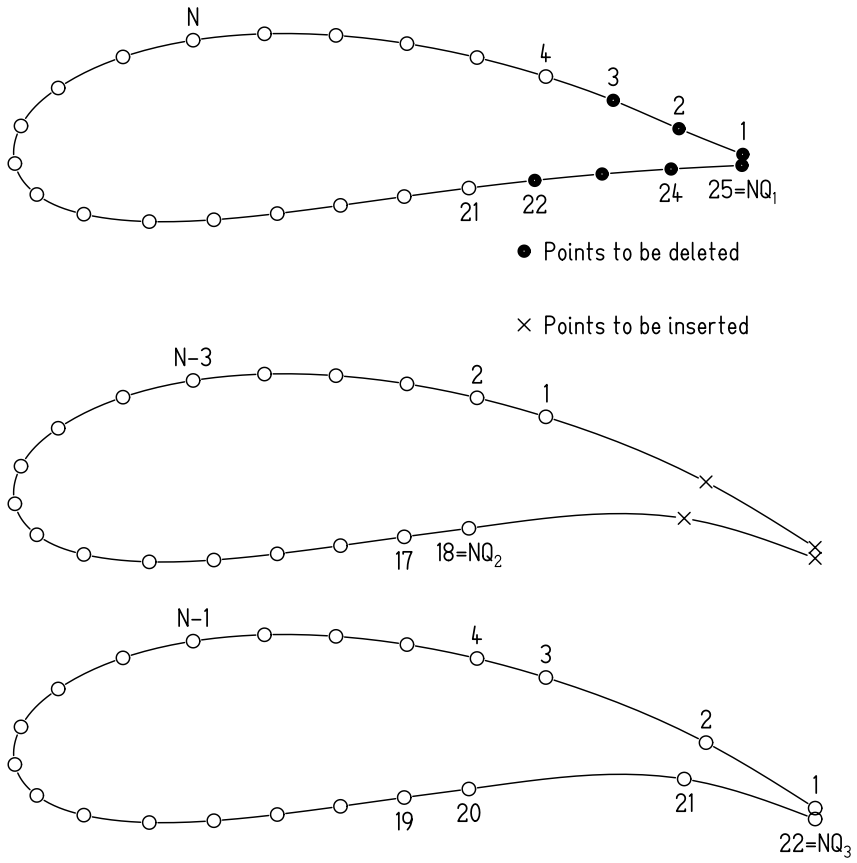

Original point numbers (before deleting points by FLAP line with *NUPU* = 1)

Point numbers after deleting points by FLAP line with *NUPU* = 1 and before inserting points by FLAP lines with *NUPU* = 2 and 3.

Point numbers after inserting points by FLAP lines with *NUPU* = 2 and 3.

Figure 10: Alteration of airfoil point numbers during exercise of variable-geometry option.

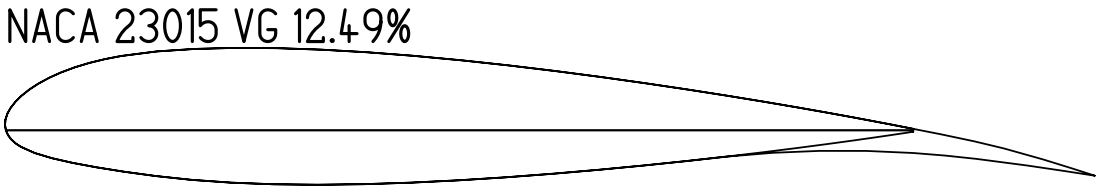

Figure 11: NACA 23015 airfoil with and without variable-geometry modification.

5.4.3 Modification of Individual Points

If *NUPA* $\neq$ 0, individual points are modified.

NUPE, *NUPI*, and *NUPU* are ignored.

$F_1 = n_i$, which is the point number, the ordinate y/c of which is changed by F_2.

F_2 is the vertical component of the change perpendicular to the surface in percent chord. Positive F_2 denotes a change toward the exterior of the airfoil (i.e., a bump); negative F_2, a change toward the interior (i.e., a dip).

(F_3, F_4) and so on allow six more points to be modified.

For example,

```
FLAP19␣␣␣␣␣3␣.01␣37␣-.01
```

which moves point number 3 toward the exterior of the airfoil by 0.01-percent chord and point number 37 toward the interior by the same amount. The modified airfoil replaces the original one because *NUPE* = 9.

5.4.4 Moment Reference Points

The ALFA line invokes Subroutine MOMENT, which computes the pitching-moment and hinge-moment coefficients c_m and c_h, respectively, for each angle of attack. The reference point for c_m is normally the quarter-chord point and, for c_h, the leading edge. The coefficients are stored so they are available for other (e.g., boundary-layer) computations. Depending on the print mode mcm, the coefficients can be listed immediately after they are computed. A FLAP line with *NUPU* = 0 automatically shifts the reference point for c_h to the flap hinge point. The computation of c_h is performed such that only that portion of the airfoil aft of the reference point contributes to c_h. The hinge-moment coefficient c_h is nondimensionalized by the airfoil chord, not by the flap chord. This works properly only if the coordinates are not normalized by a FXPR or PAN line with *NUPI* $\neq$ 0.

Occasionally, moments relative to other reference points must be computed, which can be accomplished by means of a FLAP line with *NUPI* $\neq$ 0.

NUPA, *NUPE*, and *NUPU* are ignored.

If *NUPI* = 1, the reference point for both c_m and c_h is shifted to

$$x/c = 0.01F_1 \qquad y/c = 0.01F_2$$

If *NUPI* = 2, the reference point for both c_m and c_h is shifted to the point specified by F_1 and F_2 as with *NUPI* = 1 but the calculation of c_m excludes that portion of the airfoil forward of the reference point.

If *NUPI* $>$ 3, the F-numbers are ignored and the reference point for c_m is the flap hinge point. The calculation of c_m is performed as with *NUPI* = 2.

This FLAP line immediately initiates the computation of c_m and c_h about the new reference point for all α values in the currently valid ALFA line. Depending on the print mode specified in this ALFA line, a listing of the moment coefficients is produced, in which the reference point is given.

The option *NUPI* = 1 is useful in two specific cases. It can be used to determine the aerodynamic center, for which c_m is constant with α and the value of c_h can be used to evaluate the bending moment of ribs in a wing.

The options *NUPI* $>$ 3 are relevant only in conjunction with other FLAP lines because the values of c_m and c_h would otherwise be identical. These options can be exercised, however, after a FLAP line with *NUPE* = 9. Another FLAP line then allows another flap to be introduced and the moment relative to the previous reference point (e.g., the previous flap hinge point) to be computed. The authority of Flettner flaps or trim tabs can thus be analyzed.

The following input lines produce the listing below.

```
REMO1          *PLISTING CHAPTER FLAP-LINE
FXPR     4
NACA 0009          61    0    0   09
ALFA101003 -10 0 10
FLAP  1    26.148 0
ALFA
FLAP  2    40 0
ALFA
FLAP 9     25 0 3 5
ALFA101003 -10 0 10
FLAP  3
ALFA101003 -10 0 10
FLAP       8 -1.49 2 10
ALFA101003 -10 0 10
```

```
PANEL METHOD NACA 0009 9%   CL=-0.000000486, 6.74718 ALPHA0=-0.000004127 MACH=0

Airfoil NACA 0009 9%         Moments
delta=0 deg.,Hinge at x=0 y=0
Alpha relative to the  chord l.
ALPHA       CM         CH         CL         CL(LIN)
-10.00   0.013212   0.301082  -1.168387     -1.100000
  0.00   0.000000   0.000000   0.000000      0.000000
 10.00  -0.013212  -0.301081   1.168386      1.100000

Airfoil NACA 0009 9%         Moments
delta=0 deg.,Hinge at x=0.26148 y=0
Alpha relative to the  chord l.
ALPHA       CM         CH         CL         CL(LIN)
-10.00  -0.000007   0.111141  -1.168387     -1.100000
  0.00   0.000000   0.000000   0.000000      0.000000
 10.00   0.000007  -0.111141   1.168386      1.100000

Airfoil NACA 0009 9%         Moments
delta=0 deg.,Hinge at x=0.4 y=0
Alpha relative to the  chord l.
ALPHA       CM         CH         CL         CL(LIN)
-10.00   0.060703   0.060703  -1.168387     -1.100000
  0.00   0.000000   0.000000   0.000000      0.000000
 10.00  -0.060702  -0.060702   1.168386      1.100000

PANEL METHOD NACA 0009 9%   CL=0.363964, 6.742775 ALPHA0=3.089734 MACH=0

Airfoil NACA 0009 9%         Moments
delta=5 deg.,Hinge at x=0.75 y=0
Alpha relative to the  chord l.
ALPHA       CM         CH         CL         CL(LIN)
-10.00   0.011974   0.000741  -0.808646     -0.760129
  0.00  -0.049861  -0.004984   0.363829      0.339871
 10.00  -0.108545  -0.010336   1.524523      1.439871

Airfoil NACA 0009 9%         Moments
delta=5 deg.,Hinge at x=0.75 y=0
Alpha relative to the  chord l.
ALPHA       CM         CH         CL         CL(LIN)
-10.00   0.000741   0.000741  -0.808646     -0.760129
  0.00  -0.004984  -0.004984   0.363829      0.339871
 10.00  -0.010336  -0.010336   1.524523      1.439871

PANEL METHOD NACA 0009 9%   CL=0.783348, 6.719803 ALPHA0=6.649134 MACH=0

Airfoil NACA 0009 9%         Moments
delta=10 deg.,Hinge at x=0.9192 y=-0.014887
Alpha relative to the  chord l.
ALPHA       CM         CH         CL         CL(LIN)
-10.00  -0.014017  -0.000858  -0.391355     -0.368595
  0.00  -0.019818  -0.001147   0.781171      0.731405
 10.00  -0.024346  -0.001359   1.928365      1.831405
```

Six blocks of results are produced. Each contains a table with α, c_m, c_h, c_ℓ, and $c_\ell(lin)$, where c_ℓ is computed from the potential-flow (i.e., inviscid) velocity distribution and $c_\ell(lin)$ includes viscous effects merely by setting the lift curve slope to 2π or 0.11 per degree.

The first block contains c_m about the quarter-chord point and c_h about the leading edge. Because no portion of the airfoil is forward of the reference point for c_h (i.e., the leading edge), c_h is identical

to the moment coefficient about the leading edge.

The second block contains c_m about $x/c = 0.2605$, $y/c = 0$, which is the aerodynamic center. The hinge-moment coefficient c_h is still computed about the leading edge.

The third block contains c_m and c_h about $x/c = 0.4$, $y/c = 0$, which is a hinge point. The contribution of the portion of the airfoil forward of the hinge point is excluded.

The fourth block, which concerns a 25-percent-chord flap deflected $5°$, contains c_m about the previous hinge point $x/c = 0.4$, $y/c = 0$ and c_h about $x/c = 0.75$, $y/c = 0$, which is the hinge point introduced by a preceding FLAP line.

The fifth block contains c_m and c_h about $x/c = 0.75$, $y/c = 0$.

The sixth block, which concerns an additional 8-percent-chord flap deflected $10°$, contains c_m about $x/c = 0.75$, $y/c = 0$ and c_h about the new hinge point $x/c = 0.9192$, $y/c = -0.0149$.

5.5 ALFA Line

The ALFA line initiates:

the storage of up to 22 angles of attack specified by the F-numbers (all α values remain available for other options),

the inviscid computation of the pitching-moment and hinge-moment coefficients for the specified angles of attack (these coefficients also remain available for other computations), and

additional listings specified by print modes mxy, mpa, and mcm.

One last option, which lists the second derivatives of the velocity or pressure distributions at various angles of attack, is described at the end of this section.

NUPA and *NUPE* determine the print modes.

If *NUPA* = 0, mxy, mcm, and mpa remain as previously set.

If *NUPA* $\neq$ 0, mxy = *NUPE* and mcm = *NUPA*.

If *NUPA* = 1, mxy = *NUPE*, mcm = *NUPA*, and, additionally, mpa = *NUPE* + 1.

If $mxy \neq 0$, the airfoil coordinates and the velocity, or pressure, distributions for all the specified α (up to 14) are listed. This is called an x-y-V listing. If $mxy = 0$, no listing is produced.

If $mcm = 1$, the pitching-moment c_m and hinge-moment c_h coefficients for all the specified values α are listed. If $mcm \neq 1$, no listing is produced.

If $mpa = 0$, no listing from Subroutine PANEL is produced.

If $mpa = 1$ or 2, only the headline from Subroutine PANEL is listed.

If $mpa > 3$, the headline, the airfoil coordinates, and the vorticities for $\alpha = 0°$ and $\alpha = 90°$ from Subroutine PANEL are listed.

The default values are $mxy = 1$, $mcm \neq 1$, and $mpa = 1$.

The print modes are summarized in the following table.

NUPA	*NUPE*	Output
0	ignored	x-y-V listing as before
1	0	c_m and c_h listing, headline from PANEL, no x-y-V listing
1	1	x-y-V listing, c_m and c_h listing, headline from PANEL
1	≥ 2	x-y-V listing; c_m and c_h listing; headline, vorticities, and slopes from PANEL
≥ 2	0	mpa for PANEL listing remains as before, no x-y-V listing
≥ 2	≥ 1	x-y-V listing, mpa for PANEL listing remains as before

Note that the print mode mpa cannot be set to 0 in an ALFA line. This must be done in an FXPR or PAN line. Setting mpa in the ALFA line (i.e., *NUPA* $= 1$) is only useful if the moment coefficients are to be listed.

NUPI and *NUPU* specify the details of the x-y-V listing and also the corresponding plot produced by a DIAG line.

If *NUPI* $= 0$, the α values are relative to the zero-lift line and the x-y-V listing and the DIAG plot contain velocity distributions.

If *NUPI* $= 1$, the α values are relative to the x-axis and the x-y-V listing and the DIAG plot contain velocity distributions.

If *NUPI* $= 2$, the α values are relative to the zero-lift line and the x-y-V listing and the DIAG plot contain pressure (C_p) distributions.

If *NUPI* $= 3$, the α values are relative to the x-axis and the x-y-V listing and the DIAG plot contain pressure (C_p) distributions.

If *NUPU* $=$ 0–22, *NUPU* specifies n_α, which is the number of F-numbers (i.e., α values) to be read. The number of F-numbers n is determined from the input. If $n > n_\alpha$, n_α is set to n. Thus, it is simplest to set *NUPU* to 1 and let the code count the α values.

If *NUPU* $>$ 22, a listing containing only the point numbers, x, y, and ν is produced and n_α is set to 0.

If *NUPU* $= 0$, *NUPI*, n_α, and the values of α_i from the preceding ALFA line with *NUPU* $\neq 0$ are used.

The F_i, where $i = 1$, ..., n_α, specify the angles of attack α_i in degrees.

If $F_i = -99.ab$, $\alpha_i = \alpha_k^*$, where $k = ab$. If $k = 0$ or $k > n_\alpha$, then $k = i$.

This option allows α^* values from the airfoil design to be used as α_i. (Remember that the velocity over airfoil segment i is constant at this α.) This option is useful if the values of α_i^* have been changed by iteration during the design procedure. If this option is specified after an airfoil analysis or if $k = i < n_\alpha$, the α_i is skipped.

Internally, the code uses the angle of attack relative to the zero-lift line. If *NUPI* $= 1$ or 3, all angles of attack relative to the x-axis are converted to values relative to the zero-lift line and then back to values relative to the x-axis for output only. If the option $F_i = -99.ab$ is used with *NUPI* $= 1$ or 3, the α_i^* are converted to values relative to the x-axis for output.

The following examples illustrate the use of the ALFA line.

```
ALFA21␣␣␣1␣1␣-99␣-99.05␣3
```

No moment coefficients are listed ($mcm =$ *NUPA* $= 2 \neq 1$), the x-y-V listing containing velocities

is produced (*NUPA* $\neq$ 0 and, therefore, $mxy =$ *NUPE* $= 1$; *NUPI* $= 0$), and $\alpha_1 = 1°$, $\alpha_2 = \alpha_2^*$, $\alpha_3 = \alpha_5^*$, and $\alpha_4 = 3°$, all relative to the zero-lift line (*NUPI* $= 0$).

`ALFA␣␣3␣␣1␣2␣4␣6␣8␣10`

Print modes mcm and mxy remain as previously set (*NUPA* $= 0$). If $mxy \neq 0$, the x-y-V listing containing pressure coefficients is produced (*NUPI* > 2) with $\alpha = 2°$, $4°$, $6°$, $8°$, and $10°$ relative to the x-axis (*NUPI* $= 3$).

`ALFA` [no additional input]

NUPI, n_α, and the values of α_i from the preceding ALFA line with *NUPU* $\neq 0$ are used and print modes mxy, mcm, and mpa remain as before.

`ALFA20`

NUPI, n_α, and the values of α_i from the preceding ALFA line with *NUPU* $\neq 0$ are used. The moment-coefficient listing and the x-y-V listing are not produced (*NUPA* $= 2 \neq 0$; therefore, $mxy =$ *NUPE* $= 0$).

A special option lists the second derivatives of $v(\phi)$ in the x-y-V listing. This allows the curvature of $v(\phi)$, usually in the ramp area, to be checked. (See ref. [3].) If an $\alpha_i \neq 0$ and $\alpha_{i+1} = \alpha_i$, the second derivative of the velocity (or pressure) distribution is listed for α_{i+1}.

5.6 DIAG Line

The DIAG line initiates the plotting and labelling of two different diagrams: the x-y-V diagram, which contains the airfoil shape and velocity or pressure (C_p) distributions or a so-called pressure-envelope diagram, which is relevant for cavitation on hydrofoils.

If *NUPA* $\neq 0$, the lines in the x-y-V diagrams are plotted as polygons instead of splined curves. The coordinate points, in this case, can be distinguished by the corners of the polygons.

If *NUPE* $= 1$, experimental data are inserted into the x-y-V diagram (see below).

NUPI determines the type of diagram to be plotted and the line type to be used (see below).

NUPU specifies the plot mode mbt, by which different sets of data can be plotted in one diagram, $V(s)$ near the leading edge can be plotted, and the airfoil points can be identified by symbols.

The three digits of *NUPU* are designated abc.

If $c = 0$, one set of data is plotted, axes are drawn, and the diagram is terminated (i.e., closed to further plotting).

If $c = 1$, one set of data is plotted and the diagram remains open to further plotting.

If $c = 2$, one set of data is plotted into the open diagram, axes are drawn, and the diagram is terminated.

If $c = 3$, one set of data is plotted into the open diagram, which remains open to further plotting.

If $b \neq 0$, the airfoil points are identified by symbol b, as defined in figure 12. In this case, only the first eight symbols are available; symbol 9 is a flag perpendicular to the airfoil surface.

If $a \neq 0$, $V(s)$ near the leading edge is plotted. The velocities on the lower surface are plotted as negative values.

Obviously, plot mode mbt is valid only for the one DIAG line in which it is specified.

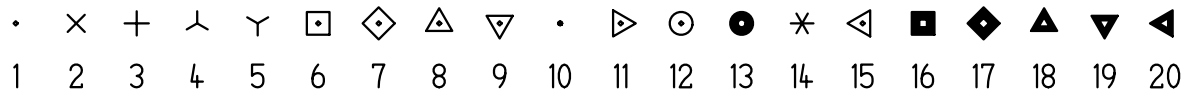

Figure 12: Available symbols and their numbers. Symbol 10 is a flag perpendicular to the local tangent.

5.6.1 Pressure-Envelope Diagram

If *NUPI* = 1, a pressure-envelope diagram is plotted. The abscissa is $-C_{p,min}$ and the ordinate, α. All α values in the preceding ALFA line are used. The size of the frame depends on the α values. If the vertical extent of the frame must be increased to accommodate a succeeding set of data, this can be accomplished by setting F_1 and $F_2 \neq 0$.

If $F_1 \neq 0$, $F_1 = \alpha_{min}$ in degrees.

If $F_2 \neq 0$, $F_2 = \alpha_{max}$ in degrees.

5.6.2 x-y-V Diagram

If *NUPI* $\neq$ 1, the x-y-V diagram is plotted.

If *NUPI* = 0, the curves in the x-y-V diagram are solid.

If *NUPI* $\geq$ 2, *NUPI* is the line type as defined in Chap. 6.7.4.

The x-y-V diagram contains the airfoil shape and the velocity or pressure distributions for all α values in the preceding ALFA line. The ordinate is V, if *NUPI* = 0 or 1 in the ALFA line or $-C_p$, if *NUPI* = 2 or 3.

Scaling

Usually, the diagrams are produced by means of a printer, in which case, it is helpful to specify the size of the diagrams in the input. The length of the x/c-axis in the velocity or pressure distribution is specified by $100F_1$, which is the unit length (i.e., $x/c = 1$) of the x/c-axis in mm. The default value is 200 mm.

For example,

`DIAG␣␣␣␣␣␣␣140`

which specifies a length of 140 mm for the x/c-axis.

Note that the x/c-axis can extend beyond $x/c = 1$ for airfoils with flaps or variable geometry. Only DIAG lines that open a diagram (i.e., *NUPU* = 0 or 1) can alter the unit length.

Extension of Frame

The size of the frame for the x-y-V diagram is determined from the data available when the diagram is opened (i.e., *NUPU* = 0 or 1). The data to be plotted from this line, including the experimental data, if *NUPE* = 1, are evaluated before the frame is opened and the frame is sized accordingly. Without additional input, the upper edge of the frame is set to $V = 2.5$ or $C_p = -3$. The curves

are not plotted beyond this limit.

The upper edge of the frame can be extended by specifying F_1 in a DIAG line with *NUPU* = 0 or 1, in which case F_2 specifies V_{limit} or $(C_p)_{limit}$.

The upper edge of the frame will be extended if the limit specified by F_2 is greater than that derived from the data. This can be applied in two ways as follows.

If the data corresponding to the first DIAG line (i.e., *NUPU* = 0 or 1) exceeds the default limit $V = 2.5$ or $C_p = -3$ and the entire curves are to be plotted.

If, following a DIAG line with *NUPU* = 1, the curves from succeeding DIAG lines with *NUPU* = 2 or 3 require a larger frame than those from the first DIAG line.

Labelling

Without additional input, the axes are labelled "α relative to the x-axis" or "α relative to the zero-lift line" and all α values used for the diagram are plotted in the upper, right corner. The airfoil name and thickness in percent chord, valid for the DIAG line terminating the diagram (i.e., *NUPU* = 0 or 2), are plotted inside the airfoil or, if the airfoil is too thin, below it.

If *NUPU* = 0 and only one α value is input, this value is included in the label "α = ... relative to the ..." and the plotting in the upper, right corner is omitted.

In all DIAG lines with *NUPI* = 0, additional input can begin at least three columns after the last F-number; if no F-number is present, in column 13 or higher. One or more DLFF sentences can be given that contain one or more groups of three numbers as follows.

$\pm i$, $\pm x/c$, e, $\pm i$, $\pm x/c$, e, ...

Each group of three numbers plots the i^{th} α value near the corresponding curve. The value is plotted such that the corner e of the label rectangle (fig. 13) is located at x/c along the curve. If the sign of x/c is negative, the curve corresponding to the lower surface is labelled; if positive, the curve for the upper surface is labelled. If a minus sign precedes i, "α =" is plotted ahead of the α value. The input $e = 1$ at the end of a sentence can be omitted; the next sentence must then begin with $\pm i$ for the next group.

The label rectangle encompasses the label and a small gap. The e values corresponding to the four corners are shown on the left side of figure 13. The right side of figure 13 shows an example in which corner 4 is located along the curve.

If labelling information is input, the α values are not plotted in the upper, right corner.

Figure 13: Label rectangles.

Note that the character "F" in any DLFF word can be used to continue the input in the next line.

The airfoil name to be plotted can be changed by inputing *N and the new name as a character string at least three columns after the end of the last DLFF sentence. The name must be terminated by two spaces. Thus, the name cannot contain two successive spaces.

After *Z, a character string can be given that will be plotted after the label(s) explaining the first α value.

After *i, where i = 1, 2, ... 9, a character string can be given that will be plotted after the label initiated by the i^{th} group of three numbers.

If only one α value is valid, its value is omitted in the label(s) along the curve.

If $i < -30$, $|i| - 30$ specifies the number of the α value and the c_ℓ value is written near the curve instead of the α value. This is normally done in the first group. This option is useful if the Mach number is not zero. The α label is then omitted.

If "F" is the last character of a character string, the current flap data are plotted as "c_f% Flap δ_f°", where c_f is the flap chord and δ_f is the deflection. These data are not plotted if $\delta_f = 0^\circ$. The input *iF or *ZF adds only the flap data to the labels.

Font @1 (see ref. [6]) is the default font for the airfoil name and, therefore, switching to capital Latin letters is superfluous, in this case.

Experimental Data

Experimental data can be inserted into an x-y-V diagram. If *NUPE* = 1 in the DIAG line that opens a diagram (i.e., *NUPU* = 0 or 1), the succeeding lines, which have "X", "Y", or "E" in the first column, specify the experimental data as follows.

The X lines contain the x/c values.

The Y lines contain the velocities, if the preceding ALFA line has *NUPI* $\leq$ 1, or pressure coefficients, if *NUPI* $\geq$ 2.

The E line terminates the experimental data.

The X and Y lines are read by the same subroutine as are the experimental data for the CDCL diagram (see Chap. 6.7). Thus, the same options are available. The first line in the key is solid with the explanation "Theory".

The available symbols are shown in figure 12.

The following example produces the diagram shown in figure 14.

```
REMO1          *P   *9US
TRA1    88 0 5 60 -5
TRA29   88 4 17.5 2 -1 .6 4 17.5 2 -1 .6 3 0 0
ALFA201  2 -99.9 0
DIAG 1   1 0 2.2   1 .65 2 -2 .3 3 1 -.25 3   *2@1Plain
X  100  45 50 60 65
Y  100  135 140 135 160  2   *T@1Fictitious Experiment
E
FLAP       25 0 3 15
ALFA  1  2 3 0
DIAG     2          -1 .1 2 2 .16 3 2 -.7 2 1 -.2 F
1    *ZF  *2, @1Flap   *3, @1Flap
```

The velocity distributions for two different flap deflections (0°and 15°) are plotted in one diagram by means of DIAG lines with *NUPU* = 1 and *NUPU* = 2. The labels "α =" are added when i is negative. The labels "Plain" and "25% Flap 15°" are inserted after the labels with $i = 1$, which occcurs once in each DIAG line. The label "Flap" is inserted after the α labels corresponding to the second and third groups of three numbers. Ficticious experimental data are included.

The following example produces figure 15.

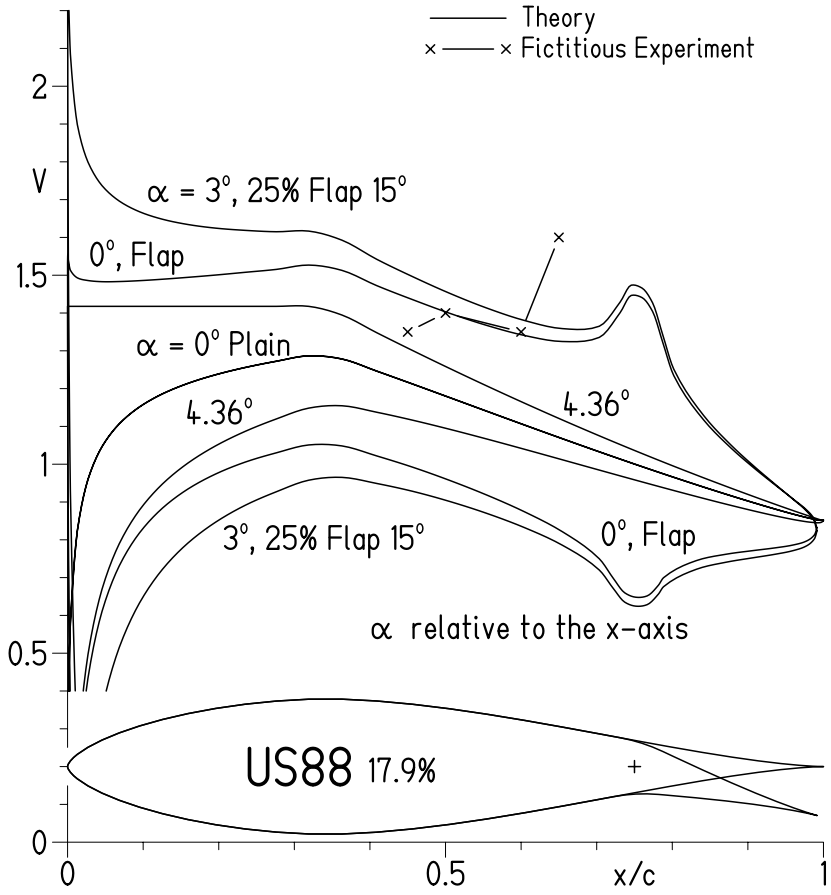

Figure 14: Velocity distributions for unflapped and flapped US88 airfoil.

```
REMO1         *P
TRA1  1111 0 5 60 -5
TRA2  1111 4 17.5 2 -1 .7 4 17.5 2 -1 .7 3 .2 0 0
ALFA      1 0
DIAG      1 0 1.6
FLAP 9      25 0 3 5
ALFA  1001 0
DIAG      3          1 .12 3     *Z@1Flap
FLAP        8 -1.49 2 10
ALFA  1001 0
DIAG      2          1 .4 2     *Z@1Double Flap
```

The FLAP lines of this example are the same as the last two FLAP lines in the example for listing the moment coefficients. The velocity distributions for three shapes are plotted in one diagram by *NUPU* = 1, 3, and 2. Only one α value is given. This value is included in the explanation line and omitted from the labels near the curves. The additional text given after *Z is plotted at the location given by the group of three numbers. Using *1 instead of *Z would have the same effect.

The third example illustrates the smoothing option for Wortmann airfoils. The velocity distributions for the original coordinates and those after three smoothings are shown in figure 16.

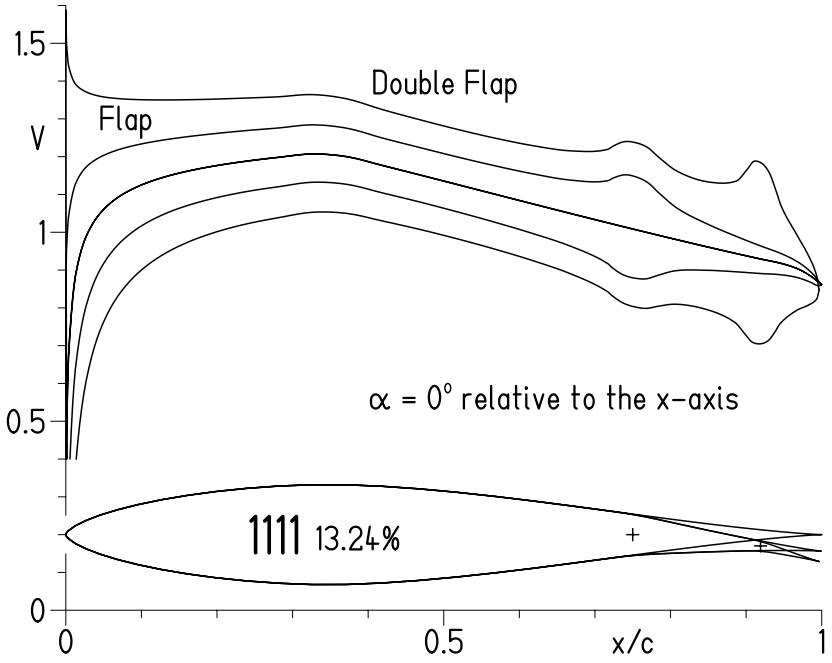

Figure 15: Velocity distributions for airfoil 1111, unflapped and with single and double flaps.

```
FXPR                FROM THE NEW BOOK     FIG. 13
FX 63-137
FX63-13701  000  000   82   40  249  169  501  373  818  630 1189  921
FX63-137 7 1601 1219 2043 1514 2516 1794 3018 2052 3553 2284 4114 2479
FX63-13713 4711 2631 5323 2729 5962 2768 6605 2745 7273 2668 7927 2530
FX63-13719 8590 2343 9204 2098 9804 181310331 147510823 111211221  716
FX63-1372511578  30711833 -10312042 -48612137 -84812191-116712128-1460
FX63-1373112024-168811792-189511522-203411122-216110704-222010165-2277
FX63-13737 9622-2263 8975-2256 8323-2180 7611-2122 6864-1978 6089-1855
FX63-13743 5304-1699 4480-1482 3625-1254 2740 -995 1820 -636  985 -317
FX63-13749  000  000
ALFA     1 4 8 12
DIAG     1
FXPR    30           FROM THE NEW BOOK
FX 63-137
FX63-13701  000  000   82   40  249  169  501  373  818  630 1189  921
FX63-137 7 1601 1219 2043 1514 2516 1794 3018 2052 3553 2284 4114 2479
FX63-13713 4711 2631 5323 2729 5962 2768 6605 2745 7273 2668 7927 2530
FX63-13719 8590 2343 9204 2098 9804 181310331 147510823 111211221  716
FX63-1372511578  30711833 -10312042 -48612137 -84812191-116712128-1460
FX63-1373112024-168811792-189511522-203411122-216110704-222010165-2277
FX63-13737 9622-2263 8975-2256 8323-2180 7611-2122 6864-1978 6089-1855
FX63-13743 5304-1699 4480-1482 3625-1254 2740 -995 1820 -636  985 -317
FX63-13749  000  000
ALFA     1 4 8 12
DIAG     2         -1 .2 1 2 .19 3 3 .4 2 2 -.16 4 3 -.25 1
```

5.7 PUXY Line

The PUXY line writes the airfoil coordinates x/c and y/c and the inner normal angles β to a file having the name of the input file and the extension "PU".

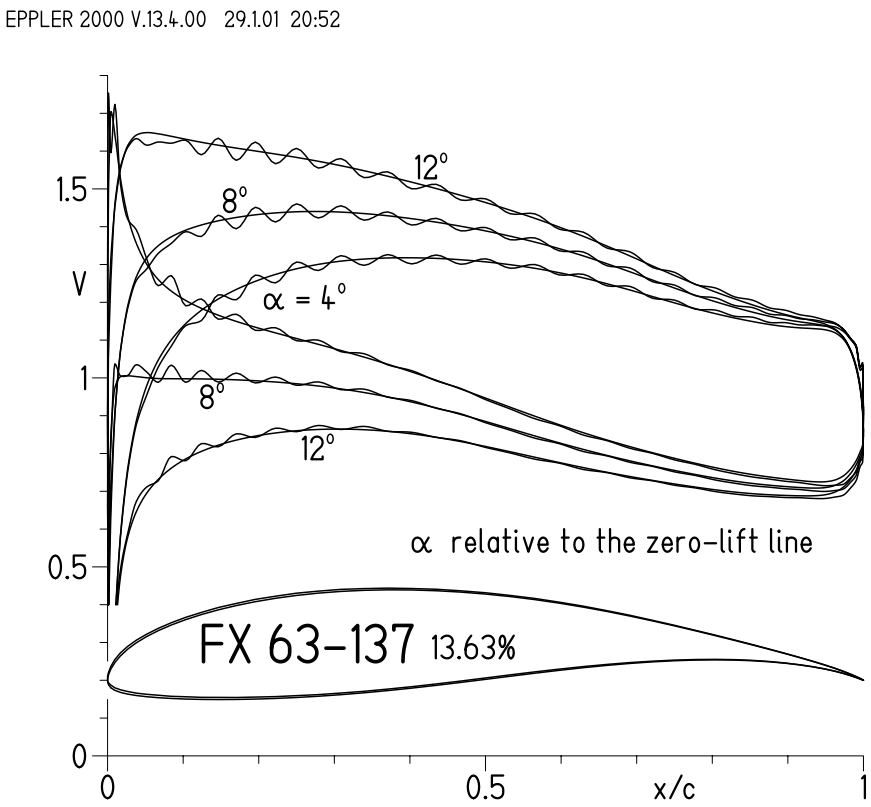

Figure 16: Velocity distributions for original and smoothed FX 63-137 airfoil.

Columns 1–5 in each output line contain the airfoil name. If this name comes from the analysis mode, characters 3–7 of the name are used. If this name comes from the design mode, a space followed by the four digits of the airfoil number are used. Columns 6–8 contain the number of the first point written in that line. Columns 9–80 contain four groups of three numbers each, which are the x/c, y/c, and β values for one point. No decimal points are written. The x/c and y/c values in this file can be read using format F6.5 and the β values, format F6.4.

6 Boundary-Layer Analysis

6.1 Fundamentals

The computation of the boundary-layer development is performed by means of an integral method (see ref. [3]). This method requires as input the Reynolds number R and the potential-flow velocity distribution $U(s)$, where s is the arc length from the stagnation point along the surface of the airfoil. The velocity distributions are computed in either the design or the analysis mode.

The basic results of this approximate method are the momentum thickness $\delta_2(s)$ and the shape factor $H_{32}(s)$. Also the displacement thickness $\delta_1(s)$ and the shape factor $H_{12}(s)$ are evaluated. The momentum thickness is most significant for the viscous drag; the shape factor indicates the shape of the boundary-layer profile. Increasing H_{32} corresponds to a more favorable pressure gradient. All results together allow the approximate evaluation of displacement, separation, and transition of the boundary layer, the airfoil drag, and the occurence and effect of laminar separation bubbles.

The prediction of boundary-layer separation has not been changed since 1963 (ref. [4]). Separation

is predicted when H_{32} decreases to 1.51509 in a laminar boundary layer and when H_{32} decreases to 1.46 in a turbulent boundary layer. A displacement iteration was developed in 1980 (ref. [2]).

6.1.1 Criteria for Boundary-Layer Transition

In code versions since 1980, boundary-layer transition was predicted by means of a local criterion. In 1996, a new empirical transition criterion was implemented that considers the instability history of the laminar boundary layer, which avoided the long computing time of the e^N method while achieving similar results, in most cases.

Since then, computing power has increased dramatically, which has negated the disadvantage of the e^N method. Moreover, the faster computers allowed a very large number of solutions of the Orr-Sommerfield equation to be computed and tables to be constructed from which the amplification rates of the Tollmien-Schlicting (TS) waves can be evaluated with adequate precision by interpolation. This increases the speed of the e^N method such that the boundary-layer computations require only 10 to 30 times more time than with the empirical criterion, which is compensated by the higher computer speed.

The laminar boundary layer is initially stable. During its development, a combination of Reynolds number and shape factor must be found for which the first TS wave becomes unstable. This stability limit has been evaluated for many shape factors. A table was then constructed that allows the stability limit for a given boundary-layer development to be evaluated precisely by interpolation. This evaluation also yields the frequency of the first unstable TS wave.

The amplification rate of a TS wave depends on the local Reynolds number and the shape factor of the boundary-layer flow in which it develops and on its frequency. An amplification table must therefore contain values depending on three parameters. In stability theory, these three parameters are the Reynolds number based on the displacement thickness δ_1, the shape factor H_{12}, and a nondimensional frequency β. The current amplification table contains more than 40,000 values.

The boundary-layer computation begins with the search for the first unstable TS wave with its nondimensional frequency β_{crit}. This yields also the natural frequency f_{crit}. A frequency range with 64 frequencies f_i is defined around f_{crit}. For all f_i, the amplifications are evaluated and their natural logarithms are summarized into the amplifications $\ln a_i(s)$. At any position s along the airfoil surface, the maximum amplification

$$n(s) = \max \{\ln a_i(s)\}$$

is evaluated by quadratic interpolation. If n reaches the specified value N, transition is assumed. During the development of the laminar boundary layer, the frequency of the most amplified TS wave varies considerably. Some of the TS waves that are initially amplified may be damped later whereas others may be amplified. Sometimes, the frequency of the most amplified TS wave is outside the defined frequency range. The boundary-layer computation is then halted and restarted at the first instability using an expanded frequency range. Two typical examples of amplifications for many frequencies are shown in figure 17. The amplifications are plotted using dashed lines where the length of the dash is proportional to the frequency. Thus, higher frequencies are represented by shorter dashes and lower frequencies, by longer dashes. This gives a qualitative impression of the length of the TS waves. The ordinate is the airfoil point number. The amplifications are plotted only for these points although they are usually computed at many intermediate points as well. The examples in figure 17 show that higher frequencies are often damped out after initially being amplified, whereas lower frequencies are amplified later and finally reach the transition value.

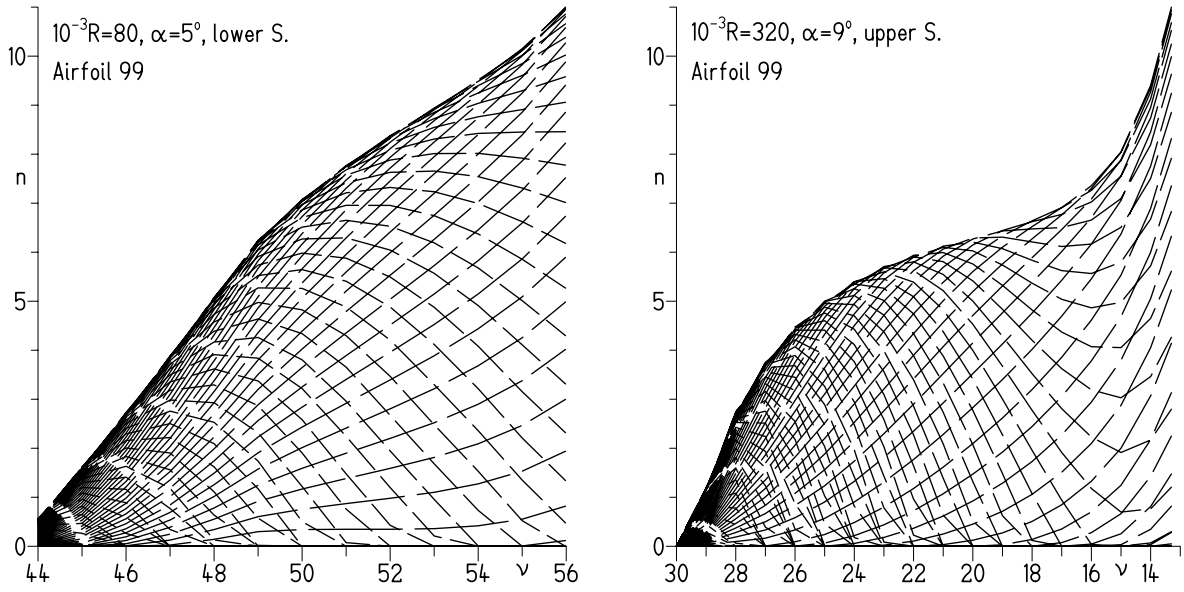

Figure 17: Examples of amplification diagrams.

This method seems straightforward, although the value of N must be determined empirically. The amplification is only a factor by which very small initial disturbancies are amplified. The amplitude of the TS waves at the beginning of the transition process has been extensively investigated. Measurements in low-turbulence wind tunnels correspond to an N of 11 to 13. Measurements in flight correspond to N values up to 15. Note that the N values of 11, 13, and 15 represent amplifications of 59,874, 442,413, and 3,269,017, respectively.

The default value of N in the code is 11, which corresponds to a low-turbulence wind tunnel but may be conservative for flight. The value of N can be specified in the input.

For previous transition criteria, a roughness factor $r > 0$ could be specified that accounts for free-stream turbulence and/or surface roughness. For the e^N method, the roughness factor specifies a reduced N-factor N_r as follows.

$$N_r = N(1 - 0.165\, r)$$

Thus, an r of 6 specifies an N-factor N_r of $0.01N$, which means transition will occur immediately after the initial instability. This simulates a very rough surface and/or a very turbulent free stream. A roughness factor r of 0 corresponds to natural transition on a smooth surface with very low free-stream turbulence.

The effect of single roughness elements has also been included, which simulates turbulators, flap hinges, or poorly-faired spoilers, for example. If the boundary layer is turbulent at the location of the roughness element, δ_2 is increased by an amount that depends on the height of the element and the local shape factor. If the boundary layer is laminar at the location of the roughness element, transition is assumed to occur at that location and δ_2 is not increased.

6.1.2 Profile Drag

The profile-drag coefficient c_d is calculated after each boundary-layer computation. This is usually performed according to the Squire-Young formula

$$c_d = 2\,\delta_{2,te}\left(\frac{V_{te}}{V_\infty}\right)^{\frac{5+H_{12,te}}{2}} \tag{3}$$

The subscript te denotes "at the trailing edge." In previous versions of the code, this formula was modified for separated flows by using, instead of $H_{12,te}$,

$$H_{12}^* = min\,(H_{12,te}, 2.5) \tag{4}$$

An upper limit for $H_{12,te}$ had to be introduced that was relevant mainly if the turbulent boundary layer separated early, when U was high.

Recently, a new formula

$$c_d = 2\,\delta_{2,te}\frac{\lambda\,[\lambda - (1-\lambda)(1-\kappa)H_{12,te}]}{1+\kappa(1-\lambda)} \tag{5}$$

was developed (ref. [5]), where

$$\lambda = \frac{V_{te}}{V_\infty} \tag{6}$$

and κ is a parameter that cannot be determined precisely. For $\kappa = 0.7$, this formula yields drag coefficients that, in normal cases, deviate little from those resulting from the Squire-Young formula and it does not require modification for early separation. The shape factor $H_{12,te}$ is limited to its value at separation only if $V_{te} < V_\infty$. This formula now replaces equation 3. It can, as was possible with the old formula, be applied during the computation of the boundary layer, where it indicates those portions of the boundary-layer development that contribute most to the drag. (See ref. [3].)

6.1.3 Bubble Drag

At low Reynolds numbers, the occurrence of laminar separation bubbles is the reason for most and sometimes large differences between wind-tunnel measurements and numerical predictions based on boundary-layer theory. The boundary-layer method in the previous versions of the code used an analogy between the turbulent boundary layer just after transition and the laminar separation bubble. This analogy has been used since 1982 to issue a warning when additional drag from bubbles was to be expected. Since 1996, a technique for estimating the bubble drag was derived from recent experimental results. This model, however, had a shortcoming that was present in most other simulations as well. Near the leading edge, where laminar separation occurs in a very thin boundary layer, the predicted bubble drag was too high. This has been corrected. Theoretical investigations showed that, following separation, a thin laminar boundary layer exhibits a considerably adverse pressure gradient. Accounting for this pressure gradient led to much better agreement with experiments for thin and thick boundary layers.

Another finding from the theoretical investigations was the existence of an explosively increasing dissipation coefficient near transition in the separated boundary layer. This has been confirmed experimentally. Introducing this phenomenon into the bubble model further improved the predictions over a wide range of Reynolds numbers.

6.2 EHNN Line

The EHNN line specifies only the value of N $(= EHNN)$.

$F_1 = EHNN$

The default value of $EHNN$ is 11. The value of $EHNN$ remains valid until it is changed by another EHNN line.

6.3 RE Line

The RE line normally specifies up to five pairs of numbers, each containing a transition mode MU and a Reynolds number R. Boundary-layer computations for each MU-R pair are performed using the velocity distributions $V(x, \alpha)$ for all the α values in the preceding ALFA line. Single roughness elements can also be specified. The code terminates if there is no ALFA line somewhere before the RE line. The results from the boundary-layer analysis are listed and plotted according to print mode mpr and plot mode mpl. A summary of the results is stored in blank COMMON arrays CW, SA, and SU, which remain available for other computations. Other options in the RE line allow certain parameters to be specified without initiating a boundary-layer computation.

6.3.1 Print and Plot Modes

If *NUPA* = 1–8, mpr = *NUPE* and mpl = *NUPI*, where

if $mpr = 0$, the listing is suppressed;

if $mpr = 1$, the listing of the summary is produced, which contains the lift, drag, and pitching-moment coefficients, including viscous corrections and drag from laminar separation bubbles; the arc lengths of the turbulent and separated flows on both airfoil surfaces; and a warning "*", if a drag contribution from laminar separation bubbles is present;
an information on the sequence of the most significant boundary-layer points on both surfaces, separated by a slash "/", where it designates

"i" beginning instability
"s" laminar separation
"r" laminar reattachment
"t" laminar–turbulent transition
"R" reattachment after separation bubble
"S" turbulent separation
"A" reattachment after turbulent separation

if $mpr = 2$–9, the listing containing, in addition to the summary, the boundary-layer development along both surfaces for each MU-R pair and all the α values in the preceding ALFA line is produced. The arc lengths s/c starting at the stagnation point, the potential-flow velocity U/U_∞, and the point numbers, beginning with zero, are given in the first three columns. Then, for each MU-R pair, two columns are produced. The first one contains H_{12} for $mpr=$ 4 and 8; for all others, it contains H_{32}. The second column contains:

if $mpr = 2$, the momentum thickness given as $10^2\delta_2$ (entitled "100DLT2");

if $mpr = 3$, the Reynolds number based on the momentum thickness and the local velocity, given as $10^{-3}R_{\delta_2}$ (entitled "RD2/1000");

if $mpr = 4$, the displacement thickness, given as $10^2\delta_1$ (entitled "100DLT1");

if $mpr = 5$, the contribution to the vicous drag resulting from equation 5 using the local H_{32} and δ_2 (entitled "CD(s)");

if $mpr = 6$, the difference between the natural logarithm of the local maximum amplification factor and the currently valid N (entitled "NDIFF");

if $mpr = 7$, the local skin-friction coefficient c_f (entitled "CDsf(s)");

if $mpr = 8$, the decimal logarithm of the Reynolds number R_{δ_1} based on the displacement thickness δ_1 and the local velocity V (entitled "LOG(RD1)"; and

if $mpr = 9$, the product δ_2 times R_{δ_2}, which is important for the pressure gradient in the laminar separation bubble (entitled "D2*RD2").

If only one MU-R pair is specified, three additional columns are produced containing the velocity outsinde of a present separation, the slope dn/ds of the maximum amplification function, given as $\delta_1(dn/ds)$, and the maximum amplification function $n(s)$ itself (entitled "UBD", "D1*dn/ds", and "n(s)"); if suction is active, the two last columns contain v_0 and c_Q, desuignated "V0" and "CQ".

if $mpl = 0$, the diagram is suppressed;

if $mpl = i \leq 5$, the boundary-layer development for the i^{th} MU-R pair is plotted as R_{δ_2} versus H_{32} (see refs. [1] and [3]). Two plots are generated: the left one is for the upper surface and the right one, for the lower surface. Each plot contains one curve for each α value in the preceding ALFA line. The diagram is closed afterwards; and

if $mpl = 6$–8, only the curves for the first MU-R pair are plotted as follows:

if $mpl = 6$, the diagram is opened, the curves for the first MU-R pair are plotted, and the diagram remains open for further plotting;

if $mpl = 7$, the curves for the first MU-R pair are plotted into the open diagram, which is then closed; and

if $mpl = 8$, the curves for the first MU-R pair are plotted into the open diagram, which remains open for further plotting.

If *NUPA* $= 0$, mpr and mpl remain as previously set. The default values are $mpr = 1$ and $mpl = 0$.

If $0 < NUPU < 99$, the amplification diagrams, as shown in figure 17, are plotted for all boundary-layer computations initiated by this RE Line. Thus, the number of figures is 2 times the number of angles of attack times the number of MU-R pairs (i.e., one figure for each surface at each α for each MU-R pair). The number of figures is limited to $NUPU$ if $NUPU < 99$ and to 999 if $NUPU = 99$.

6.3.2 Reynolds Numbers and Transition and Bubble-Drag Modes

If *NUPA* $\neq 9$ and *NUPU* $= 0$, the boundary-layer computation is performed. F-numbers F_1–F_{10} are interpreted as follows.

$F_1 = MU$, which contains five digits $sa.bcd$, which are interpreted as described below.

$F_2 = 10^{-3}R$, where R is the Reynolds number.

If $F_2 = 0$, the MU-R pairs and the values of x_T/c from the preceding RE line are used.

$(F_3, F_4) = (MU_2, R_2)$ and so on up to $(F_9, F_{10}) = (MU_5, R_5)$.

F-numbers F_{11}–F_{20} specify single roughness elements (see Chap. 6.3.3).

The odd F-numbers $F_1, F_3, \cdots, F_9$ each contain five digits $sa.0c$, which are interpreted as follows.

s is the suction mode MA, which is normally omitted or 0.

a is the transition mode.

$a = 1$ or 2 (i.e., fixed transition) is no longer valid, having been superseded by single roughness elements.

$a = 3$ specifies natural transition.

$a > 3$ specifies free transition with roughness factor $r = a - 3$.

c is the bubble-drag mode.

$c = 0$ computes the bubble drag on both the upper and lower surfaces and does not plot warning triangles in the CDCL diagram;

$c = 1$ computes the bubble drag on both the upper and lower surfaces and plots warning triangles in the CDCL diagram;

$c = 2$ computes the bubble drag on the upper surface only and does not plot warning triangles in the CDCL diagram;

$c = 3$ computes the bubble drag on the lower surface only and does not plot warning triangles in the CDCL diagram; and

$c = 4$ does not compute the bubble drag on either the upper or the lower surface and does not plot warning triangles in the CDCL diagram.

In this case, previous data sets now yield different results. The natural transition mode, $MU = 3$, now specifies transition prediction using the e^N method and inclusion of bubble drag on both surfaces.

6.3.3 Single Roughness Elements

The single roughness elements have two different effects. If the boundary layer is turbulent at the location of the roughness element, δ_2 is increased by an amount that depends on the height of the element and the local shape factor. If the boundary layer is laminar at the location of the roughness element, transition is assumed to occur at that location and δ_2 is not increased. The latter effect simulates fixed transition in a wind tunnel, for example.

The elements are specified by F-numbers F_{11}–F_{20}.

F_{11}–F_{20} contain five digits $abb.cc$, which are interpreted as follows.

$|abb|$ specifies the location of the roughness element x_R in percent chord. If $x_R = 0$, no roughness element is introduced by that F-number.

cc, which is interpreted as $0.cc$, specifies the roughness height in percent chord. Note that cc can have more than two digits and, therefore, the roughness height can be less than 0.0001c (e.g., 0.1 mm for a chord of 1 m).

F_{11} and F_{12} specify roughness elements on the upper and lower surfaces for the first MU-R pair,

F_{13} and F_{14} specify roughness elements on the upper and lower surfaces for the second MU-R pair,

and so on up to F_{19} and F_{20}.

Accordingly, roughness elements can be specified on either surface for each MU-R pair. If fewer roughness elements than MU-R pairs are specified, the last pair of roughness elements is used for all remaining MU-R pairs. Usually, only one pair of roughness elements is specified, which is then valid for all MU-R pairs. In most applications, the locations of the roughness elements are the same for all wind-tunnel or flight conditions.

F_{11}–F_{20} are read from each RE line that specifies at least one Reynolds number. The roughness elements remain in effect until an RE line with $F_2 \neq 0$ is read.

The F-numbers are counted. If less than five MU-R pairs are specified and F_{11} is specified, the F-numbers between the last MU-R pair and F_{11} must be specified as zero.

For example,

```
RE␣␣␣␣␣␣␣␣␣␣3␣4000␣3␣2000␣0␣0␣0␣0␣0␣0␣60.1␣80.1
```

which specifies roughness elements on the upper surface at $x/c = 0.60$ and on the lower surface at $x/c = 0.80$, each with a height h/c of 0.0010. These elements are also used for the second Reynolds number.

6.3.4 Labelling and Scaling

The boundary-layer development diagram contains R_{δ_2} in a logarithmic scale versus H_{32} in a linear scale. Two plots are produced, one for the upper surface and one for the lower surface. Each plot contains one line for each α value in the currently valid ALFA line. Each plot contains the stability limit $R_{\delta_2}(H_{in})$, and a vertical line for laminar separation. See reference [3].

A boundary-layer development diagram is initiated by *NUPI* = 1–8. The different modes for opening and closing the diagram are described in Chapter 6.3.1.

The diagram can be supplemented by additional text. If *Z is given after the optional information for curve labelling (see below), the character string following *Z is inserted between the airfoil name and the Reynolds number. All the options described in Chapter 5.6 are available. If *A and two spaces are given following or immediately preceding the *Z sequence, the explanation blocks are moved above the plots.

Starting in column 51, groups of three numbers

$\pm i$, $\pm R$, e; $\pm i$, $\pm R$, e, ...

can be given. Each group initiates labels to be inserted near the corresponding curves. Corner e of the label "$\alpha = \alpha_i^\circ$" is located near the point where $R_{\delta_2} = R$ along the curve for the i^{th} angle of attack α_i (see "DIAG Line", Chap. 5.6). If i is given without a minus sign, the label "$\alpha =$" is omitted. If $e > 4$, corner $e = e - 4$ is located near the same point and the Reynolds number is plotted instead of α_i. If the specification for the last curve is made with $e > 4$, α_i is substituted for R in the headlines.

The plot for the upper surface is labelled if the sign of R is positive; a minus sign initiates the labelling of the plot for the lower surface.

If *NUPA* = 9 and $F_1 \neq 0$, F_1 is the width in mm of the boundary-layer development diagram. The default width is 208 mm. No boundary-layer computation is performed. This width remains valid until another RE line with the same option is given.

6.3.5 Interpolation of Drag and Lift Coefficients

A RE line with *NUPA* = 8, initiates in succeeding boundary-layer computations drag coefficients c_d for given c_ℓ^* or vice versa to be evaluated by interpolation; no boundary-layer computation is performed. The interpolation is performed for each boundary-layer computation initiated following this line.

F_1 specifies the number n of the MU-R pair in the RE line or the twist angle-chord pair in the FLZW line to be considered.

If $F_2 > 0$, $F_2 = c_\ell^*$.

If $F_2 < 0$, $|F_2| = 100 c_d^*$.

$(F_3, F_4) = (n,\ c_\ell^*$ or $c_d^*)$ up to (F_9, F_{10}).

For example,

```
RE␣␣8␣␣␣␣␣␣1␣.8␣2␣-1.5␣3␣.2
```

performs interpolations for each succeeding boundary-layer computation and the following results are listed:

for the first MU-R pair, c_d at $c_\ell^* = 0.8$;

for the second MU-R pair, c_ℓ for $c_d^* = 0.015$; and

for the third MU-R pair, c_d at $c_\ell^* = 0.2$.

To obtain precise results, the α values in the preceding ALFA line should result in a c_d or c_ℓ close to the specified c_d^* or c_ℓ^*.

6.4 FLZW Line

The FLZW line initiates aircraft-oriented boundary-layer computations, where the Reynolds number R varies with the aircraft lift coefficient C_L and the local chord c. A local twist angle Θ, which must be specified relative to the zero-lift line of the entire wing, can also be given. The α values in the preceding ALFA line are taken as the local angles of attack relative to the zero-lift line. If the α values in the ALFA line are specified relative to the chord line, they are converted to α relative to the zero-lift line by adding the zero-lift angle before these computations. Thus, the aircraft lift coefficient is

$$C_L \approx 0.11\,(\alpha + \Theta) \tag{7}$$

and the aircraft speed is

$$v = \frac{v_1}{\sqrt{C_L}} \tag{8}$$

where

$$v_1 = \sqrt{\frac{2gm}{\rho S}} \tag{9}$$

is the aircraft speed at $C_L = 1$, g is the acceleration due to gravity in m/s^2, m is the aircraft mass in kg, ρ is the air density in kg/m^3, and S is the wing area in m^2. To prevent v from reaching unrealistically high values as C_L approaches 0, a maximum aircraft speed v_{max} is specified and

$$v = min\left\{\frac{v_1}{\sqrt{0.11\,(\alpha + \Theta)}}, v_{max}\right\} \tag{10}$$

The speed v is used to calculate the Reynolds number

$$R = \frac{v\,c}{\nu} \tag{11}$$

which, therefore, depends not only on the local angle of attack and aircraft mass but also on the local twist angle and the local chord.

Note that if a Mach number $M \neq 0$ is specified before an FLZW line, the variation of Mach number with angle of attack is considered. Because the C_L also depends on the Mach number, an iteration process is necessary to obtain agreement between C_L, M, and v. Accordingly, each α requires three to five runs of the panel method, which increases the computing time.

Also note that, if the computation is to be performed with roughness elements, they must be specified in the last RE line preceding the FLZW line. This RE line must specify at least one Reynolds number.

Everything else is processed exactly as it is for an RE line, including the print and plot modes and storage of the results.

NUPA, *NUPE*, and *NUPI* (see "RE Line", Chap. 6.3).

NUPU $= MU$, which contains up to three digits $a0c$, as defined for the RE line. If MU contains only one digit, it is interpreted as a; two digits are interpreted as $a0$. All options described for the RE line are allowed. Fixed transition (i.e., $a = 1$ or 2) requires the transition locations to be specified in the preceding RE line.

$F_1 = W/S$, which is the wing loading (aircraft mass/wing area) in kg/m^2.

$F_2 = v_{max}$, which is the maximum aircraft speed in m/s.

$0.1\,F_3 = \rho$, which is the air density in kg/m^3.

If $F_3 = 0$, ρ remains as previously set. The default value is 1.229 kg/m^3.

$F_4 = 10^6\nu$, which is the kinematic viscosity in m^2/s.

If $F_4 = 0$, ν remains as previously set. The default value is 13.6 $\times$ 10^6 m^2/s.

$F_5 = c_1$, which is the local chord in m.

If $F_5 = 0$, the FLZW line does not initiate a boundary-layer computation; instead, the values of v_{max}, ρ, and ν are stored for a succeeding PLW line.

$F_6 = smmmb.cc$, where s may be a minus sign, $sb.cc$ is the local twist angle Θ_1 in degrees, and mmm is the transition mode for the chord specified by F_5. This option is only permitted if *NUPU* in the FLZW line is zero. If not, m is included in the twist angle, which can then be greater than 10°. If *NUPU* $= 0$ and the twist angle is less than 10°, the transition mode is taken from the first transition mode in the preceding RE line. If $mmm = 0$, it is set to 300.

$(F_7, F_8) = (c_2, \Theta_2)$ and so on up to $(F_{13}, F_{14}) = (c_5, \Theta_5)$.

6.5 PLW Line

The PLW line initiates an aircraft-oriented boundary-layer computation using the specified aircraft data and resulting in a speed or a power polar for the given aircraft. The wing planform is specified and, therefore, the aspect ratio ÆR can be computed and the influence of the local chords on the

Reynolds number can be considered. Knowing ÆR allows the induced-drag coefficient C_{D_i} to be computed

$$C_{D_i} = k \frac{C_L^2}{\pi \text{ÆR}} \tag{12}$$

where k is the so-called k-factor. The default value, 1.03, assumes a good planform. The effect of wing twist is not considered. The parasite-drag area A_p (= parasite drag/dynamic pressure) is assumed to be constant and, thus, the aircraft parasite-drag coefficient is

$$C_{D_p} = \frac{A_p}{S} \tag{13}$$

where S is the wing area.

If the influence of various airfoils on the wing mass is to be evaluated for a given aircraft configuration, the thicknesses of the airfoils must be considered. The PLW line contains an option for this purpose that allows the wing planform to be alterred such that the absolute thickness of the different wings is the same. To achieve this, a reference thickness t^*/c must be specified and, if an airfoil having a thickness t/c is to be evaluated, the chords are multiplied by t^*/t before any computations are performed. A mass penalty due to the increased wing area that arises from the greater chords is also computed. This procedure allows the influence of the airfoil on the overall aircraft performance to be evaluated in a more realistic manner than if the same planform were used for airfoils having different thicknesses.

Everything else is processed as it is for an FLZW line. The α values in the preceding ALFA line are used. Because the aircraft speed increases rapidly as the lift coefficient decreases, more α values should be specified in the lower lift-coefficient range. The values of v_{max}, ρ, and ν from the preceding FLZW line are used. The print and plot modes for the boundary-layer computation cannot be changed by an PLW line.

NUPA, *NUPE*, and *NUPI* specify options for plotting the computed speed polar (see below).

NUPU = MU (= $a0c$), which is transition mode as described for the FLZW line.

$F_1 = t^*/c$, which is the reference airfoil thickness in percent chord.

> If $F_1 < 0$, $t^*/c = t/c$, which is the thickness of the airfoil being evaluated in percent chord.
>
> If $F_1 = 0$, MU, t^*/c, W^*, DWS, A_p, and the reference planform remain as previously specified.

$F_2 = W^*$, which is the aircraft mass in kg.

$F_3 = DWS$, which is the mass penalty factor in kg/m^2 (see below).

$10^{-3}F_4 = A_p$, which is the parasite-drag area in m^2.

$F_5 = c_1^*$, which is the local chord in m.

$F_6 = db_1$, which is the length of the spanwise section having chord c_1^* in m.

$(F_7, F_8) = (c_2^*, db_2)$ and so on up to $(F_{N-1}, F_N) = (c_{N-1}^*, db_{N-1})$, where $N \leq 14$.

F_{N+1} = k-factor; if $k = 0$, the default value, 1.03, is used.

The wing planform is specified in F_5–F_N by spanwise sections having constant chords. A linearly tapered wing of 15-m span having a root chord of 1.2 m and a tip chord of 0.6 m could, therefore, be described by three, 5-m sections ($db = 5$) having average chords c_i of 1.1 m, 0.9 m, and 0.7 m. The same planform could be described by five, 3-m sections ($db = 3$) having average chords c_i of

1.14 m, 1.02 m, 0.90 m, 0.78 m, and 0.66 m. Note that the sum of all the db values is the span of the aircraft, not the half span.

The chords finally evaluated are

$$c_i = c_i^* \frac{t^*}{t} \tag{14}$$

The wing area is

$$S = S^* \frac{t^*}{t} \tag{15}$$

where the reference wing area S^* is

$$S^* = \sum_i c_i^* db_i \tag{16}$$

The aircraft mass is

$$W = W^* + (S - S^*) DWS \tag{17}$$

If no alteration of the planform is intended, F_1 must be negative, which sets $t^*/c = t/c$.

The speed polars computed by PLW lines can also be plotted. The scales of the axes are adapted to the results.

The results from several PLW lines can be plotted in one diagram. The labelling options consider two different kinds of comparisons:

One airfoil with different PLW lines for evaluating different aircraft layouts.

Different airfoils for evaluating their influence for the same or similar layouts.

Speed polars, which show the sink rate and L/D versus aircraft speed, and power polars, which show the power required (in kW) versus aircraft speed, can be plotted.

If *NUPA* = 1, 2, 6, or 7, the arrays containing the polar results are cleared and the results for the current polar are stored for later processing.

If *NUPA* = 1 or 6, the current polar is plotted in a new diagram, the axes are drawn and labelled, and the diagram is closed. The results for this polar remain available for further plotting.

If *NUPA* = 3 or 8, the results for the current polar are stored and all the polars stored thus far are plotted, the axes are adapted to the maximum and minimum results, and the diagram is closed. The results remain available for further plotting.

If *NUPA* = 4 or 9, the results for the current polar are added to the arrays without first clearing them.

If *NUPA* $<$ 5, the axes do not necessarily include the zero points.

If *NUPA* $>$ 5, the axes include the zero points.

If *NUPE* $\neq$ 0, *NUPE* specifies the symbol number. The symbols and their corresponding numbers are shown in figure 12.

If *NUPE* = 0, the results for the current polar are not stored. If *NUPA* $\neq$ 0, all polars stored thus far are plotted as for *NUPA* = 3 or 8.

If *NUPI* = 0 (or even), a speed polar is plotted.

If *NUPI* = 1 (or odd), a power polar is plotted.

Several options for additional labelling are available as follows.

After *N, the airfoil name can be replaced by the given character string as in other diagrams.

After *S, a character string can be given that indicates the span. The current span is inserted automatically following the explanation. If only *S␣␣ is given, the span and "m" are plotted (i.e., the span is assumed to be in m).

After *W, a character string can be given that indicates the aircraft mass. The current mass is inserted automatically following the explanation. If only *W␣␣ is given, the mass and "kg" are plotted.

After *A, a character string can be given that indicates the wing area. The current wing area is inserted automatically following the explanation. If only *A␣␣ is given, the wing area and "m^2" are plotted.

After *T, a character string can be given that is added at the end of the corresponding line in the key.

In a line that terminates the diagram (i.e., *NUPA* $= 1$ or 3), a character string can be given after *Z that is inserted at the end of the caption.

It should be remembered that the font for capital Greek letters (see ref. [6]) is valid after the airfoil thickness is written and that no space is present between the thickness and the first character of the strings. Thus, the first string after the airfoil name should begin with a space followed by @1 or @2 to specify the desired font.

The caption and the key are positioned where, in most cases, sufficient space exists. It can occur, however, that the caption or the key intersects the curves. Therefore, two options are available by which other positions can be specified as follows.

After *L, two DLFF words can be given that specify the upper, left corner of the key.

After *M, two DLFF words can be given that specify the upper, left corner of the caption.

The coordinates are given in the units of the diagram (i.e., velocity and either sink rate sink or power).

The following example produces the diagram shown in figure 18.

```
REMO11     0 0 0 .3 .3
FXPR     5
NACA 43012         61   40   30   12
ALFA20   1 1.3 1.6 2 2.2 2.4 3 4 5 6 8 10 12 14 15 16
FLZW     3 30 60
PLW 21   3 -1 400 10 .05 .9 6 .7 6 .5 6   *T @1A
FXPR     4
NACA 4412          61   04   40   12
ALFA
PLW 42           *T @1B
FXPR     4
NACA 6412          61   06   40   12
ALFA20   1 1.3 1.6 2 2.4 2.6 3 4 5 6 8 10 12 14 15 16
PLW 33      *T @1C  *S, @1SPAN  *W, @1W=  *A, @1A=  *Z +++  *M70 4.6
```

6.6 PLWA Line

The PLWA line allows the wing area S, the aircraft mass W, and the parasite-drag area A_p specified by the preceding PLW line to be modified. Any number of PLWA lines can succeed one PLW line. The effect of the modifications on the lift and parasite-drag coefficients only is computed.

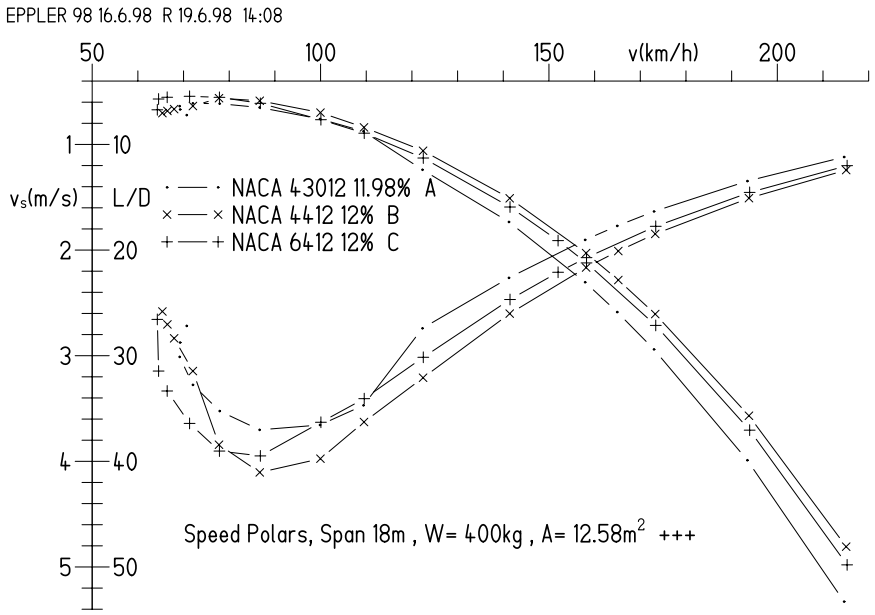

Figure 18: Speed polars of one aircraft with three different airfoils.

Because the lift coefficients are affected, the aircraft speeds and the induced-drag coefficients are also affected. No influence on the Reynolds number from the altered chords and speeds is considered; the profile-drag coefficients from the computations initiated by the PLW line are used.

NUPA, *NUPE*, and *NUPI* specify options for plotting the speed polar, as described for the PLW line.

NUPU $= NMOD$, which is the number of modifications.

$F_1 = \Delta S$, which is the change in wing area in m^2.

$F_2 = \Delta W$, which is the change in aircraft mass in kg.

$10^{-3}F_3 = \Delta A_p$, which is the change in parasite-drag area in m^2.

The code adds $n\Delta S$ to S, $n\Delta W$ to W, and $n\Delta A_p$ to A_p, where $n = 1 \rightarrow NMOD$, and lists the resulting polars. Thus, if $NMOD = 3$, three polars are generated. If only one parameter is to be changed, the other changes must be set to 0.

NUPA, *NUPE*, and *NUPI* perform the same functions as in the PLW line, although some restrictions apply. The PLWA line produces more than one polar if *NUPU* > 1. Such a PLWA line specifies the one value of *NUPA* that will be used for all the polars. If *NUPU* > 1, only *NUPA* $= 4$ or 9 makes sense with respect to the sequence of the plots. Moreover, all the polars resulting from *NUPU* > 1 are plotted with the one symbol specified by *NUPE* in this line. It is, thus, not possible to have different symbols for the curves of the different polars and only one explanation option can be used. Therefore, it is recommended that the plotting option in the PLWA line be exercised only with *NUPU* $= 1$, which means that only one modification of the aircraft parameters is initiated by each PLWA line. There may be more than one PLWA line after a PLW line, of course, and each may exercise the plot option in exactly the same way as the PLW line with no restrictions on the *NUPA* and *NUPE* values.

6.7 CDCL Line

The CDCL line plots the boundary-layer summary (i.e., section characteristics), which contains the lift, drag, and pitching-moment coefficients, including viscous corrections. In addition, the transition and separation locations are shown. The abscissa for the transition and separation curves is x_T/c and x_S/c; the ordinate, c_ℓ. The plotted arc lengths s_T/c and s_S/c along the airfoil surface from the transition point and the separation point, respectively, to the trailing edge are thus $s_T/c > 1 - x_T/c$ and $s_S/c > 1 - x_S/c$.

A CDCL line normally follows an RE line but may also follow an FLZW or PLW line. It should be remembered, however, that the Reynolds number varies with the lift coefficient in the latter cases. The curves plotted correspond to the various chords c and, for the FLZW line, to the twist angles Θ as well.

The curves for the first MU-R or c-Θ pair specified in the preceding RE , FLZW, or PLW line are solid followed by up to five different types of broken lines, each corresponding to a different pair. The types of broken lines drawn can be changed.

The results from several CDCL lines can be plotted in one diagram, as described for the DIAG line, Chapter 5.6, and the STRK line, Chapter 5.2. Because the frame dimensions must be determined when the diagram is opened, if the diagram is to remain open for further plotting, it may be necessary to specify a larger frame, which is accomplished by means of the F-numbers in the CDCL line that opens the diagram.

The minimum c_d along the c_d-axis is not necessarily zero. If the minimum drag coefficient in the results to be plotted by the CDCL line that opens the diagram is greater than 0.01, which occurs frequently for low Reynolds numbers, the minimum c_d along the c_d-axis is automatically shifted in steps of 0.005.

There are options for additional labelling similar to those for the DIAG line. The CDCL line also allows the insertion of experimental data.

If *NUPA* = 1–8, the types of broken lines can be specified (see below).

If *NUPA* = 9, the width of the plot can be specified or an empty grid can be plotted (see below).

Thus, if *NUPA* $\neq$ 0, a diagram is not plotted; only the parameters for the line types or the scale factor are specified and, therefore, another CDCL line with *NUPA* = 0 must be given to plot the boundary-layer summary.

If *NUPA* = 0, the boundary-layer summary is plotted.

If *NUPE* = 1–8, experimental data are read from the succeeding lines (see below). This option is valid only for CDCL lines that open the diagram (i.e., *NUPU* = 0, 1, 4, or 5).

If *NUPE* = 9, only experimental data are plotted. The frame and the axes are specified by the F-numbers (see below).

NUPI is ignored.

NUPU specifies the options for plotting the results from more than one boundary-layer computation in one diagram and the insertion of the explanation blocks.

If *NUPU* contains two digits ab, $LAUF = a$, where,

> if LAUF $\neq$ 0, the line types of the current MU-R pairs and the labels are included in the key (see below). The line types for the next CDCL plot are not reset to the first line type but, rather, set to the next one in sequence.

if LAUF = 9, the airfoil thickness is omitted after the airfoil name as are the default explanations of the line types.

The second digit b of *NUPU* initiates the following.

If *NUPU* = 0 or 4, only one boundary-layer summary is plotted, the axes are drawn and labelled, and the diagram is closed. The frame is adapted to this summary; no further input is necessary.

If *NUPU* = 1 or 5, the diagram is opened, one summary is plotted, and the diagram remains open to further plotting.

If *NUPU* = 2, one summary is plotted into the open diagram, the axes are drawn, the diagram is then closed to further plotting.

If *NUPU* = 3, one summary is plotted into the open diagram, which remains open to further plotting.

Two explanation blocks can be included. The first one explains the symbols for the laminar separation bubble warning. The second one provides brief definitions of the abbreviations "T.", "S.", "U.", and "L.". The explanation blocks are plotted by increasing *NUPU* by 4 in the CDCL line that initiates the diagram. The second block is omitted if the option for inserting labels near the curves, as described below, is not exercised. Thus, if *NUPU* = 4 or 5, a diagram is opened as with *NUPU* = 0 or 1 and, in addition, the explanation blocks are plotted.

6.7.1 Extension of Frame

The upper and lower edges of the frame are determined when only the c_ℓ values of the first summary (i.e., CDCL line with *NUPU* = 1 or 5) are available. If *NUPE* = 1, experimental data will be inserted later. Additional CDCL lines (with *NUPU* = 2 or 3) may plot summaries in the same diagram that include c_ℓ values that exceed the minimum or maximum c_ℓ of the first summary. Therefore, F_1–F_5 of the CDCL line opening the diagram (i.e., *NUPU* = 0, 1, 4, or 5) allow the frame to be extended and the key in the upper, left corner to be shifted. First,

$$\begin{aligned} c_{\ell,max} &= max\{c_{\ell_i}, F_4\} \\ c_{\ell,min} &= min\{c_{\ell_i}, F_5\} \end{aligned} \tag{18}$$

are evaluated. Thus, F_4 and F_5 specify the minimum c_ℓ range, which may be extended by the c_{ℓ_i} but not reduced. Both $c_{\ell,max}$ and $c_{\ell,min}$ are rounded to one digit after the decimal point to coincide with the tic marks at along the c_ℓ-axis. The default values are $F_4 = F_5 = 0$.

Then, F_1–F_3 allow the upper and lower edges $c_{\ell,up}$ and $c_{\ell,low}$ of the frame to be shifted relative to $c_{\ell,max}$ and $c_{\ell,min}$, respectively.

F_1 shifts the key in the vertical direction; $F_1 > 0$ shifts it up; $F_1 < 0$, shifts it down.

$F_m = max(F_1, F_2)$ extends the upper edge $c_{\ell,up}$ of the frame.

F_3 extends the lower edge $c_{\ell,low}$ of the frame.

$$\begin{aligned} c_{\ell,up} &= c_{\ell,max} + max\left\{F_1 + 0.4, F_m + 0.15 + 0.41\ BF\right\} \\ c_{\ell,low} &= min\left\{-0.25, c_{\ell,min} - 0.15 - F_3\right\} \end{aligned} \tag{19}$$

where $BF = 1$ if the explanation blocks are to be plotted and $BF = 0$ otherwise. The values of F_m and F_3 should be as large as the amount by which succeeding c_{ℓ_i} exceed $c_{\ell,max}$ and $c_{\ell,min}$.

6.7.2 Labelling

Without additional input, the axes are labelled and the airfoil name is plotted in the upper, left corner. After the name, the thickness, and, if present, the turbulator locations are plotted. Below this, the line types and their corresponding explanations are plotted in a key. Normally, these explanations contain the Reynolds numbers from the RE line or the chords from the FLZW line that precedes the CDCL line that terminates the diagram (i.e., *NUPU* = 0, 2 or 4). For each Reynolds number or chord, the line type is drawn followed by the Reynolds number or chord and the roughness factor r, if it is not zero.

The explanation is supplemented by "without b.d." if the bubble-drag contribution is not included in the plotted c_d values; "with b.d. u." or "with b.d. l." is added if the bubble drag is included for only the upper or lower surface, respectively.

Labels can be placed near the transition and separation curves for the upper and lower surfaces as well as near the c_ℓ and c_m curves. The input for this option begins at least three columns after the last F-number or in column 13 or higher if no F-numbers are specified. One or more DLFF sentences can be given, which contain up to 14 groups of three DLFF words as follows.

k, c, $\pm e$, k, c, $\pm e$ ...

These groups determine the positions of the six labels "T.U.", "T.L.", "S.U.", "S.L.", "$c_\ell(\alpha)$", and "$c_m(\alpha)$", in that order. The abbreviations stand for "transition upper surface", "transition lower surface", "separation upper surface", and "separation lower surface", respectively. The groups of three numbers contain

k, which is the number of the MU-R pair in the preceding RE line or the c-Θ pair in the preceding FLZW line.

c, which, for the first five labels, is the c_ℓ value where corner e of the label rectangle will be located near the k^{th} curve. For the last label, c is the α value for corner e, in which case, $c = 0$ is not useful and, therefore, $c = 0$ plots the label at the left end of the k^{th} c_m curve if $e = 0$ and at the right end if $e = 1$.

$|e|$ is the corner number (see "DIAG Line", Chap. 5.6).

If $e > 0$, the next group of numbers specifies the position of the next label.

If $e < 0$, the next group numbers plots the same label in a different position. Thus, it is possible to plot one label in several positions. The last label $c_m(\alpha)$ alone can be plotted only once. For this label, a negative e supresses the "(α)", which is occasionally necessary because of the limited space near the c_m curves.

If $k = 0$, the corresponding label is not plotted. The values c and e can be omitted if $k = 0$, after which the input must begin with a new DLFF sentence. Its first word is the value k of the next group of three numbers. Thus, in this case, two spaces must be input between the last word of a group and the first one of the following group. If a group has three numbers, the next group can follow without beginning a new DLFF sentence.

The corner e of the label rectangle is positioned at the lower or upper end of the k^{th} curve, if the specified c is less than the minimum or greater than the maximum value of c_ℓ (or α), respectively, along the corresponding curve.

Occasionally, the c_ℓ value where the corner e is to be positioned occurs more than once along the curve, for example, if c_ℓ decreases beyond stall. In this case, the first occurrence of the c_ℓ value in the sequence of the currently valid ALFA line is selected. The second occurrence can be selected

by increasing k by 5. Thus, $k = 7$ specifies the second occurrence of the c_ℓ value c along the curve specified by $k = 2$.

If k is negative, the label-rectangle position is independent of the curve. In this case, e specifies the horizontal coordinate x/c of the upper, left corner of the label rectangle and c, the c_ℓ value.

After the group of numbers that inserts the last label $c_m(\alpha)$, up to six more DLFF words W_L–W_{L+5} can be given.

W_L and W_{L+1} contain the horizontal and vertical positions, respectively, of the upper, left corner of additional text given after *E, which can be given at least three columns after the last DLFF word. The horizontal position is given in the units of the c_d-axis (i.e., between 0 and 35); the vertical position, in the units of the c_ℓ-axis. An example of this option is given in figure 19, where "1935" is plotted at 12, 0.5.

W_{L+2}–W_{L+5} specify a position of the explanation blocks different from the default position. For example, if high c_ℓ values occur, the explanation blocks can be placed within the diagram. If W_{L+2}–W_{L+5} are not zero, they specify the coordinates of the upper, left corners of the explanation blocks. W_{L+2} and W_{L+3} position the block that explains the bubble warnings; W_{L+4} and W_{L+5}, the block that defines the abbreviations. W_{L+2} and W_{L+4} specify the horizontal positions; W_{L+3} and W_{L+5}, the vertical positions. The positions of both blocks must be specified if the default position of either is changed.

The *N and *Z options are exercised as described under "DIAG Line", Chap. 5.6.

After *i, where $i = 1, 2, \ldots, 7$, additional text can be given that will be inserted between the i^{th} line type and its explanation. Here, i may be greater than the total number of line types, in which case, additional text lines are plotted below the line types and their explanations. This option is primarily useful in conjunction with $LAUF \neq 0$ or when experimental results are included. Here also, an "F" at the end of the string plots the current flap data and *iF adds only the flap data to the labels. After the flap data, the labels "R =" or "c =" are plotted to clarify the succeeding numbers.

The options may require more than one input line. An "F" can be inserted in the DLFF words, which continues the input on the next line. Moreover, in the first line that contains an * option, ** can be given and then a second line containing further * options can be given.

6.7.3 Experimental Data

Experimental data can be included in the diagram as follows.

If *NUPE* = 0–8 and *NUPU* = 0, 1, 4, or 5 (i.e., a CDCL line that opens the diagram), the frame dimensions and the airfoil name are determined by the results to be plotted by this line, including the experimental data if *NUPE* $\neq 0$ (see below).

If *NUPE* = 9, *NUPU* is ignored and the frame dimensions and the airfoil name must be specified in the CDCL line. The values of $c_{\ell,max}$ and $c_{\ell,min}$ are given in F_4 and F_5, respectively, as previously discussed. The airfoil name is specified after *N, as in other lines.

$F_4 = c_{\ell,max}$, which determines the upper edge of the frame, as previously discussed.

$F_5 = c_{\ell,min}$, which determines the lower edge of the frame, as previously discussed.

$F_6 = c_{d,min}$, which shifts the c_d-axis as is normally performed automatically if $c_{d,min} > 0.01$. The default value is 0.

$F_7 = \alpha_{min}$, which determines the left end α_{left} of the α-axis as follows

$$\alpha_{left} = max\{\alpha_{min} - 4°, -10°\}$$

$F_8 = \alpha_{max}$, which determines the right end α_{right} of the α-axis as follows

$$\alpha_{right} = min\{\alpha_{max} + 3°, 19°\}$$

$F_9 = t/c$, which is the airfoil thickness in percent chord. If this value is not specified, the thickness is not plotted after the airfoil name.

$F_{10} = c_{m,min}$, which is the minimum pitching-moment coefficient. The default value is -0.1.

$F_{11} = c_{m,max}$, which is the maximum pitching-moment coefficient. The default value is 0.

The experimental results are specified in additional lines, which are not in the normal format. In the first column, they contain a single-letter identifier "L", "D", "M", "T", "A", "X", "Y", or "E". Following the identifier, they contain the Lift coefficients, Drag coefficients, Moment coefficients, Transition locations x_T/c, or Angles of attack, in degrees. The E line terminates the experimental data.

Occasionally, drag or transition data are given for α values instead of c_ℓ values. The α values must then be transformed into c_ℓ values, which can be accomplished by means of Y lines. The Y line contains α values that are transformed into c_ℓ values using the preceding A and L lines. Following the Y line, D and T lines with "A" in the second column are permitted, in which case, the c_ℓ values are determined from the Y line, not the preceding L line. An X line is not necessary but is allowed and treated as a TA line.

All lines, except the E line, contain up to three DLFF sentences, beginning in column 4. The first DLFF sentence normally contains $N > 1$ experimental values as DLFF words. For example,

D␣␣.0048␣.0049␣.0051␣.0060␣.0075␣␣

Preceding the DLFF sentence, which contains five words in this example, a DLFF sentence containing only one word can be given. This word specifies the factor by which all the words in the succeeding sentence are divided. For example,

D␣␣10000␣␣48␣49␣51␣60␣75␣␣

which is equivalent to the previous example. In many cases, it is easier to use the factor. With the factor, $N = 1$ experimental value is allowed in the second DLFF sentence.

The D, A, and T lines specify abscissas, whereas the L and M lines specify ordinates. The data remain available until other data are read. Thus, for example, one set of c_ℓ values can be used for both c_d and α values.

A third DLFF sentence may be included following the experimental data. It contains only one word that specifies the symbol number. The symbols are connected by straight lines if the distance between the points is sufficient. If the number of abscissas and ordinates is not the same, the longer set is truncated, starting with the last value. The truncation applies only to the diagram; all the data remain available for further plotting.

If a symbol number is specified, two symbols and a connecting line are plotted in the key. The explanation for this line can be specified in the CDCL line, as previously explained, or following *T, which must be given at least three columns after the symbol number. The continuation option "F" can be used, if necessary.

The symbols are shown in figure 12. A flag perpendicular to the curve is not available in this case.

For example,

```
D␣␣10000␣48␣49␣51␣60␣75
L␣␣10␣␣1␣3␣5␣7␣9␣11␣␣5␣␣␣*T@1Exp.␣1
A␣␣-1␣0␣1␣2␣3␣4␣␣5
E
```

which plot five data points as c_d versus c_ℓ using symbol 5. The c_ℓ value of 1.1 is not used. The explanation for this line is "Exp. 1". Then, six data points are plotted as c_ℓ versus α, also using symbol 5. The c_ℓ value of 1.1 is used in this plot.

6.7.4 Line Types

The line types j are defined by lengths ℓ_i in mm of the lines and the spaces. Line type $j = 1$ is a solid line. For $j > 1$, the line type is specified by m_j numbers from the array ℓ_i (12 floating-point numbers), beginning with $i = n_j$. The first length ℓ_i, where $i = n_j$, is drawn; the next length ℓ_{i+1}, is not drawn (i.e., a space); and so on. After the last ℓ_i, where $i = n_j + m_j - 1$), the cycle is repeated starting with the first ℓ_i. The variable m_j must be divisible by 2 and less than 9. The variables m_j and n_j are stored in arrays containing five integers each.

The default values for j = 2, 3, 4, 5, 6 and i = 1, 2, ..., 12 are

m_j = 2, 4, 6, 8, 2 $\qquad$ n_j = 1, 3, 3, 3, 5
ℓ_i = 5, 2, 10, 2, 2, 2, 2, 2, 2, 2

which specify the following line types (the line segments are underlined, the space segments are not)

$j = 1$ ——————————————————
$j = 2$ — — — — — — — — — — 5mm, 2mm
$j = 3$ ——— – ——— – ——— – ——— – 10mm, 2mm, 2mm, 2mm
$j = 4$ ——— – – ——— – – ——— – – 10mm, 2mm, 2mm, 2mm, 2mm, 2mm
$j = 5$ ——— – – – ——— – – – 10mm, 2mm, 2mm, 2mm, 2mm, 2mm, 2mm
$j = 6$ – – – – – – – – – – – – – – – – 2mm, 2mm

If *NUPA* $\neq 0$ and $F_2 \neq 0$, new values for ℓ_i, m_j, and n_j are specified. In this case, the five digits of F_1 specify n_2–n_6; the five digits of F_2, m_2–m_6; and F_3–F_{14}, the ℓ_i.

For example,

```
CDCL1␣␣␣␣␣␣11553␣24422␣5␣2␣.5␣2␣10␣2␣2␣2
```

which specifies the following line types.

$j = 1$ ——————————————————
$j = 2$ — — — — — — — — — — 5mm, 2mm
$j = 3$ —— · —— · —— · —— · —— · —— · 5mm, 2mm, 0.5mm, 2mm
$j = 4$ ——— – ——— – ——— – ——— – 10mm, 2mm, 2mm, 2mm
$j = 5$ ——— ——— ——— ——— ——— 10mm, 2mm
$j = 6$ · 0.5mm, 2mm

6.7.5 Scaling

The width of the CDCL diagram is normally 379 mm. This width is multiplied by a scaling factor SCF. The default value of SCF is 1. If *NUPA* = 9 and $F_1 > 0$, $SCF = F_1$.

For example,

```
CDCL9␣␣␣␣␣␣␣␣.7
```

which sets SCF to 0.7. Note that only the scale is changed; no plotting is performed.

6.7.6 Empty Grid

An empty grid, plotted on a transparency, is useful for the evaluation of the CDCL diagram.

If *NUPA* = 9 and $F_1 < 0$, a grid with $\Delta c_{\ell,1} = 0.1$ and $\Delta c_{d,1} = \Delta c_{\ell,1}/100$ is plotted. A second grid with $\Delta c_{\ell,2} = 0.5$ and $\Delta c_{d,2} = \Delta c_{\ell,2}/100$ is plotted to make every fifth line bolder. The first grid is plotted with line width $PENAX$; the second, with 2 $\times PENAX$. The value of $PENAX$ can be specified in a REMO line (see Chap. 2.2.2).

If $F_2 \neq 0$, $\Delta c_{\ell,1} = F_2$.

If $F_3 \neq 0$, $\Delta c_{\ell,2} = F_3$.

6.7.7 Examples

The first example plots a diagram for the NACA 23012 airfoil (fig. 19). The diagram remains open for the plotting of results for the same airfoil with a simple flap. Because the flapped airfoil is expected to produce higher c_ℓ values, the key and, accordingly, the frame are extended upward by $F_1 = 0.6$. The option with $LAUF \neq 0$ is exercised to include the explanations for the first plot as well. The explanation block is included because *NUPU* = 5 in the first CDCL line and labels are inserted near the curves.

Both CDCL lines contain an "F" at the end, which continues the DLFF words in column 1 of the next line. There, three spaces must be present to terminate the previous DLFF sentence. Additional text can then be inserted in the third and fourth line explanations. The ** option is used in the second CDCL line to include another line, which, in this case, is not necessary.

Note that the text in the second line explanation specified by *BF plots only an additional "b". The "F" normally causes the flap data to be inserted but, in this case, no flap data are available. Also, the error in the input NACA airfoil name, 2301W, is corrected because the name is determined from the input parameters.

```
REMO1           *P
FXPR     5
NACA 2301W         61   20   30   12
ALFA     8 0 2 4 6 8 10 12 14
RE         3 1000 3 2500
CDCL    15 .6       1 .25 2 1 .35 1 6 1.04 1 0  2 1.1 3 1 4.5 3 F
    *1FB    *2BF
FLAP       25 .5 3 10
ALFA     8 4 6 8 10 12 14 16 18
RE
CDCL     6          1 .9 2 1 .8 1 2 2 3 0  1 1.5 1 1 0 0 12 .5 F
      **3F   *4F
     *E1935
ENDE
```

The second example illustrates the insertion of labels for two different airfoils SU1 and SU2 plotted in one diagram (fig. 20). This example also demonstrates the independent evaluation of the effect of laminar separation bubbles on the upper and lower surfaces. Again, $LAUF \neq 0$ in the first CDCL line and the frame is extended by 0.6 to accommodate the expected higher c_ℓ values of the second

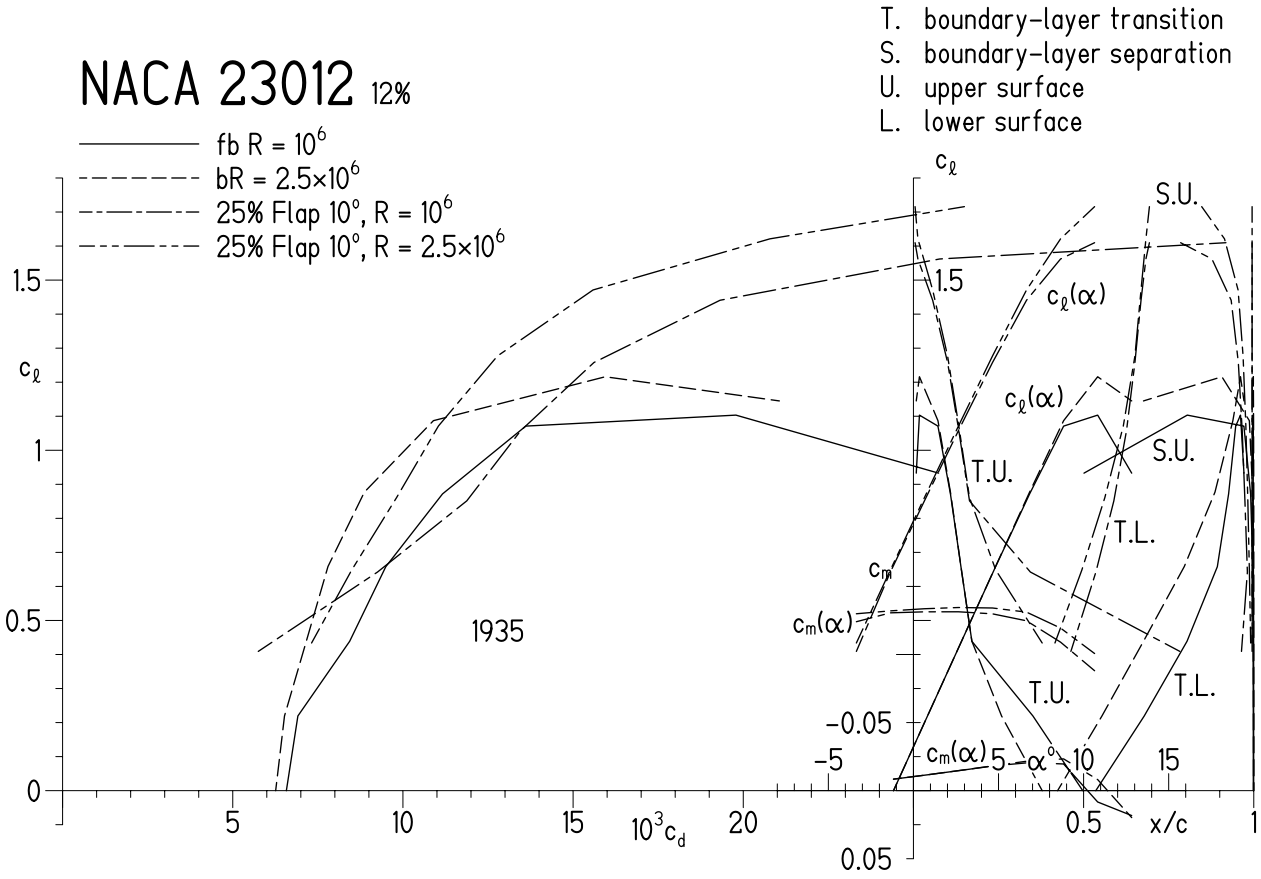

Figure 19: Diagram for unflapped and flapped NACA 23012 airfoil.

airfoil. (In this case, it would have been simpler to evaluate the more highly cambered SU2 airfoil first; then no extension of the frame would have been necessary.) The airfoil name is changed to include both airfoil names. The thickness of the second airfoil, 15.87%, is plotted after the thickness of the first airfoil using the *Z option. The line explanations are supplemented by the corresponding airfoil names.

For each airfoil, three boundary-layer calculations are performed for one Reynolds number $R = 600{,}000$: one with $MU = 3$, one with $MU = 3.04$, and one with $MU = 3.02$. The drag is thus computed once including the bubble drag from both surfaces, once including no bubble drag, and once including bubble drag from only the upper surface, which is denoted in the corresponding line explanation by an additional "u.". The difference between the polar curve exhibiting the lowest drag and the middle curve is, therefore, the bubble drag from the upper surface. The difference between the middle curve and the curve exhibiting the highest drag is the bubble drag from the lower surface. At high lift coefficients, the second airfoil exhibits bubble drag only from the upper surface. Thus, the middle and highest-drag curves coincide.

```
REMO1            *PTEST FOR USERS GUIDE
TRA1      1 15.5 4.1 2 5 2 6 2 7.1 2 8.3 2 9.6 2 11 2 12.5 0 14 60 3
TRA25     1 4 15.5 2 .7 .68 4 13.5 2 .3 .68 1 .3 0     18.3%
ALFA      8 0 2 4 6 8 10 12 14 16
RE          3 600 3.04 600 3.02 600
CDCL     15 .6       2 1.3 4 1 1.2 1 1 2 2 1 .1 2 2 .2 3 1 0 F
0    *1@1SU1,    *2@1SU1,   *3@1SU1,   *NSU1, SU2   *Z, 15.87@3Z
TRA1      2 20.5 5 2 6.5 2 8 2 9.5 2 11 2 12.5 0 14 60 8
TRA25     2 4 20.5 2 .7 .68 4 16.5 2 .3 .68 1 .3 0       15.87%
ALFA      8 5 7 9 11 13 15 17 19 21
RE
CDCL      6          2 1.9 4 1 1.7 1 2 5 3 0  2 1.9 1 1 0 F
1     *4@1SU2,    *5@1SU2,    *6@1SU2,
```

The third example illustrates the insertion of experimental data (fig. 21). Note that the line ex-

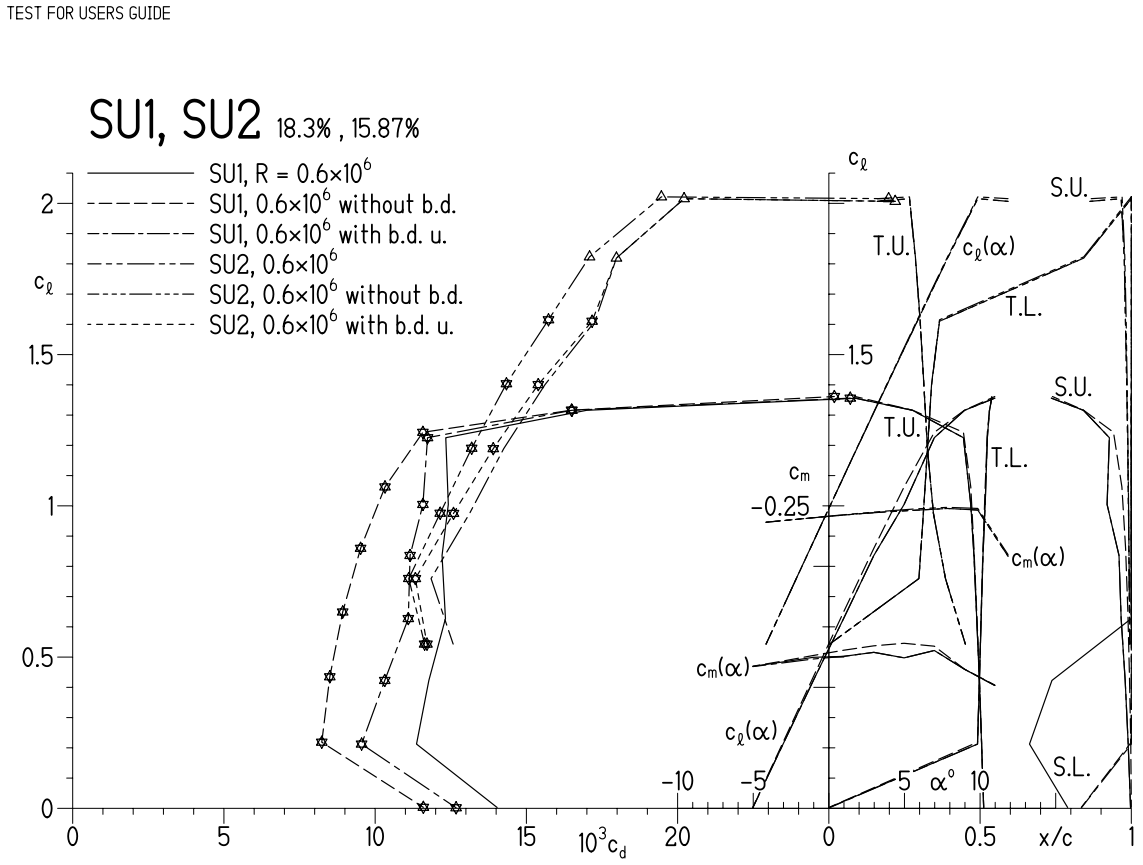

Figure 20: CDCL plot for SU1 and SU2 airfoils.

planation for the experimental data (ref. [14]) is given after *3 in the CDCL line, although only two MU-R pairs are specified. Because bubble drag is likely for the given Reynolds number, the computations have been performed with and without the bubble-drag option. It is unnecessary to specify the option for bubble drag from the upper surface only because the lower surface exhibits no bubbles within the low-drag, lift-coefficient range.

```
REMO11      0 0 0 .3 .3   *P@1TEST E 387
TRA1   387 14.5 -11.5 16.5 -6 18.5 -.5 20.5 5.2 22.5 5.5 24.5 5.9
TRA1   387 26.5 6.5 28.5 7.3 30.5 8.5 0 9.2 33.5 2.5 35.5 3.9 37.5 4.9
TRA1   387 39.5 5.6 41.5 6.15 43.5 6.5 60 6.7
TRA21  387 5 0 0 0 1 4 0 0 0 1 0 0 0 2
ALFA20  14 1 1.5 2 3 4 5 6 7 8 9 10 11 11.5 12
RE          3 200 3.04 200
CDCL 1              1 .8 1 1 .25 3 1 1.1 4 0  1 .7 1 1 3 2
L  100  -9 16 23 35 56 67 85 97 108 115 118    RE=200 000
D  10000  210 130 94 98 113 122 130 128 132 169 250  6   *T@1Exp. Delft
E
```

The fourth example illustrates the insertion of experimental data where more than one MU-R pair

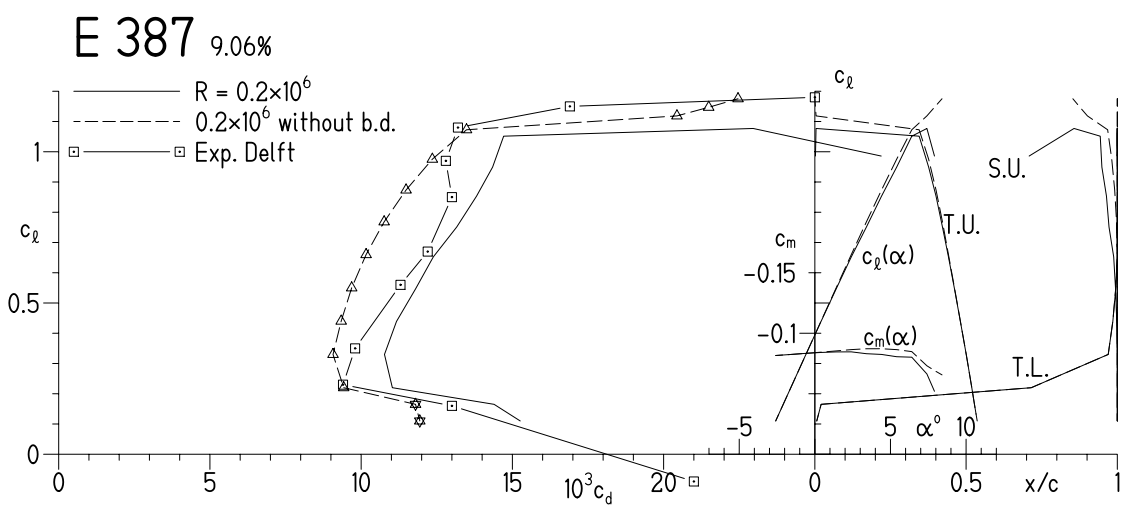

Figure 21: Diagram for E 387 airfoil, including experimental data.

is specified (fig. 22). The experimental data are fictitious. The key is shifted upward by $\Delta c_\ell = 0.2$ because it would otherwise have interfered with the curves.

```
REMO1             *P@1Test Exp. Data
TRA1     8 27.5 10 29.5 11 0 12 60 4
TRA26    8 4 17.5 2 -1 .7 4 17.5 2 -1 .7 6 0 0
ALFA20  11 2 3 4 6 8 10 11 12 13 14 15
RE          3 2000 3 6000
CDCL 1          1 .5 2 1 1.2 1 1 2 4 0  2 .25 3 2 6 3
L  100  20 30 70 100 130 140
D  10000  100 75 80 85 95 200  12    *T@1Exp. Re = 2@3M10@H6@J
A  10  -40 -30 10 45 70 90  4
L  100  10 30 70 100 125 150
D  10000  100 60 62 65 105 160  6    *T@1Exp. Re = 6@3M10@H6@J
E
```

The final example plots a diagram containing only experimental data (fig. 23).

```
CDCL 9      -.3 0 0 1.2 -.1 .011 -8 13 16.01   *NExonly
L  100  12 23 34 45 56 67 78 89 100 105
D  10000  123 98 94 104 112 119 125 134 160 240  F
6   *T@1Special Experiment
T  100  90 86 82 78 74 70 65 60 50 10  6
A  10  -80 -67 -54 -41 -30 -19 -8 3 40 90  6
Y  10  -70 -60 -50 -40 -20 0 5 6 10 30
M  100  -5 -5 -6 -6 -6 -7 -7 -7 -8 -4  6
TA 100  10 50 70 80 85 90 95 99 100 100  6
E
```

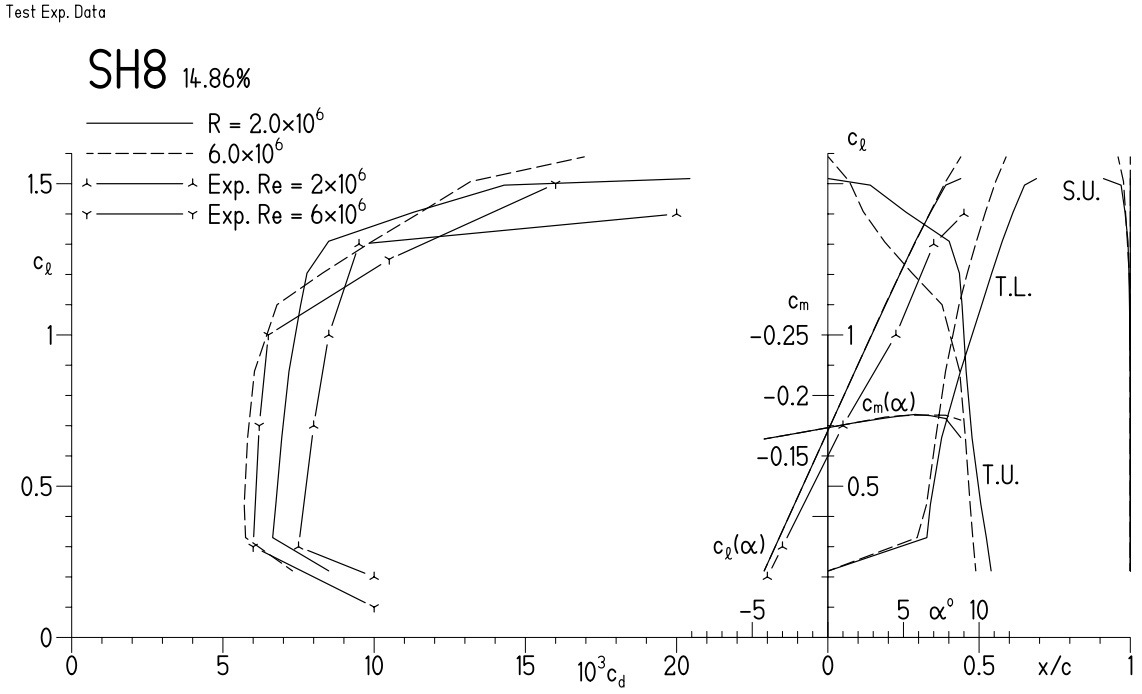

Figure 22: Diagram for two Reynolds numbers, including experimental data.

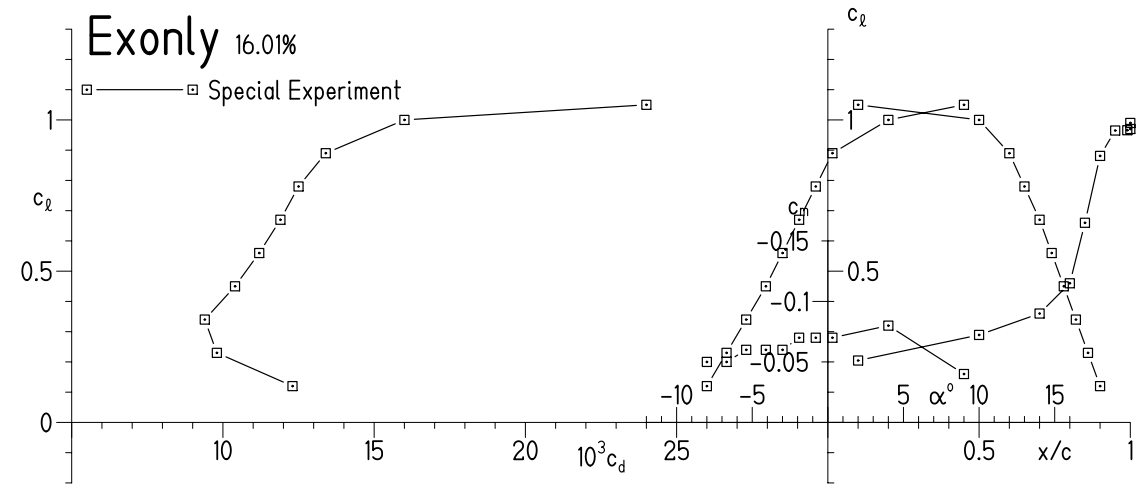

Figure 23: Diagram containing only experimental data.

6.8 DPIT Line

The DPIT line initiates a boundary-layer displacement iteration. Because the iteration process can diverge, the DPIT line should normally specify only one iteration. A maximum of five angles of attack from the currently valid ALFA line can be specified for the displacement iteration. The succeeding RE (or FLZW or PLW) line initiates the normal boundary-layer computation for all α values in the ALFA line (without displacement iteration). The displacement thickness is then smoothed and added to the airfoil contour for all α values specified in the DPIT line and for all Reynolds numbers specified in the RE line. The 'modified' airfoil shapes are then analyzed using the panel method. The resulting $c_\ell(\alpha)$ and $c_m(\alpha)$ are stored. The c_d and c_ℓ values from the normal (i.e., uniterated) computation are listed and plotted; only the α and c_m values are alterred.

If no displacement iteration is performed, the viscous effects are assumed to reduce the lift-curve slope from the potential-theory value to 2π. The displacement iteration determines this reduction

from the displacement effect. Therefore, it is possible that the lift-curve slope after the displacement iteration is greater than 2π, which occurs in experiments as well.

The linear portions of the lift and moment curves are adapted to least-squares fits of the values from the displacement iteration. The correction due to boundary-layer separation is then added (see ref. [1]).

The modified values α_c are listed in the boundary-layer summary as "AC = ...". If no displacement iteration is performed, $\alpha_c = \alpha$.

The least-squares fits of the lift and moment curves are undefined if the displacement iteration is performed for only one α. In this case, the slopes of the curves are taken from the uniterated computations and only a horizontal translation of the curves is performed.

If only two α values are specified for the displacement iteration, the least-squares fits are merely straight lines through two points. If one of these points corresponds to an α at which extensive separation occurs, the corresponding c_ℓ will be reduced considerably and the least-squares fit will be unrepresentative of the linear portion of the lift curve. It is, therefore, recommended that the displacement iteration be performed only for α values within the linear portion of the lift curve (i.e., for α values at which no significant separation occurs).

The DPIT line must immediately precede a line initiating a boundary-layer computation (i.e., RE , FLZW, or PLW line).

NUPA, *NUPE*, *NUPI*, and *NUPU* are ignored.

If F_1–$F_5 > 0$, the F-numbers specify the angles of attack for which a displacement iteration is performed and also the plot mode mbt. The F_i are given as $abc.de$, where

> abc is interpreted as an integer n. A displacement iteration is performed for the n^{th} angle of attack in the preceding ALFA line and for each Reynolds number in the immediately succeeding RE , FLZW, or PLW line.
>
> If $d > 0$, a diagram containing the airfoil contour, including the displacement thickness, and the velocity distribution for the specified angle of attack is plotted after each displacement iteration. The plot mode mbt is set to $d - 1$ and interpreted as described under "DIAG Line", Chapter 5.6, and reviewed below. The RE , FLZW, or PLW line must specify only one Reynolds number if $d = 2$ or 3.
>
> If $d = 1$, one set of data is plotted, axes are drawn, and the diagram is terminated (i.e., closed to further plotting).
>
> If $d = 2$, one set of data is plotted and the diagram remains open to further plotting.
>
> If $d = 3$, one set of data is plotted into the open diagram, axes are drawn, and the diagram is terminated.
>
> If $d = 4$, one set of data is plotted into the open diagram, which remains open to further plotting.
>
> If $e \neq 0$, e displacement iterations are performed for the angle of attack specified by abc. Note that $e = 0$ and $e = 1$ are equivalent. The specification of $e > 1$ is not recommended.

If $F_5 < 0$, the curvature of the displacement surface $d^2\delta_1/dx^2$ is limited to $SLM = -0.bcde$. This limit is used until it is reset by another DPIT line with $F_5 < 0$. Only four angles of attack can be specified in DPIT lines with $F_5 < 0$.

The DPIT line is valid for only one airfoil. A TRA2, FXPR, or FLAP line invalidates the DPIT line.

A new DPIT line must be given if a displacement iteration is to be performed for the new or flapped airfoil.

An important restriction applies to the performance of multiple displacement iterations (i.e., $e > 1$). If $e > 1$ is specified in one or more of the F-numbers, the succeeding RE line must contain only one Reynolds number; similarly, the succeeding FLZW line must contain only one chord. If, as recommended, only one displacement iteration is initiated by each F-number (i.e., $e = 0$ or 1), no restriction applies to the RE or FLZW lines.

The first example plots the results of the displacement iterations for $R = 3 \times 10^6$ at $\alpha = 2^\circ$ and 8° into the diagram that remained open after the uniterated velocity distributions were plotted (fig. 24). Only one Reynolds number is permitted because the second F-number in the DPIT line must specify plot mode $mbt = 3$, which cannot be specified more than once. Figure 24 illustrates not only the effect of the displacement iteration on the velocity distribution but also on the airfoil contour. Slight irregularities in the iterated velocity distributions occur near the transition locations; these also occur in experiments.

```
REMO1                *P
TRA1      9 0 10 60 3
TRA26     9 4 16.5 2 -1 .6 4 16.5 2 -1 .6 6 0 0 0
ALFA      2 2 8
DIAG      1         -1 .3 1 2 .6 2 2 -.4 4
ALFA      9 0 2 4 6 8 10 12 14 16
DPIT        2.40 5.30
RE          3 3000
```

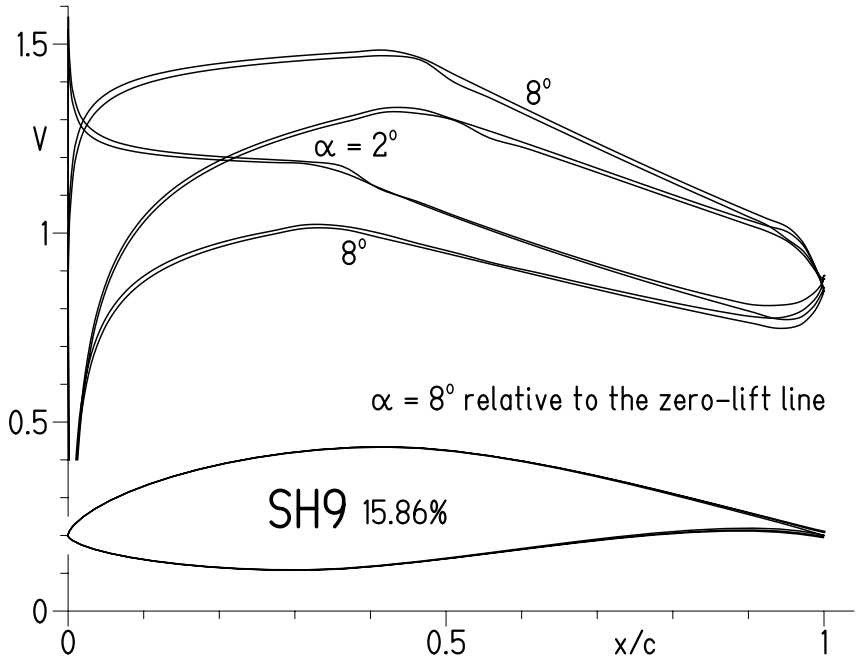

Figure 24: Effect of displacement iteration on velocity distributions.

In the second example, the first DPIT line specifies two α values, the second and the seventh (i.e., $\alpha = 2^\circ$ and 12°), for displacement iterations. The succeeding RE line and the CDCL line with *NUPU* $= 1$ initiate the diagram shown in figure 25, to which results without iteration are later added. The iteration affects only the lift and moment curves.

```
REMO1             *PDPIT TEST
TRA1      9 0 10 60 3
TRA26     9 4 16.5 2 -1 .6 4 16.5 2 -1 .6 6 0
ALFA      1 0 2 4 6 8 10 12 14 16 18
DPIT        2 7
RE  120     3 1000
CDCL     81 -.3      *1@1With displ. it.
DPIT        0
RE          3 1000
CDCL     82    2 1.05 4 2 .3 3 1 1.4 4 0  2 .25 3 2 -10 4
```

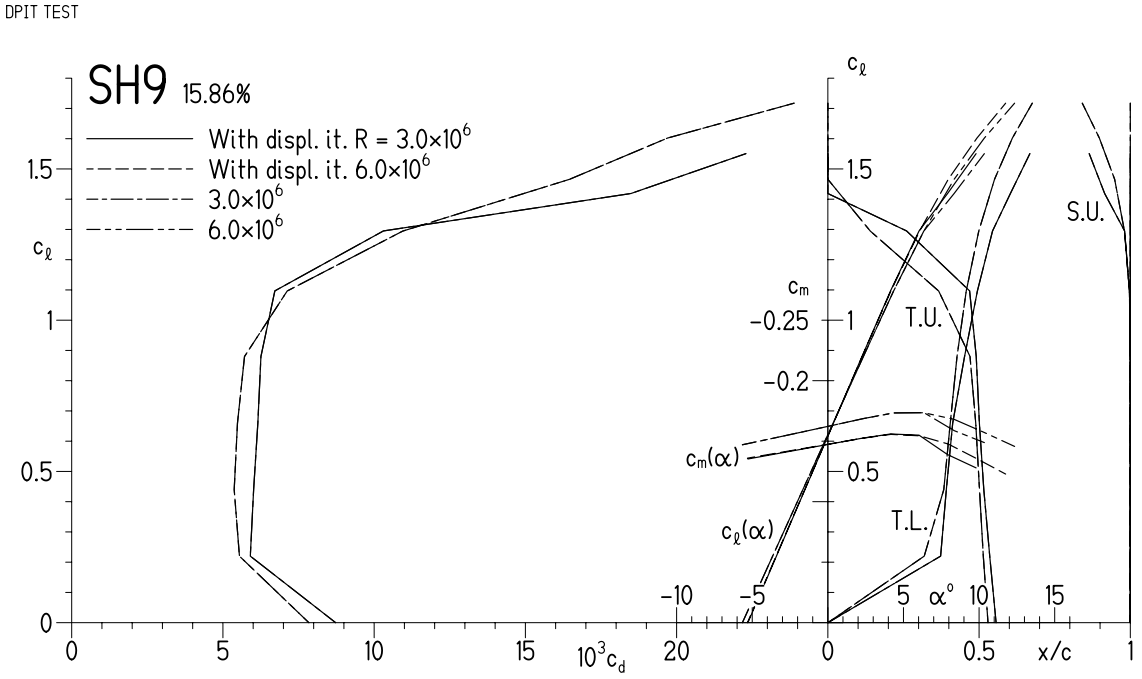

Figure 25: Boundary-layer summary diagram with and without displacement iteration.

7 Rules for Input and Flow Chart

7.1 Input-Line Sequence

The following table presents an input-line summary along with rules for the sequence of the input lines.

Line	Must be preceded by
REMO	—
TRA1	—
TRA2	TRA1
RAMP	TRA1
ABSZ	—
FXPR	—
PAN	TRA2
FLAP	TRA2 or FXPR
ALFA	TRA2 or FXPR
PUXY	TRA2 or FXPR
DIAG	ALFA

Line	Must be preceded by
STRD	—
STRK	STRD, TRA2 or FXPR
EHNN	—
RE	ALFA
FLZW	ALFA
PLW	FLZW
PLWA	PLW
CDCL	RE or FLZW or PLW
MACH	—
DPIT	ALFA

7.2 Flow Chart

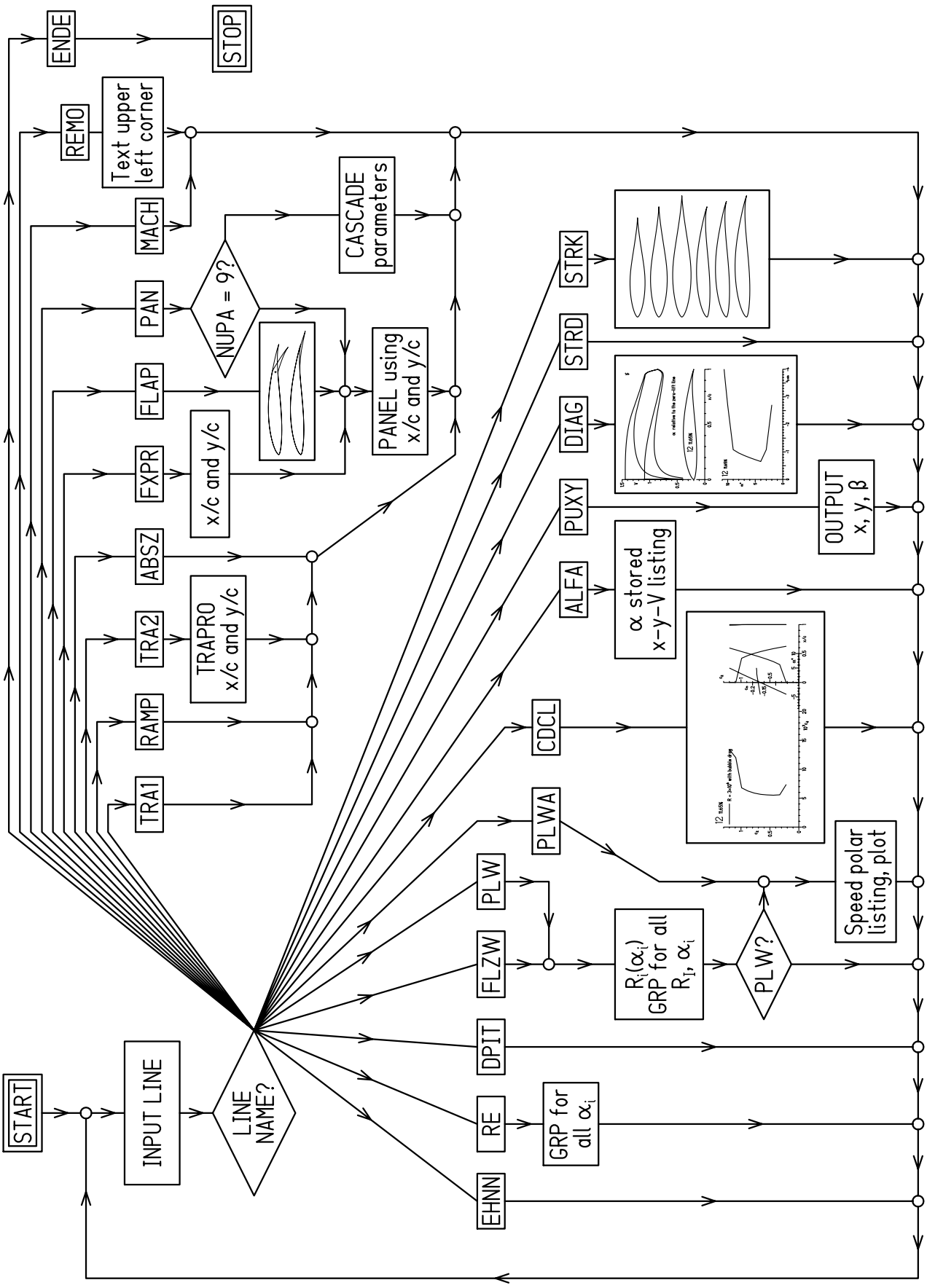

References

[1] Eppler, Richard; and Somers, Dan M.: A Computer Program for the Design and Analysis of Low-Speed Airfoils. NASA TM-80210, 1980.

[2] Eppler, Richard; and Somers, Dan M.: Supplement to: A Computer Program for the Design and Analysis of Low-Speed Airfoils. NASA TM-81862, 1980.

[3] Eppler, Richard: Airfoil Design and Data. Springer-Verlag (Berlin), 1990.

[4] Eppler, Richard: Praktische Berechnung laminarer und turbulenter Absauge-Grenzschichten. Ingenieur-Archiv 32 (1963), pp. 221–245. English translation NASA TM-75328 (1978).

[5] Eppler, Richard: About Classical Problems of Airfoi Drag. Aerospace Science and Technology Vol. 7 (2003), pp. 289–297.

[6] Eppler, R.: Independent Plotting. R. Eppler (Stuttgart), c.2004.

[7] Althaus, Dieter; and Wortmann, F. X.: Stuttgarter Profilkatalog I. F. Vieweg & Sohn (Braunschweig), 1981.

[8] Abbott, Ira H.; Von Doenhoff, Albert E.: Theory of Wing Sections. Dover Publ. (New York), c.1959.

[9] Jacobs, Eastman N.; Ward, Kenneth E.; and Pinkerton, Robert M.: Characteristics of 78 Related Airfoil Sections from Tests in the Variable-Density Wind Tunnel. NACA Rep. 460, 1933.

[10] Jacobs, Eastman N.; Pinkerton, Robert M.: Tests in the Variable-Density Wind Tunnel of Related Airfoils Having the Maximum Camber Unusually Far Forward. NACA Rep. 537, 1935.

[11] Labrujere, Th. E.; Loeve, W.; and Sloof, J. W.: An Approximate Method for the Determination of the Pressure Distribution on Wings in the Lower Critical Speed Range. Transonic Aerodynamics. AGARD CP No. 35, 1968.

[12] Drela, M.; and Giles, M. B.: Viscous-Inviscid Analysis of Transonic and Low Reynolds Number Airfoils. AIAA Journal, vol. 25, no. xx, 1987, pp. 1347–1355.

[13] Dini, P.; and Maughmer, M. D.: A Locally Interactive Laminar Separation Bubble Model. J. Aircr., vol. 31, no. 4, July-Aug. 1994, pp. 802–810.

[14] McGhee, Robert J.; Walker, Betty S.; and Millard, Betty F.: Experimental Results for the Eppler 387 Airfoil at Low Reynolds Numbers in the Langley Low-Turbulence Pressure Tunnel. NASA TM-4062, 1988.